University of Cyprus
Faculty of Letters

Department of History and Archaeology
MA Programme
Field Archaeology on Land and under the Sea

Master's Thesis

Thomas Stavrou

University of Cyprus
Faculty of Letters
Department of History and Archaeology

Field Archaeology on Land and under the Sea

Thomas Stavrou

3D Palaeogeographical Reconstruction of the Archaeological Site of Kition from the Late Bronze Age through to the Roman Period.

Master's Thesis

Supervisor: Dr. Apostolos Sarris

2023

Abstract:

Title: 3D Palaeogeographical Reconstruction of the Archaeological Site of Kition from the Late Bronze Age through to the Hellenistic Period.
Author: Thomas Stavrou
Department/Institute: University of Cyprus, Faculty of Letters, Department of History and Archaeology
Supervisor: Dr. Apostolos Sarris

Abstract:
The ancient settlement of Kition lies below the modern city of Larnaca, on the southeast coast of Cyprus. It lies roughly 400 meters from the nearest coastline and has irrefutable evidence that it once had an operational harbour that had direct access to the sea and participated within the Mediterranean international trade system from the Late Bronze Age through to the Hellenistic and Roman Period.
The following research has been aimed to hypothetically reconstruct a 3D model of the coastal topography and urban layout of the settlement, through the use of past coring data, sea-level indicators, and spatial interpolation techniques.
The aim of this study is to manifest the contribution of integrated approaches such as GIS, Geomorphology, Sedimentology, Palaeontology, and DTM interpolation to recreate the Palaeogeography of ancient Kition during four historical periods of succession: Late Bronze Age, Iron Age, Classical, Hellenistic and Roman periods. The basis of the topographic reconstruction relies on the effective use of generating a DTM through various interpolation techniques, taking into account known elevation points which come from previous coring studies from the Larnaca vicinity and offer paleoenvironmental information of the evolution of the coastal development. Corrections to the coring elevation points are applied based on local sea-level indicators, ensuring a more precise interpretation of the ancient sea-level. This study builds upon these previous findings and offers hypothetical terrain elevations of the various topographical features while placing basic 3D rendered architectural features onto their corresponding paleo-DTM.

Keywords: Mediterranean; Cyprus; Kition, Palaeogeographical Reconstructions, Sedimentology, Coastal Evolution, Coring, 3D Environmental Reconstruction, Paleo-DTM, Interpolation techniques

Acknowledgements

I would like to express my sincere gratitude to my supervisor Dr. Apostolos Sarris for his guidance and support with the topic and processing of data. I also thank Dr. Stella Demesticha and Dr. Miltiadis Polidorou, for personal consultations and discussion. Thank you to my family for their support and patience. Furthermore, I am grateful to my partner, Gabby for her constant support throughout the writing of this thesis.

Table of Contents

LIST OF FIGURES

LIST OF TABLES:

NOMENCLATURE & ABBREVIATIONS:

A standard series of abbreviations is unique to the chronology and ceramics of Cypriot archaeology. The dates are derived primarily from the work of the Swedish Cyprus Expedition Gjerstad (1960) and (Gifford, 1978), with updated revisions from later publications Karageorghis (1982 and 1998) and Knapp (2003).

Period:	Duration:
Neolithic	c. 7500 – 3900/3800 BC
Chalcolithic	c. 3900 – 2500 BC
Bronze Age	c. 2500 – 1050 BC
Early Cypriot (EC)	c. 2500 – 1900 BC
Middle Cypriot (MC)	c. 1900 – 1650 BC
Late Cypriot (LC)	c. 1650 – 1050 BC
Iron Age	c. 1050 – 475 BC
Geometric (CG)	c. 1050 – 750 BC
Archaic	c. 750 – 475 BC
Classical	c. 475 – 325 BC
Hellenistic	c. 325 – 100 BC
Early Roman	c. 100 BC – 300 AD
Late Roman	c. 300 AD – AD 750
Byzantine	AD 750 – 1191
Frankish	AD 1191 – 1489
Venetian	AD 1489 – 1571
Ottoman	AD 1571 – 1878
British	AD 1878 – 1960
Modern	from AD 1878

1. INTRODUCTION

Kition lies on the southeast coast of Cyprus, and currently lies beneath the modern town of Larnaca. Over time Kition experienced a coastal evolution, which is captured in both archaeological and geological records, that reveal a dynamic narrative of environmental shifts spanning millennia. A compelling example of this transformation is evident in the relocation of the Classical ship sheds, once situated on the Mediterranean shores, but now they can be found 400 meters inland. Geological, sedimentological, paleontological, and other analytical examinations have documented the progressive shifts in the ancient shoreline over the past 6000 years.

This dissertation which reconstructs the palaeogeographic Digital Terrain Model (DTM) and urban topography of Kition from the Late Bronze Age through to the Hellenistic and Roman Period is laid out over six chapters. This first chapter introduces the research goals. The second chapter provides a brief overview of the historical chronology of the urban landscape of Kition from the Late Bronze Age, through the Iron Age, into the Classical period, and finally ending in the Hellenistic and Roman period. Various features of the urban topography (e.g., temples, fortified walls, etc.) are discussed, with the focus being the two sites of *Kathari* and *Bamboula*. These features were represented in 3D reconstructions.

The third chapter discusses the various reconstructions conducted on the palaeogeography of ancient Kition. A discussion on the multidisciplinary approaches to those studies is also provided to illustrate the in-depth analysis of each reconstruction. The fourth chapter provides the methodological approach and the final 3D reconstructions of each period of Kition based on the coring data, sea-level changes, and interpolation techniques. The fifth chapter provides the 3D reconstructions for each historical period of interest based on the best interpolated DTM with basic rendered archaeological reconstructions. The concluding sixth chapter discusses findings and challenges that arose throughout the study, as well as the results of the 3D reconstructions.

The key research questions which this thesis endeavours to answer are the following:

1) Which interpolation method performs best for each specific DTM?
    a. Inverse Distance Weighted, Local Polynomial, Kriging, Natural Neighbour?
2) Do the generated interpolated DTMs identify any other potential topographic features?
3) Was the defensive wall of Kition located solely on mainland and followed the natural contours of the topography?
4) What are some of the elevation points of coastal features (spit, islands, etc.)?
    a. Are these features likely to have acted as protective agencies or impediments for ships entering/leaving the anchorage?

The objectives of this Master thesis are to:

1) Provide a 3D reconstruction of the Urban/Coastal Landscape of ancient Kition during the Late Bronze Age, Iron Age, Classical period, Hellenistic and Roman periods.
2) Compare interpolated DTM shoreline with other paleogeographic reconstructions.
3) Test the effectiveness of Interpolation as a method of portraying palaeogeography.

2. HISTORY AND CHRONOLOGY OF KITION

The location of ancient Kition on the southeast coast of Cyprus, is covered by modern town of Larnaca (**Fig. 1**). The ancient remains had long been known, recorded by travellers, and "excavated" by amateurs (Nikolaou, 1976). Regular excavations are confined to the artificial limits of protected plots: Areas I and III (*Chrysopolitissa*) and II (*Kathari*) of the Department of Antiquities' excavations; *Bamboula* of the Mission archéologique française de Kition et Salamine; and more recently *Mantovani* (Department of Antiquities) and *Pervolia* (Mission archéologique française de Kition et Salamine (Yon and Childs, 1997; Karageorghis and Demas, 1985; Fourrier, 2015a; Callot et al., 2022). Even though regular and rescue excavations are restricted to a few open plots, they have nevertheless revealed a vast array of context that covers the lifespan of the city.

Figure 1:Area of Interest with important archaeological sites of Larnaca mentioned in text.

The settlement of Kition was founded at the beginning of the 13th century BC (Late Bronze Age). Kition presents an impressively long and continuous history spanning from the time of its foundations to nowadays. As a result of the area's unceasing occupation, Kition's antiquity, presently buried underneath streets and houses of the modern-day town of Larnaca, is only

known in segments, this fragmentary evidence, notwithstanding, the digital recording of areas of archaeological interest by the French Mission, has provided a comprehensive understanding of the urban topography of Kition at a diachronic level (Callot et al., 2022; Georgiou et al., 2023).

Figure 2: Map of Cyprus with sites mentioned in text.

During the Late Cypriot (LC II) period, the site of Hala Sultan Tekke, south of Kition, appears to have been the area's primary urban centre (**Fig. 2**). Archaeological remains from the city's quarters and tombs attest to the city's participation in the Eastern Mediterranean trade network (Fischer, 2023). The excavators at Hala Sultan Tekke controversially attribute its collapse and abandonment to a group of invaders called the "Sea Peoples" (Astrom and Nys, 2001; Fischer, 2017). Although debatable, the eventual abandonment of Hala Sultan Tekke in the 12th century coincides with the expansion of Kition which may have resulted in the population of the former migrating north to Kition.

Research into the geomorphology of the Salt Lake supports an alternative theory to the abandonment of Hala Sultan Tekke. Coring data extracted from the around Hala Sultan Tekke and the Salt Lake has revealed that environmental changes significantly affected the ability of ships entering and exiting the harbour, due the progressive evolution of harbour lagoon silting overtime into a restricted Salt Lake (Gifford, 1978; Devillers et al., 2015).

Although no Bronze Age port has yet been physically identified, Kition was likely situated on a marine embayment and inlets that provided access to the open sea (Devillers et al., 2015; Knapp, 2018). As we will see in the following chapters, the later periods of Kition easily attest to the presence of a port with harbour facilities. One the other hand, many features of ancient Kition remain unknown and may have been lost due to modern construction. The same can be said about the palaeogeography of the ancient city and its dynamic coastline. However, utilizing the archaeological remains, coring data, indicators of past sea-level and the use of interpolation methods within GIS may provide an alternative hypothesis on the palaeogeography of ancient Kition.

2.1 Late Bronze Age

Founded as a major urban centre, protected by impressive walls, at the end of the Late Bronze Age, Kition experienced a monumental renewal in the 12th century, at the time of major disorder in the Eastern Mediterranean. Termed as the "crisis years," which profoundly impacted Cypriot urban towns (abandonment and shift in settlements), they were apparently urban "expansion years" for Kition (Fourrier, 2015a, Fischer and Bürge, 2017).

In the *Kathari* sector, limited evidence of Early Cypriot III and Middle Cypriot I burials implies some prior habitation. However, the emergence of an urban settlement becomes apparent only during the Late Cypriot IIC period. Notably, this period witnessed the construction of a series of small temples, separated by a sacred garden (Karageorghis and Demas, 1985). These temples,

originally constructed between 1300 – 1200 BC, have been continuously re-erected and reshaped due to destructive events, such as earthquakes, over the course of several centuries.

Figure 3: Plan of Kition Floor III (ca. 1125/1100-1050 BC) (Barnes, 2022; Adapted from Karageorghis and Demas, 1985).

Towards the end of the Late Bronze Age, several sanctuaries and related workshops were established in the *Kathari* district, as depicted in **Figure 1**. Among these, Temple 1 stands out as the most extensive and architecturally remarkable structure at *Kathari* (**Fig. 3**). The southern wall of this temple is constructed using large ashlar orthostats made of bright reef limestone. These ashlar blocks of Temple I bear graffiti markings, often depicting boats, underscoring the city's significance as a port (**Fig. 4**) (Karageorghis and Demas, 1985). In addition, a total of 147 stone anchors have been excavated from the five temples at *Kathari*, further solidifying the fact a

port must have been operational on the banks of *Kathari* during the Late Bronze Age (Frost, 1982).

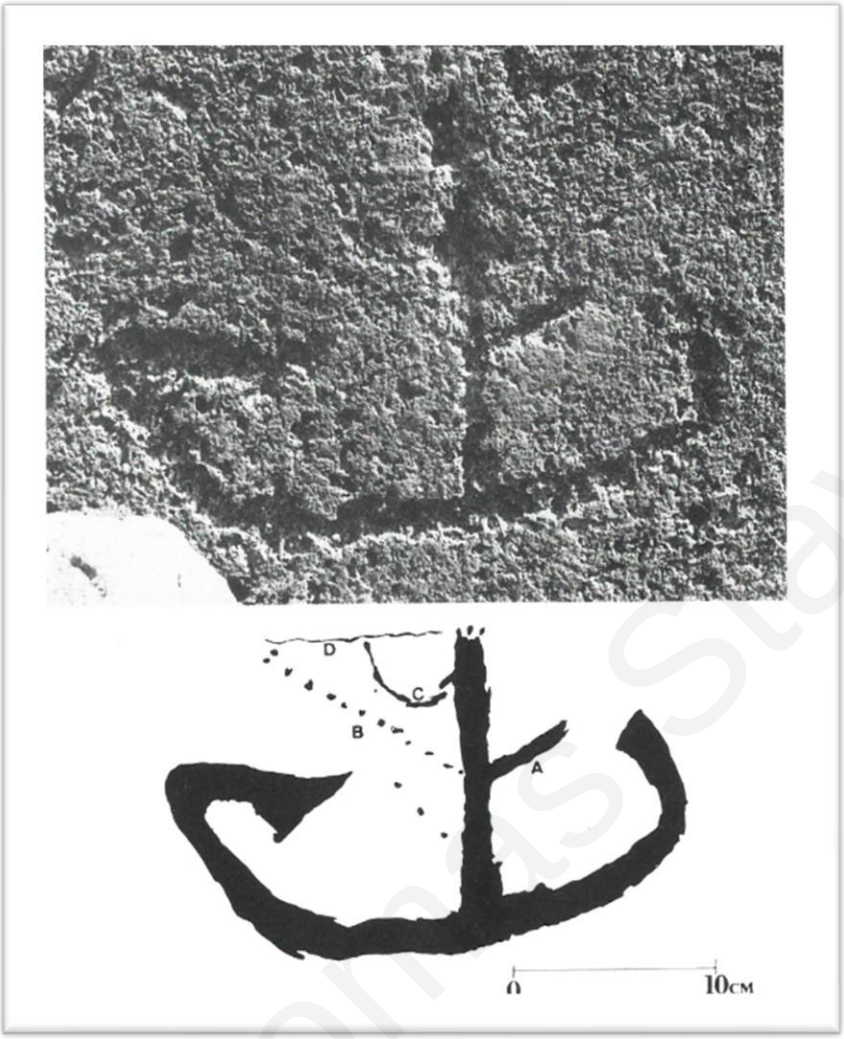

Figure 4: Boat Graffiti on Ashlar Block at Kathari (Karageorghis and Demas, 1985).

The Northern Workshops in *Kathari* reveal evidence of metallurgical activities during its earliest phase (1300-1190 BC). While no structures or installations directly correspond to it, signs of metalworking, such as copper slag and a crucible fragment found within Temple 1, indicating metallurgical activity in the vicinity of the sacred precinct since the city's foundation (Karageorghis and Kassianidou, 1999, p. 174). A different function has been proposed for the Western Workshops, which contain a wealth of artifacts associated with textile production. These workshops, active from the Late Cypriot IIC through the Cypro-Geometric I periods, hint at industrial-scale textile production (Georgiadou and Georgiou, 2019).

The proximity and activity of these sectors clearly associate with the port of the city of *Kathari*. Kition survived during the transition from the Late Bronze Age to the Iron Age, even increasing its political, commercial, and maritime activities (Parpas, 2022, p. 21). In the 13th century BC, the district at *Kathari* and the rich tombs of the necropolis bear witness to the existence of a prosperous and powerful entity, though the full nature and political structure is unknown (Karageorghis and Demas, 1985; Yon and Caubet, 1987; Yon and Childs, 1997).

During the 12th century BC, the area of *Kathari* accommodated a temple precinct (Temples 1-4), including the monumental ashlar-built temple 1. A series of industrial facilities were also established at Kathari, during this period, associated with the processing of copper (Northern Workshops) and textiles (Western Workshops) (Karageorghis and Demas, 1985; Georgiou et al.,

2023, p. 123). Recent studies of the stratigraphical record and material remains of Floor 1 suggest that *Kathari* was uninterruptedly occupied during the Iron Age (Cypriot Geometric) period (Smith, 2009; Georgiou et al., 2023)

Excavations at *Kathari* exposed part of the rampart that was established in its earliest occupation layer (Floor IV) which corresponds to the LCIIC period (13th century BC). Beginning as a mudbrick rampart, the defensive structure was replaced by a cyclopean wall of conglomerate blocks at the beginning of the 12th century (Iacovou, 2007; Georgiou, 2012; Georgiou et al., 2023, p. 123). Thus far only 125 m of this wall have been excavated at *Kathari* and another 15 m closer to *Bamboula* (Karageorghis and Demas, 1985).

The original excavators believed the wall to have enclosed "… an area of approximately 700,000 sq. m. which constitutes the Late Bronze Age town of Kition" (Karageorghis and Demas, 1985). Several hypothetical reconstructions and estimates of the shape and extent of the defensive wall around the city have been suggested, although the true extent is unknown and such large estimates should be viewed with an air of caution (Iacovou, 2007, p. 12). Whatever the case, the cyclopean wall offered protection to the city from its foundation and remained a part of the urban landscape throughout the centuries up to the 4th century BC (Yon and Childs, 1997, p. 10).

The second known cluster of Late Bronze Age urban landscape of Kition lies in the locality of Chrysopollitissa (Area 1), comprising of at least two separate units, in association with two LC chamber tombs. Evidence of metallurgical and textile production are present from this area. Evidence suggest that this was abandoned sometime during the Hellenistic and Roman Period (Karageorghis and Demas, 1985; Smith, 2009; Georgiou et al., 2023). The third cluster is still being excavated today at the site of Mantovani (or Terra Umbria). Preliminary publications demonstrate that the site yielded critical, new data, spanning from the foundation of the site in the Late Bronze Age to the Hellenistic period (Georgiou et al., 2023).

The fourth substantial cluster of Kition urban topography is the locality of *Bamboula*, also located in the northern part of the city of Larnaca (see **Fig. 1**). Unlike Kathari, *Bamboula* lacks monumental temples, although it housed textile and metallurgical workshops during the Iron Age period. The earliest evidence of occupation at the *Bamboula* site, dates to the early 13th century BC, coinciding with the contemporaneous occupation at the Kathari site located to the north. Surveys conducted in *Bamboula*, initially yielded materials from this period, which were initially considered a secondary deposit, likely of funerary origin, accumulated around the late 11th century BC. However, subsequent excavations revealed occupation layers from the 13th century BC, directly on the bedrock, along with several circular wells (**Fig. 5**). A reinterpretation of the "dump" was offered, suggesting it marked an abandonment phase (Callot et al., 2022).

Similar "pebble beds" found in Late Bronze Age (Enkomi) and Iron Age (Salamis, Amathus) contexts imply a common practice. Notably, the clearing of the rocky substrate unveiled the western limit of the port basin. This section suggests uninterrupted domestic occupation between the 13th and 11th centuries BC. The continuous stratigraphy in this steep slope area contrasts with the sanctuary, where stratigraphy only begins in the Cypro-Geometric III period (9th century BC) (Callot et al., 2022).

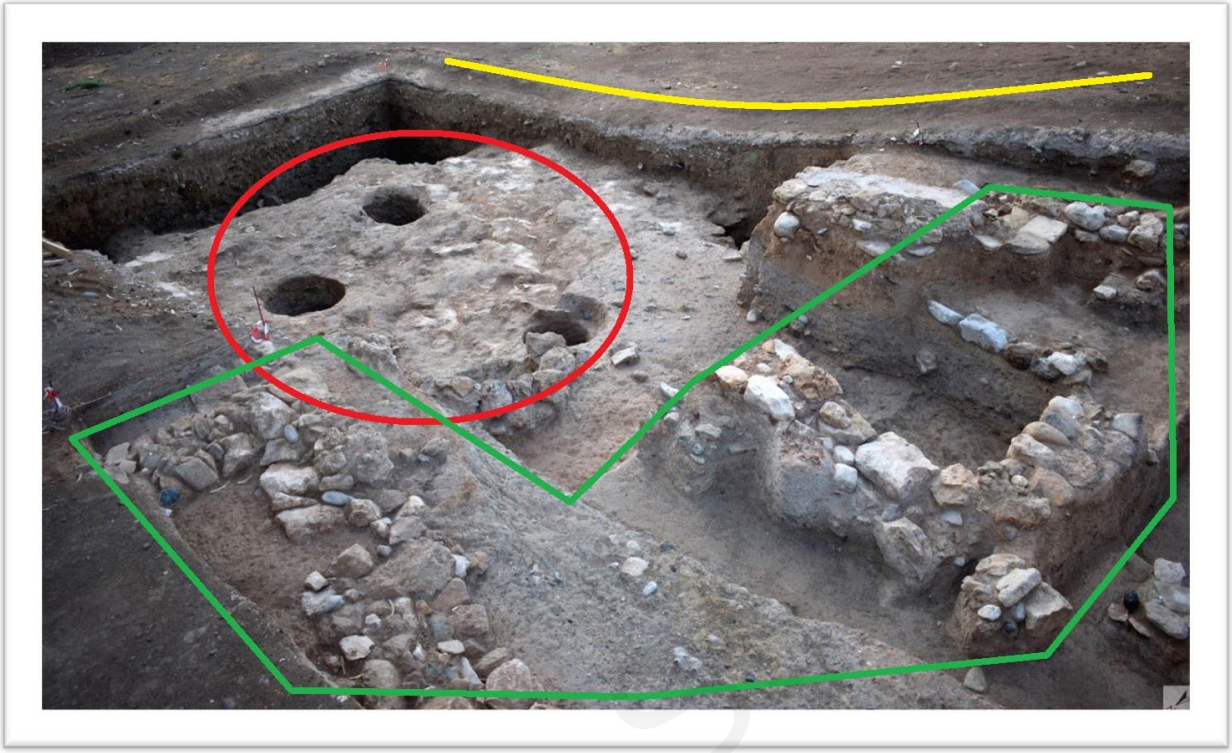

Figure 5: In the foreground, the Late Bronze Age built levels (green polygon) dating to 11th century BC. In the background are rocks and port basin (yellow line) and Late Bronze Age wells (red circle) (Callot et al., 2022).

Evidence indicates a settlement in Bamboula from the end of the 12th century to the beginning of the 11th century BC, though poorly preserved. Such as rooms delimited by walls of large pebbles and irregular limestone rubble supporting mudbrick elevations (Fig. 5 above) (Fourrier et al., 2021). Furthermore, strong evidence supports continuous habitation from the 13th to the 9th century BC, highlighted by traces of settlement dating to the tenth century found along the ramparts next to the port at Bamboula (Karageorghis and Demas, 1985; Yon and Caubet, 1987; Yon and Childs, 1997).

2.2 Iron Age

In the 1st millennium BC, Kition shared a cultural matrix with other Cypriot cities, albeit with distinct characteristics such as language and certain religious or funerary practices, aligning it more closely with the Phoenician cities on the mainland (Yon and Childs, 1997, p. 15). Despite these distinctions, evidence indicates that Kition's presence was not a result of Phoenician colonization efforts but rather represented another aspect within the city's socio-political landscape (Iacovou, 2021, p. 306).

During the beginning of the Iron Age, some topographical shifts occurred, but at a scale and in the limits of the city. The site of *Chrysopolitissa* was progressively abandoned during the 11th century BC. At *Bamboula*, a house, which may belong to a larger unexcavated city quarter, was

constructed in the first half of the 11th century close to the late Bronze Age city wall, which was still in use. At *Kathari*, a massive destruction occurred approximately in the middle of the 11th century BC, but the site was immediately reoccupied (Fourrier et al., 2021).

One notable topographic change is that of the new burial grounds. In the Late Bronze Age, tombs were located within the supposed limits of the city. From the beginning of the 11th century BC onwards, tombs were cut in the rocky plateaus that surround the northern and western parts of the city (Fourrier, 2015b).

From the 9th century onwards, Kition experienced a gradual development, which is especially apparent in the remodelling of the *Kathari* and *Bamboula* sectors. This urban development, which included the creation and improvement of public space, such as sanctuaries and streets, points to the existence of a new state power (Fourrier, 2015b). This change was likely influenced by the demands of the Assyrian empire on the Mediterranean coastal areas in the Levant and Asia Minor. During this time, Kition started regaining its position as one of the main cities of city-states. Which would lead Kition to have more control over the surrounding areas, bringing in smaller regions under its authority (Iacovou, 2018, 7-28).

The temples at *Kathari* appear to have been briefly abandoned circa first millennium BC. However, at the beginning of the 9th century BC, under Phoenician occupation, the temple complex was converted to the worship of the Phoenician goddess Astarte, the equivalent deity to Aphrodite. The renewal affected the Late Bronze Age Temple 1, whose ashlar walls were reused. A second particularly monumental reconstruction phase is also attested at *Bamboula (***Fig. 6)**. After an apparent hiatus, a sanctuary was erected in the 9th century BC. It also went through successive architectural phases, the most impressive of which is dated to the Cypro-Archaic 1 period (**Fig. 7**) (Fourrier, 2015)**.**

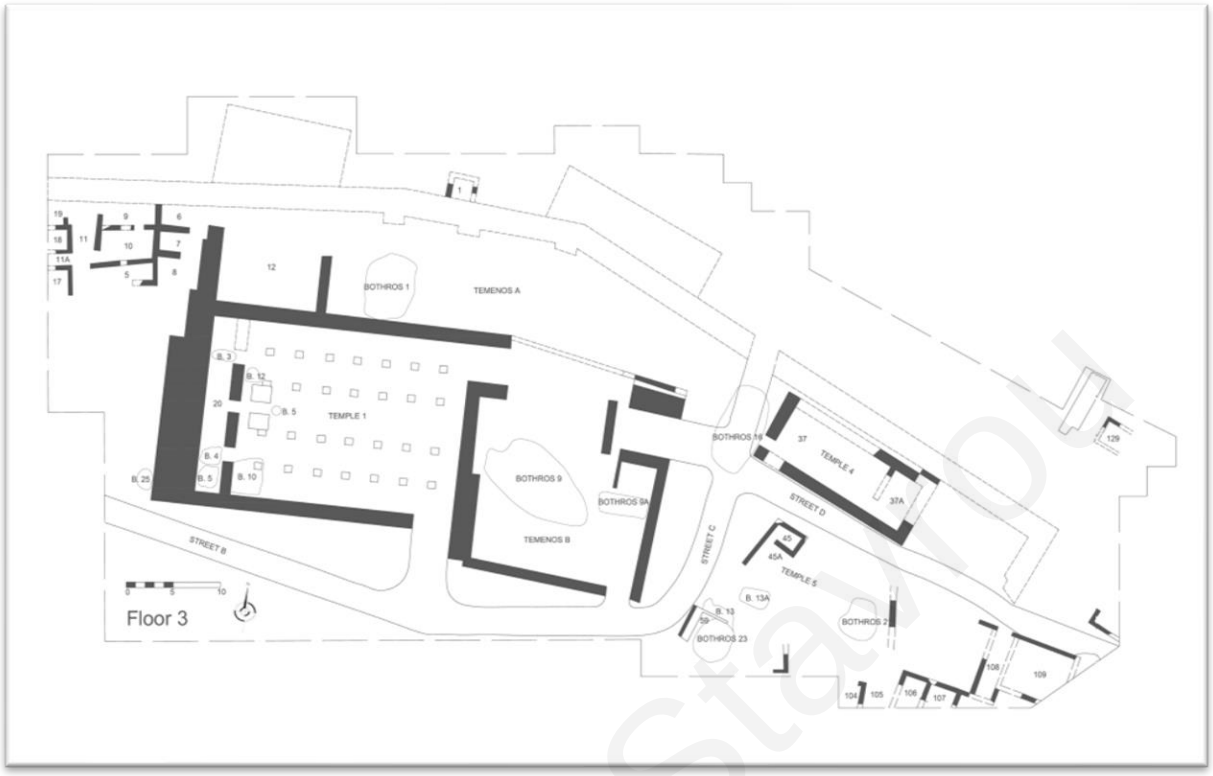

Figure 6: Plan of Kition-Kathari Floor 3 (ca. 850-707 BC) (Barnes, 2022;Adapted from Karageorghis and Demas, 1985).

As in the sanctuary of *Kathari* in the Late Bronze Age there were textile and metallurgical workshops, also found at the *Bamboula* Sanctuary during the Archaic Period. The sanctuary was established already in the Cypro-Geometric III (900/800/750 BC) if not earlier. In the Cypro-Archaic I period (ca 750-600 BC), the sanctuary underwent a radical renovation. A large central court which covered the buildings of the earlier phases was created. It was delimited to the south by a wall that separated the sacred space from a street to the east, by a portico and to the west, by a set of rooms whose contents led to their identification as craft workshops (Karageorghis and Kassianidou, 1999).

The building to the west consisted of a series of rooms and an open space and had no direct access to the sacred courtyard (**Fig. 7**). Within the rooms and the courtyard several fragments of slag and metallurgical ceramics were recovered, as well as loom weights, leading excavators to identify this building as a workshop. This draws parallels to the sanctuary of Kition *Kathari* during the Late Bronze Age mentioned above (Karageorghis and Kassianidou, 1999).

At *Kathari*, The Northern Workshops remained active during the 11th century BC, until it was abandoned when an earthquake caused damage to the structures (ca. 1125/1100 – 1050 BC). Although the temple remained in use for some time, it too was eventually abandoned sometime around 1000 BC and only reoccupied after 150 years under the Phoenician rule (ca 800-725 BC) (Karageorghis and Demas, 1985; Karageorghis and Kassianidou, 1999).

The *Chrysopolitissa* area remained abandoned until the Hellenistic era, but some buildings excavated to the southeast of the sanctuary of *Kathari* may be interpreted as houses from at least the 8th century BC onwards. Although, they are poorly preserved and have yet to be extensively excavated. Their apparent regular layout and their location south of a street might be indicative of an urban grid layout of the city (Fourrier, 2015b).

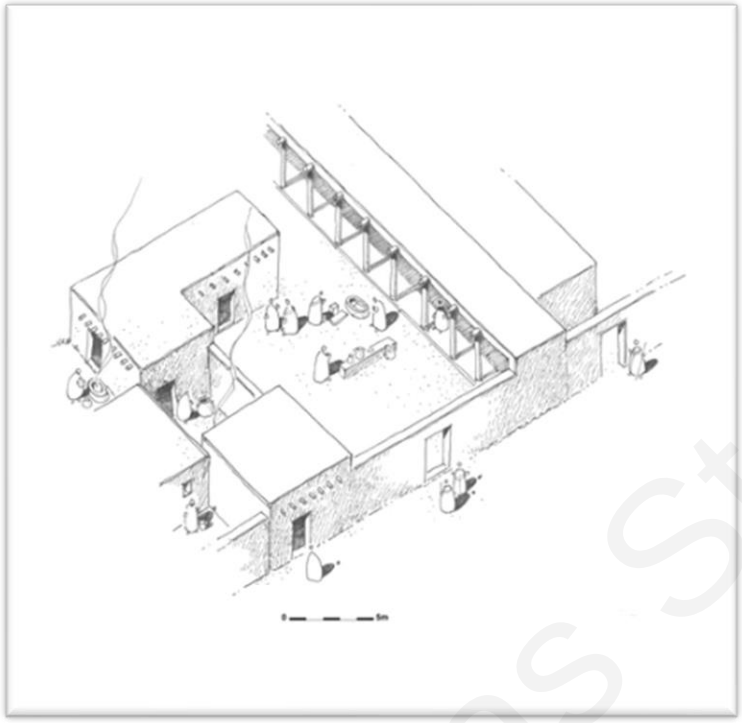

Figure 7: Reconstruction of the Sanctuary of Bamboula during the Archaic period (Fourrier, 2015).

It should be noted that over through this period of about three centuries, the material culture of Kition slowly acquired a "Cypro-Phoenician" character. This evolution is exemplified by the transformation of the ceramic repertoire, as well as by the dominant use of Phoenician script and language (Fourrier, 2015b). Nevertheless, the Iron Age city of Kition did not profoundly differ from other Cypriote urban centres. Its sanctuaries are similar to counterparts among other Cypriote urban sanctuaries, for example at Idalion (open-air sanctuary type with portico, like at *Bamboula*) and at Palaepaphos (monumental ashlar temple, like at *Kathari*) (Fourrier, 2015b).

2.3 Classical Period

The Classical period at *Bamboula* is characterized by a profound transformation. In the first half of the 5th century BC, the whole area of the Iron Age sanctuary was filled in (Caubet et al., 2015). This raised, imposing terrace was part of a new urban design of the whole *Bamboula* area, with the construction of the South Building (*Bâtiment sud)* and the ship sheds (*neosoikoi*) (Fourrier, 2015a). The construction of the South Building on the north side of the rampart, starting in the 5th century AD, rendered the defensive function of the archaic fortification obsolete. This building was originally interpreted as a temenos, by the Swedish-Cyprus excavation (**Fig. 8 and 9**) (Callot et al., 2022a, pp. 55–66).

As already mentioned, the newly rebuilt sanctuary took on a new structure and meaning within the bamboula sector. Its cultic function was evident through the presence of specific features, including altars, and votive offerings, notably the impressive series of "bothros" statues from

Swedish excavations. This function may not have been exclusive, and the place of worship might have been part of a larger urban complex, incorporating the South Building and the ship sheds, resembling a sort of palatial structure. This interpretation is supported by the presence of texts with economic content, closely resembling those found in palatial archive contexts, at Idalion (Callot et al., 2022, pp. 55–66).

Very little is known about the political history of Kition in the Classical period, and far less about the preceding periods. Nonetheless, from the 9th century BC to the end of the 6th century BC, Kition accumulated wealth from its position on the trade routes from east to west (Yon and Childs, 1997). The establishment of the Kingdom of Kition is generally attributed to the first quarter of the 5th century BC (Iacovou, 2018), although some debate exists regarding the precise timeline. While the foundation of this kingdom and the broader political landscape across the island of Cyprus falls outside the scope of the current study, it is noteworthy that Kition's influence expanded over subsequent centuries. Other cities, including Idalion and Tamassos, came under its rule, illustrating the growing political sphere of influence wielded by this growing Classical city (Cannavò, 2022).

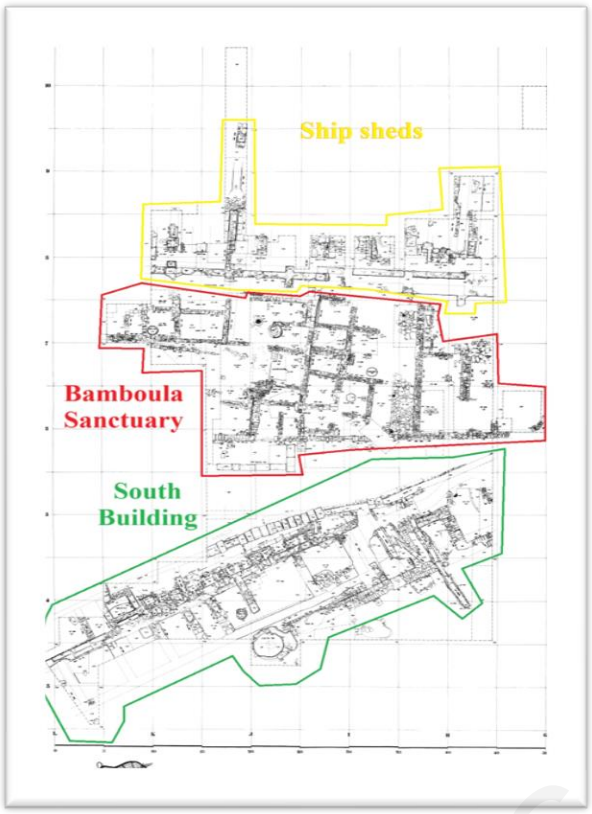

Figure 8: Plan of the Classical Ship sheds and South Building. The Archaic Sanctuary was covered and filled in which offered an open courtyard area. (After: Callot et al., 2022, pp. 65).

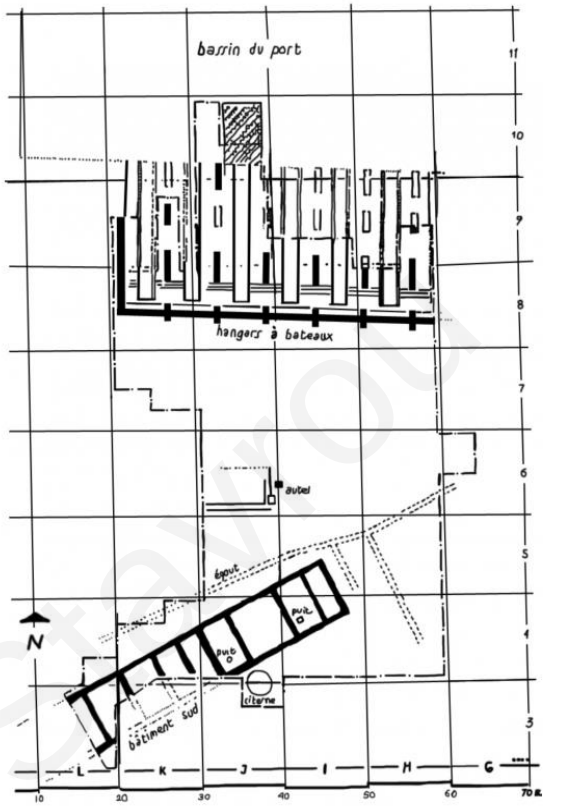

Figure 9: Layout of Bamboula during the Classical period, with the Archaic sanctuary buried and raised for an open air sanctuary (After: Callot et al., 2022, pp. 65).

The most significant developments involved the installation of *neosoikoi* (ship sheds) immediately south of the port basin (**Fig. 8, 9 and 10**). This enormous earthwork saw the necessity for the installation of long sloping ramps (intended to haul triremes to dry them) cut into the old layers, leaving in places only first occupation on the substrate of the Late Bronze Age (Fourrier and Rabot, 2020). Leaning against the robust retaining wall (wall 432) of the sanctuary terrace, these sheds required extensive earthworks to create a slope, involving backfilling to the south and excavation to the north. *Bamboula* then experienced what can rightfully be described as a comprehensive urban planning scheme, evidently carried out under the direction of royal authority (Callot et al., 2022, pp. 55–66).

Figure 10: Aerial view of the exposed archaeological remains at the archaeological site of Kition-Bamboula (Fourrier et al., 2021, p. 282).

2.4 Hellenistic and Roman periods

The end of the kingdom of Kition, marked by the execution of its last king, Pumayyaton, in 312 BC, is not evident in the stratigraphy of *Bamboula*. There are no signs of destruction or abandonment that characterize the end of the 4th century BC on the ground. On the contrary, marks of continuity are notable, both in the South Building, the sanctuary, and, as we will see, in the *neosoikoi* of the naval base. However, the Hellenistic period appears to be followed by a general decline and impoverishment of the occupation, which accelerates in the Roman period (Callot et al., 2022, pp. 55–66).

The rich ceramic assemblage from the *Bamboula* port basin and the recent discovery of a well with a chain pump, filled in the 4th century AD in the northern part of the site (Callot et al., 2022, p. 60), show that activities continued in the area, but they took a different nature. Under this aspect, the site of *Bamboula* is not significantly different from other northern sectors of the city (*Chrysopolitissa*, Areas I and III; Kathari, Area IV), which, aside from a few notable exceptions (such as Hellenistic baths), did not yield extensive structures. Instead, they produced limited sets of artifacts dating from the Hellenistic and Roman periods. The few remains from the Imperial period (largely consisting of hydraulic features such as wells and cisterns) suggest the reconstruction of a suburban landscape, including gardens and orchards, signifying a zone of urban decline. The heart of the city had already shifted further south by this time (Callot et al., 2022, pp. 55–66).

Fragmented testimonies, such as Roman amphorae found in the fill of the *Bamboula* harbour, Hellenistic baths in the *Chrystopolitissa* area, isolated Hellenistic and Roman tombs found along the outskirts of the city, testify to some kind of continuity. But the heart of the city seems to have been slowly shifting towards the south of *Bamboula* from the 3rd century BC onwards (Fourrier, 2015b).

Unraveling the Roman urban landscape of *Bamboula* poses a considerable challenge due to extensive later construction activities that obliterated many remnants. Nevertheless, intriguing evidence hints at a potential interconnected urban network spanning *Chrysopolitissa*, *Kathari*, and *Bamboula*. Archaeological discoveries, including potentially numerous hydraulic installations and mosaic baths at *Chrysopolitissa*, enclosure walls and cisterns at *Kathari*, and a lifting wheel well at *Bamboula*, collectively point towards an interconnected city layout (Fourrier and Rabot, 2020).

The *Kathari* site's religious use was largely abandoned by the 4th century BC, following the conquest of Cyprus by Ptolemy I of Egypt. Though the cult of Aphrodite (identified variously as Hera, Artemis, Isis, and Arsinoe of Egypt) continued to thrive on the island until the end of the Roman period. There is undoubtedly an urban decline from the end of the 1st century AD. After the 2nd century AD, there is very little evidence for an occupational layer, and it remained so for centuries up until the establishment of a medieval fort at *Bamboula*. (Callot et al., 2022b, pp. 203–206) Today, the area is heavily populated with the dense residential and commercial development of modern Larnaca's city centre.

3. PALAEOGEOGRAPHIC RECONSTRUCTIONS

The interest in the palaeogeography of archaeological sites in the Larnaca region has been of curiosity for many centuries. One of the earliest records, if not the first, to attempt to illustrate the topography of Ancient Kition was drawn by Richard Pococke (1738). The schematic plan of ancient fortifications of Kition (**Fig. 11**), which he estimated to be three miles in circumference. He also added that the walls seemed to have been very strong. He elaborates:

> "There is reason to think in the very ancient times that the sea washed the south walls of it, though it is now a quarter of a mile distant. To the east of the town there is a large basin, now almost filled up; it served for the security of the shipping; … this must be the enclosed port mentioned by the Ancients."

Although Pococke may have been seeking the remains of a closed harbour mentioned by Strabo (*Geography*, 14.6.3), multidisciplinary research in geomorphology and archaeology has led to an alternative and more accurate understanding of the development of the coast of Kition. Since the 1970's, a number of core drillings have been conducted throughout the area surrounding Kition, which provide a wealth of information regarding the paleoenvironmental changes that have affected the inhabitants since the city's foundation.

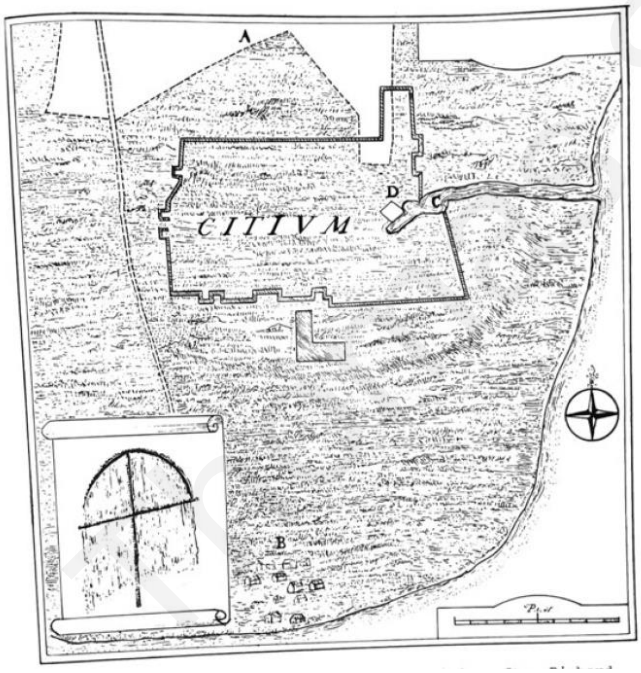

Figure 11: Kition City wall and harbour ((Nikolaou, 1976; after Richard Pococke 1738)

3.1 Analytical procedures of coring data

The processing of cores requires a certain number of analytical techniques to read the conditions of material and sediment placement within a sequence layer. Usually, cores collected are divided into several homogenous stratigraphic units which consider the colour of the sediment (according to Munsell code), the general texture, the grain size, geochemical and mineralogical composition, and the faunal content (gastropods, pelecypods, etc.) (**Fig. 12**). This protocol enables a clear understanding of the depositional environment of the sediments (e.g., open bay, lagoonal, marsh, etc.). The dating of the cores involves radiocarbon dating of organic matter, Posidonia fibers, carbon, or marine organisms. Alternatively, in rare cases, diagnostic pottery fragments are valuable dating elements extracted from core drillings (Callot et al., 2022). Moreover, recent years have witnessed the adoption of new dating methods like electron spin resonance and thermoluminescence (Peppe and Deino, 2013). These methods assess the impact of radioactivity on the accumulation of electrons in imperfections within the crystal structure of minerals to determine the age of rocks or fossils.

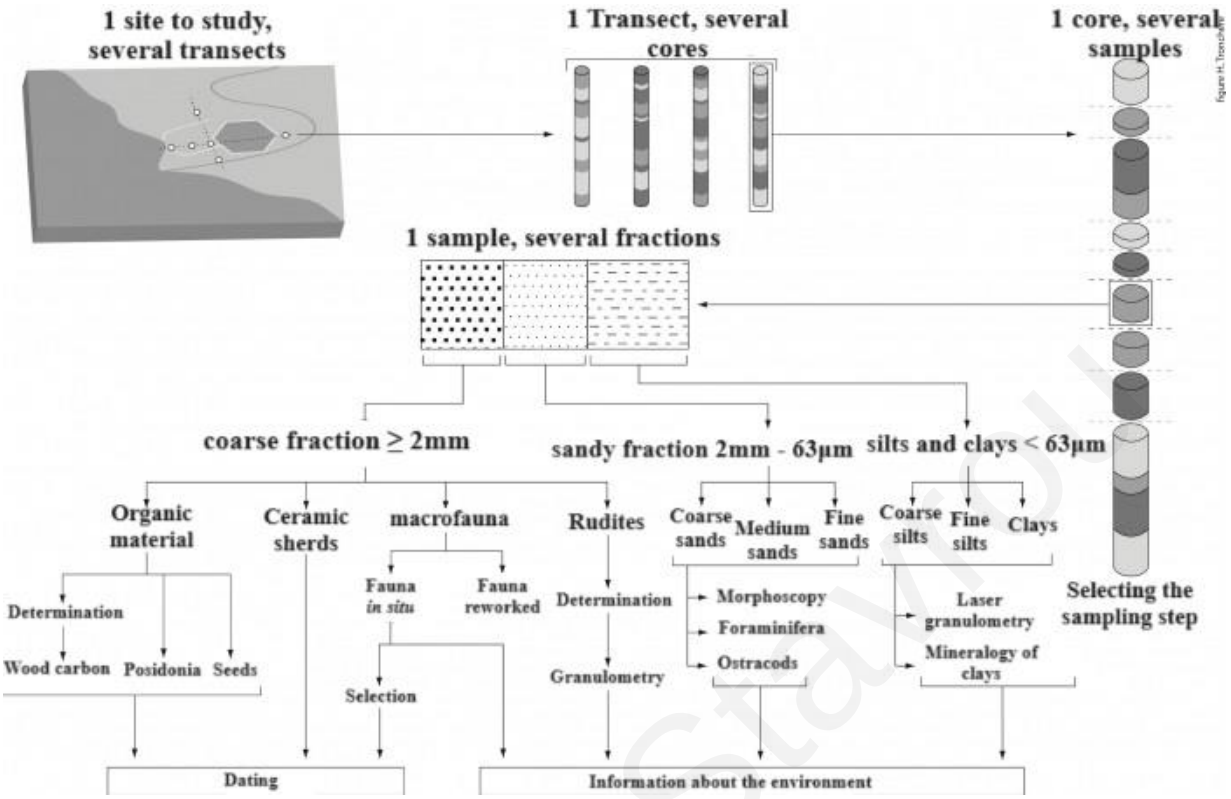

Figure 12: breakdown of the methodology of coring methodology to analyze the paleo-evolution of an environment translated by author (after Callot et al., 2022).

This results in a collection of sedimentary columns which can be further sampled and analysed for a better knowledge of the paleoenvironments, depositional environment and evolution processes of a particular area of interest. Further analytical procedures can provide us with additional information about the general geologic forces at play over time.

Granulometry is defined as the measurement of sediment grain size in a granular material as a proportion of the weight of particles of different sizes. Granulometric analysis involves the sieving of material and subsequent weighing of individual fractions as combined into mainly three groups. The smallest clay fraction usually has a 63 µm. The sand fraction contains all grains with a diameter between 63µm and 2mm, and the gravel fraction consisting of all grains with a diameter greater than 2mm (Kumar, 2011, p. 477). This important distinction, when coupled with subsequent analytical steps, yields valuable insights into the sediment's depositional environment. It aids in distinguishing areas influenced by factors like tidal waves and other natural forces, providing a means to identify various stages of evolution in a coastal site.

Following an actualist approach involves assuming that the ecological conditions of the studied faunas have remained constant throughout the Holocene period (Callot, et al., 2022, pp 25-54). This assumption allows the use of marine macrofauna, including foraminifera and ostracod macrofauna, to reconstruct ancient environments. Ostracods play a significant role in this analysis. Their bodies are enclosed within a bivalve carapace made of carbonates, primarily

found in benthic (lowest ecological zone of a body of water) environments They are extensively used in interpreting paleoenvironmental conditions, especially in fragile coastal marine ecosystems where sea level changes and climatic oscillations are recorded (Polidorou et al., 2021, pp. 1-2). The methodology of identifying marine macrofauna involves comparative analysis of ancient fossil macrofaunal assemblages and contemporary assemblages. These assemblages vary with depth, encompassing high-level fine sands, well-calibrated fine sands, Posidonia meadows, coastal detrital bottoms and seabed influenced by bottom currents (Callot et al., 2022, pp. 25–54).

Ecological data reveals that each species typically resides in relatively stable and homogenous environments. This interdependence between these organisms and their ecological parameters provides valuable insights for reconstructing Holocene environments. Certain species, characterized by a broader ecological tolerance, can adapt to environmental changes. These adaptable species, like *Cyprideis torosa*, can colonize new environments, and their increased abundance can signify environmental shifts. The lifestyle of various ostracods is influenced by primary factors such as salinity and water temperature, as well as secondary factors including bedrock, vegetation, depth and hydrodynamic conditions (Callot et al., 2022).

Wildlife density and species diversity serve as insightful indicators of environmental attributes. Greater species diversity, for instance, can signal a more open and varied environment. In contrast, a scenario characterized by a single dominant species with a high population may indicate an environment in turmoil, where only the most robust species thrive without the constraints of interspecific competition (Callot et al., 2022).

A marine bay open to the sea is likely to host a broader array of species, contributing to higher diversity. Conversely, a closed lagoon with elevated salinity levels might support only a limited number of species specially adapted to endure such extreme conditions (Callot et al., 2022). This fundamental principle serves as a cornerstone in the reconstruction of paleo-environments from the core data extracted from Kition.

3.2 Previous Reconstructions of Kition

Paleo-environmental reconstructions of the coastal sector of Kition have demonstrated through the use of core drillings that the site was once an open marine bay that became separated from the Mediterranean Sea(Gifford, 1978, Morhange, 2000, Bony, 2016). The evolution is both common and unique. It is common insofar as the general direction of change, as for most Mediterranean coasts, was towards silting up and coastline regularization, here in a fairly short period of 2600 years (Bony et al., 2016, p. 223).

Gifford (1978) initiated the use of coring to better understand the palaeographic characteristics in the Larnaca region. The study's findings identified several paleoenvironmental features of the landscape from the late Bronze Age to the Hellenistic period, with a particular focus on the Salt Lake and the site of Hala Sultan Tekke. Regarding the cores that pertain to Kition, several cores (K1-K9) identified various features (**Fig. 13**). Cores K3, 6 -9 (**Fig. 14**) located along the ancient coastal plain, identified a series of beach deposits protruding eastward, sometimes trapping

behind them depressions that became low-energy lagoonal environments collecting organic matter and biogenic carbonates.

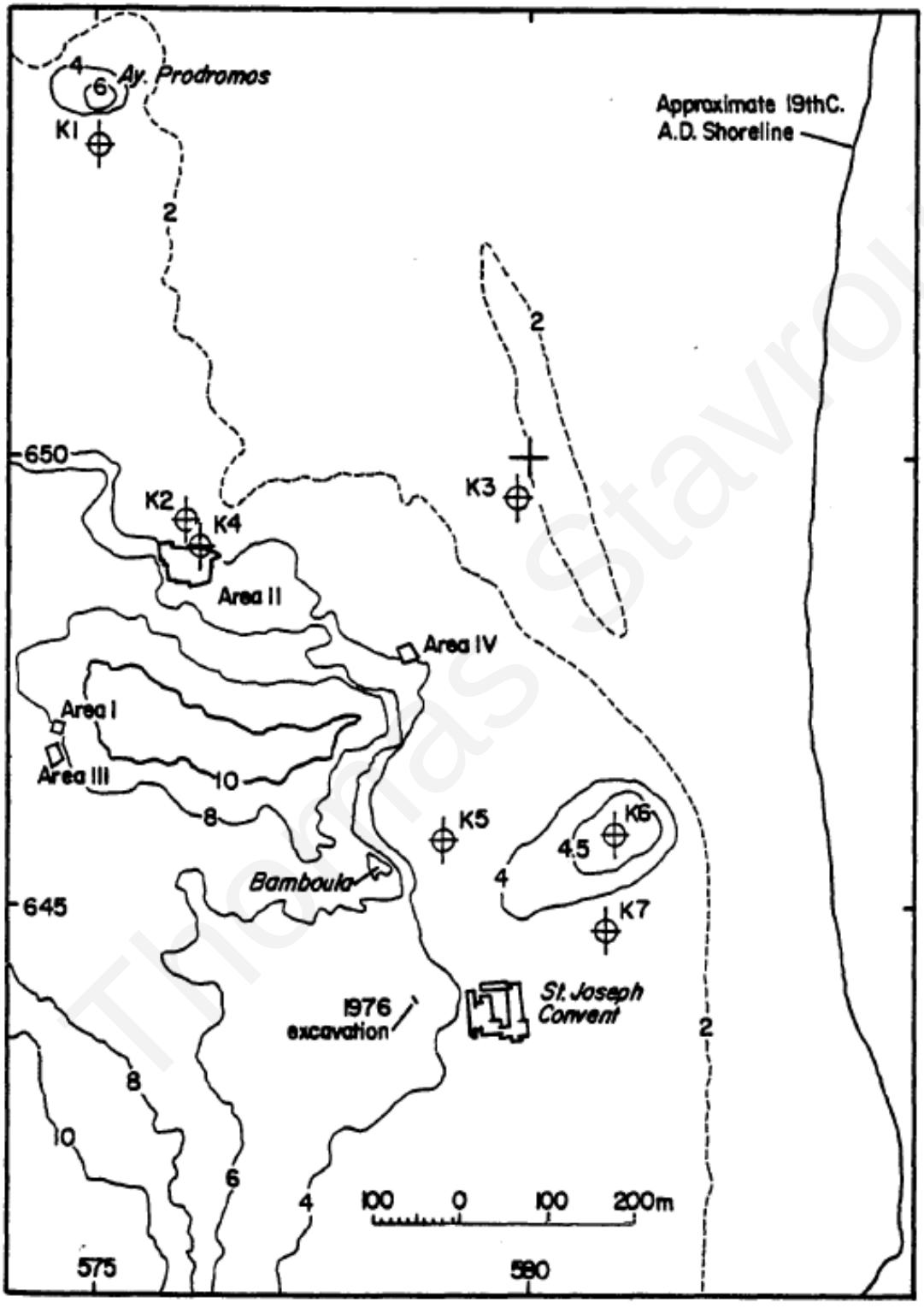

Figure 13: location of cores K1-K7 extracted from the greater Larnaca region (Gifford, 1978, p. 58)

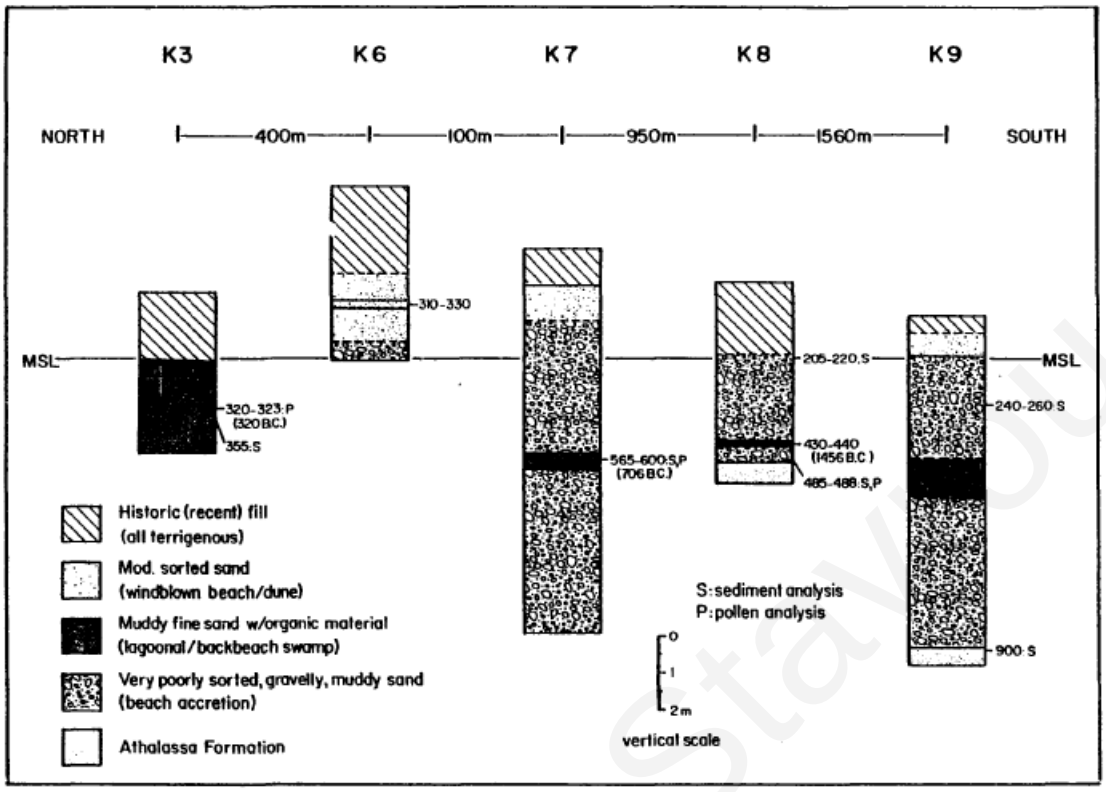

Figure 14: Core K3, K6-K9, located along the ancient coastal plain of Kition (Gifford, 1978, p. 69)

The study's reconstruction focused on the Late Bronze Age harbour site of Hala Sultan Tekke and the Hellenistic harbour of Kition. Through sedimentological sequencing and radiometric dating, a reconstruction of the Hellenistic harbour of Kition *Bamboula* was created (**Fig. 15**). The reconstruction correctly identifies the general layout of a walled city with a port harbour, similar to other Hellenistic port cities (Gifford, 1978, p. 162).

Gifford's reconstruction of Kition during the Hellenistic period produces an interesting interpretation of the geological and anthropogenic factors in shaping the coastlines. Along the coast, a beach accretion is proposed as a result of longshore drift. This produces a very shallow lagoon north of *Kathari*. He also argues that the *Bamboula* harbour follows that of the cothon type, which is protected from the sea with a narrow passageway to the sea. Following Strabo's historical accounts who speaks of a harbour "… that can be closed…" rather than a simply enclosed harbour. Secondly, he points to Kition's recognition as the centre of Phoenician influence, and the Phoenicians are believed to have specialized in the excavation of totally artificial harbour basins known as cothons (Gifford, 1978, p. 163). More recent palaeographic reconstructions, however, would point to alternative ideas to the closed harbour account.

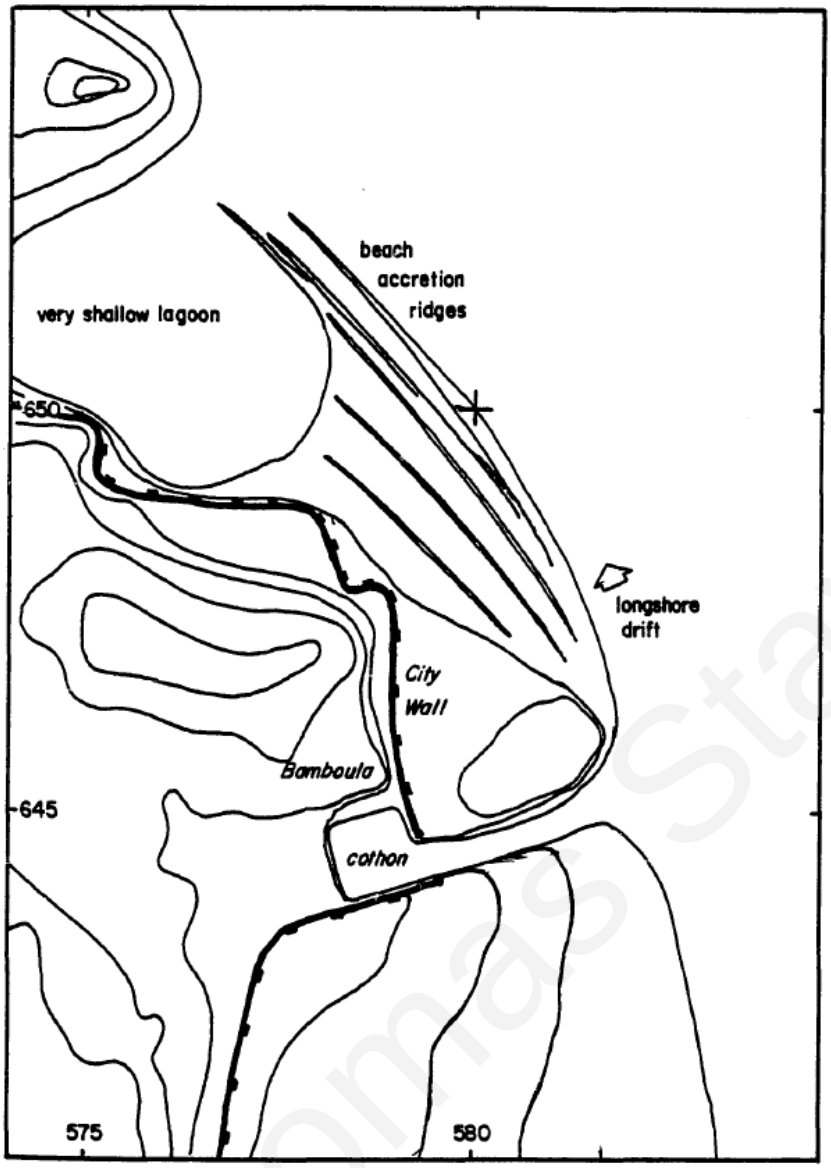

Figure 15:Hellenistic reconstruction of Kition with cothon-type harbour at Bamboula (Gifford, 1978, p. 163)

Morhange et al. (2000) provide a complete chronological reconstruction of the evolution of Kition since ca. 4000 years BP up to modern times (**Fig. 16**). Building upon previous work with the addition of 17 cores and refined analysis through sedimentological, paleontological and radiocarbon dating, provides a new paleo-environmental information for the reconstruction of shoreline changes for Kition and Larnaca Bay.

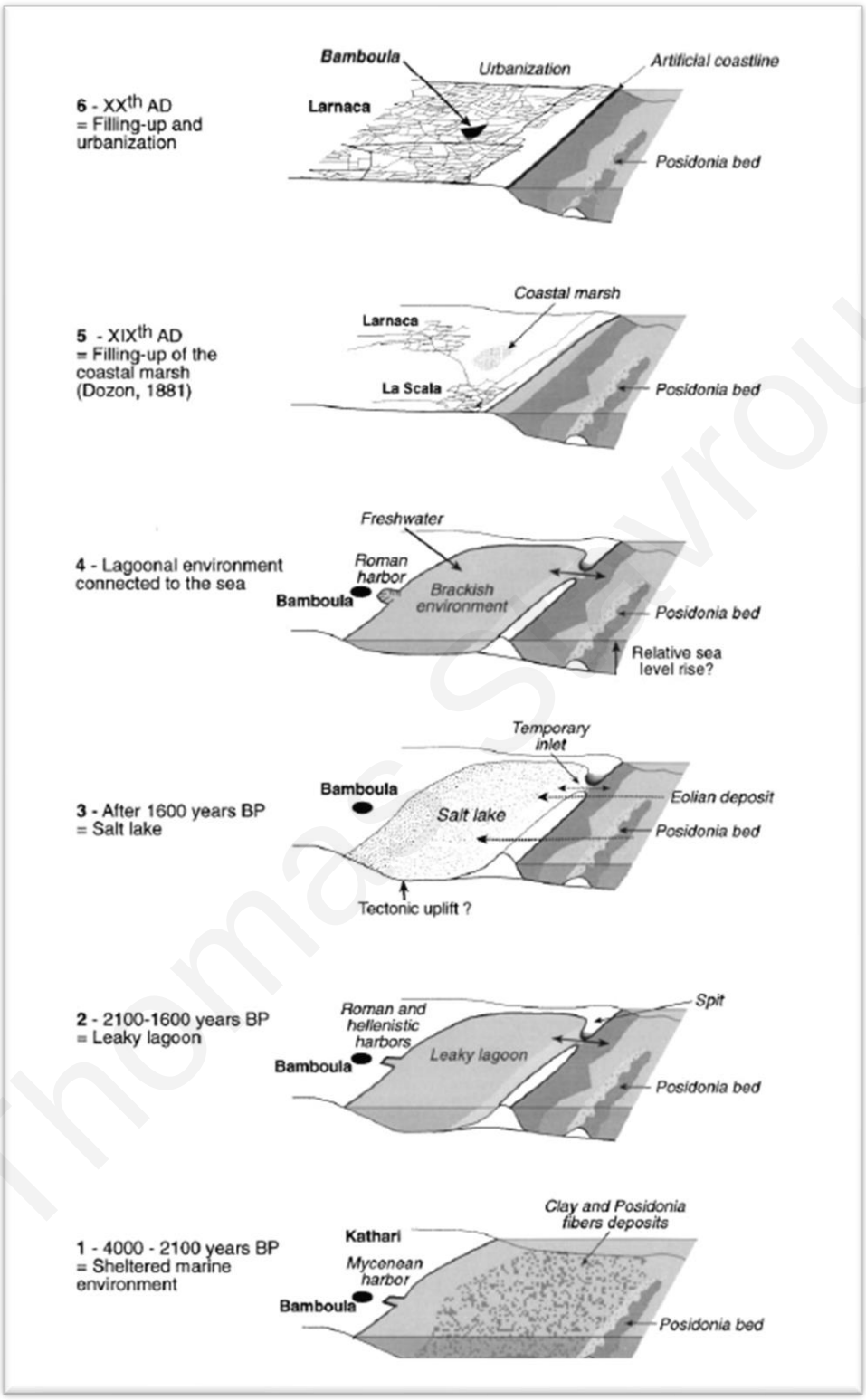

Figure 16: Reconstruction of the Paleo-environmental evolution of Kition, Larnaca coast from 4000 BP (Morhange et al., 2000, p. 227).

Figure 17: Map of Kition with core drilling locations and Bathymetric contour lines (Morhange et al., 2000, p. 206)

The cores were mainly extracted from around *Bamboula* (**Fig. 17)**. In regard to the previous study, the additional cores identified several new features, with the most significant identification being the growing coastal spit (cores CX and CXI) (**Fig. 18)** which was previously interpreted by Gifford (1978, 1985) as an accretion ridge. Spits are frequent when the coastline presents abrupt changes and longshore transport has a dominant direction creating a converging zone (Paladio-Hernandez et al., 2022). The spit formed at Kition was identified as a northerly

migrating pebble ridge that remained discontinuous, allowing passage between the coast and the sea from 4300 years BP to ca. 2000 years BP (Morhange et al., 2000, p. 225).

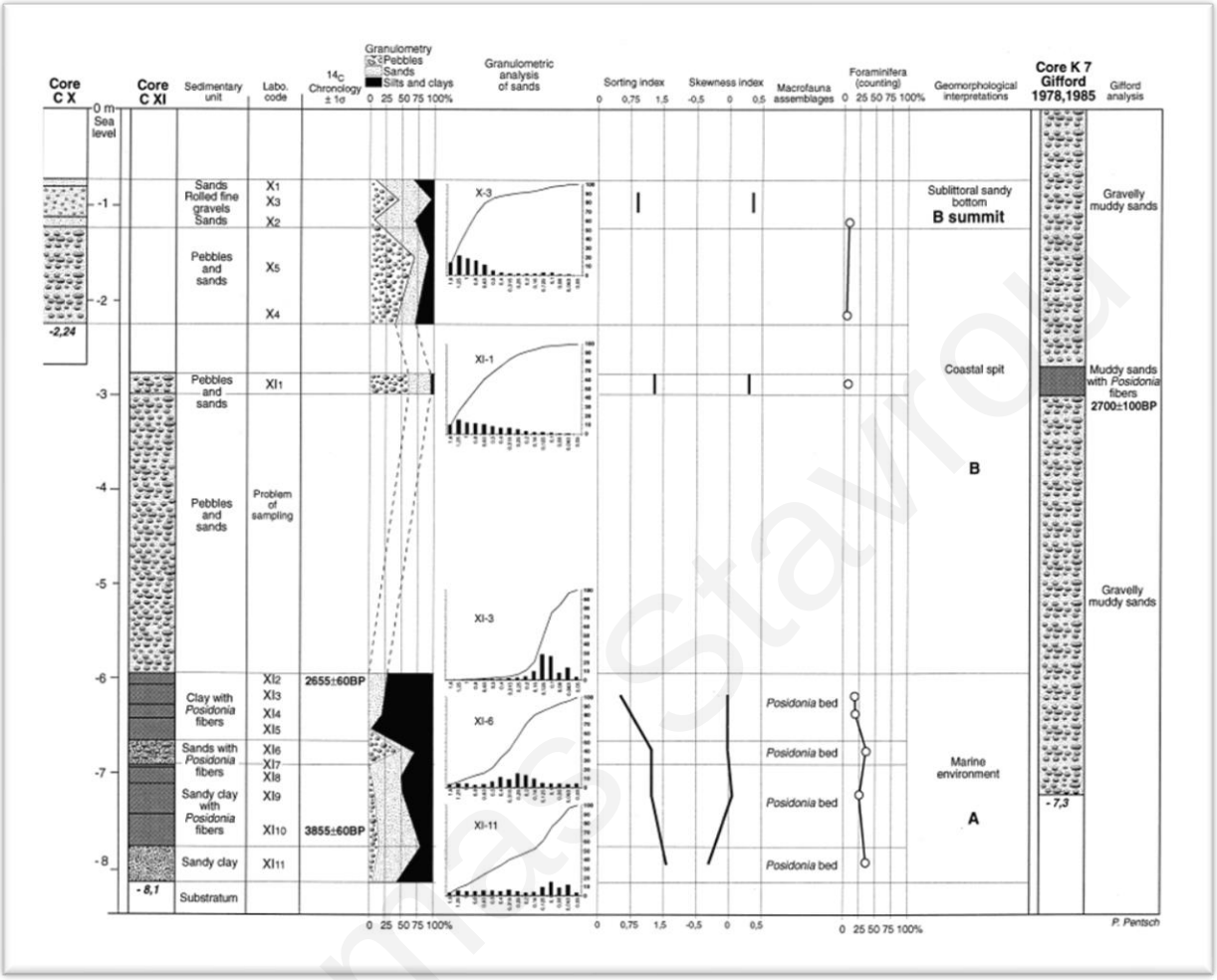

Figure 18: Core CX and CXI results of analysis from Kition. Core K& (From Gifford 1985) is added to show correlation among the stratigraphy (Bony et al., 2016, p. 218)

The overall findings from the study identify a sheltered marine bay environment for the *Bamboula* harbour between 4000-2100 years BP – which correspond to the Late Bronze Age up to the Roman period. This progressively turned into a leaky lagoon during the Roman period (2100-1600 BP), followed by a Salt Lake (1600 BP), brackish environment and finally into the modern urbanized environment **(Fig. 16)**.

A key contrast in the reconstructions is the different interpretation of geological processes in the Larnaca region. Gifford considered a higher sea-level, and further proposed a subsidence of the area. This is contrary to the results of Morhange, who identified uplift as an explanation for the rapid transformation of the lagoon of *Bamboula* (Morhange et al., 2000, pp. 225–229).

Once again, a more precise knowledge of the paleoenvironment was discovered thanks to additional core samples extracted near Kition. Bony *et al.* (2016) investigated the existence of a

secondary port located at the *Kathari* sector of the city, while also exploring the organization of the city within a changing coastal environment (Fourrier, 2014).

This research conducted a comprehensive investigation involving four additional core drillings within the *Kathari* sector, contributing to a more nuanced comprehension of the paleoenvironmental context of ancient Kition (**Fig. 19**). The findings highlighted two pivotal aspects of the Kition coastal landscape. Firstly, it illustrated the potential of *Kathari* as a viable port, emphasizing its direct adjacency to the sacred precinct's shoreline while also capitalizing on potentially sheltered conditions. Secondly, it underscored the profound impact of the pebble ridge formation on coastal evolution, that acted as a protective barrier against storms and facilitated the establishment of port activities.

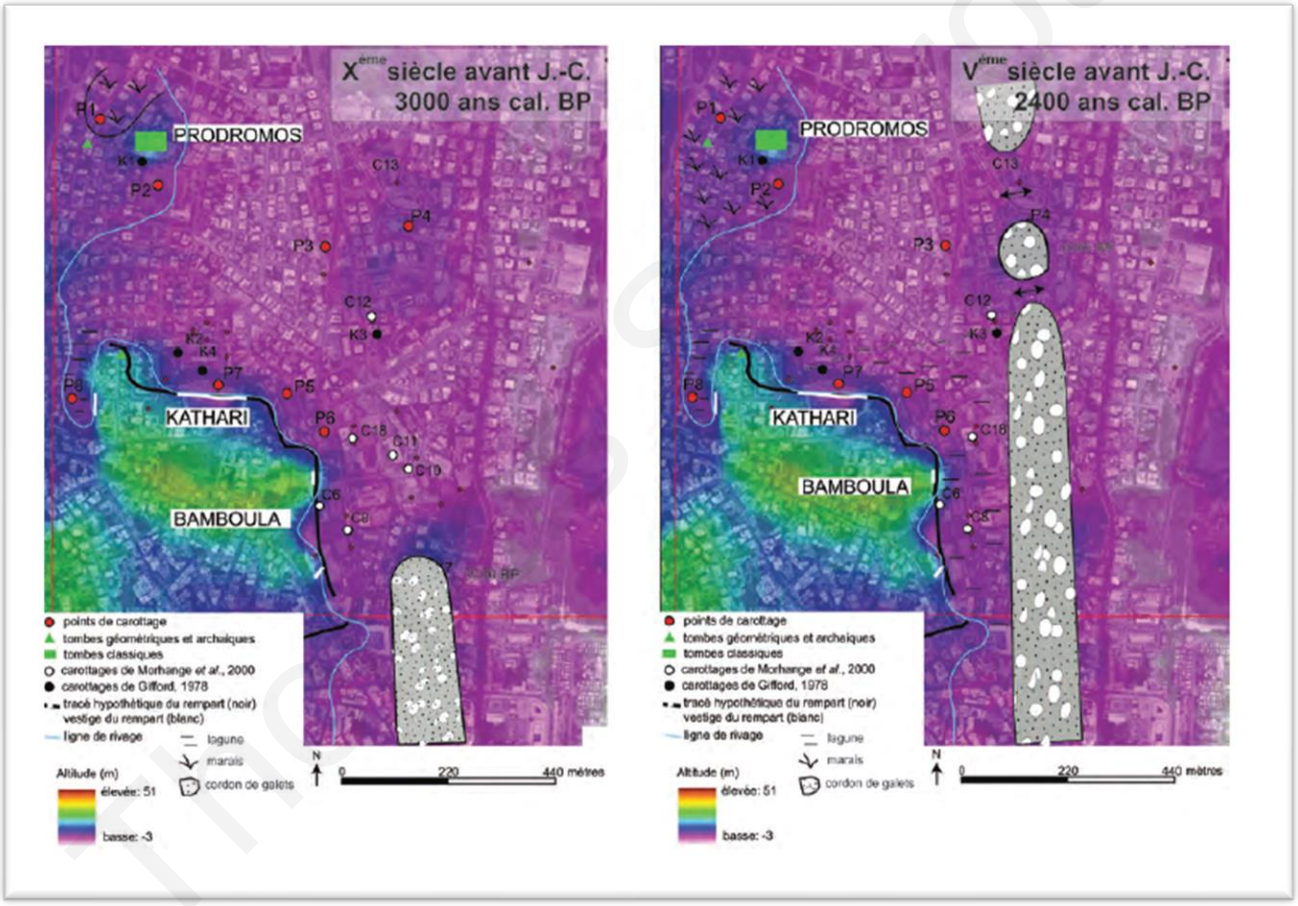

Figure 19: Reconstruction of the paleo-environment of Kition 3000 years cal. BP (on left) and 2400 years cal. BP (right). The two reconstructions emphasize the northly migrating spit over six centuries (from 1000 BC to 400 BC) (Bony et al., 2016).

A recent publication further builds upon our understanding of ancient Kition by providing a comprehensive collection of the current literature pertaining to the history of Kition as well as its palaeogeography evolution. The initial chapter delves into the general geography, geomorphological evolution of the site, the entire Larnaca region, and the historical context. This volume amalgamates over 30 years of fieldwork and research, providing an extensive overview

of palaeogeography studies in the region**. Figure 20** illustrates the most recent diachronic reconstruction of the coastal landscape evolution of Kition and the Salt Lake complex.

To summarize the current understanding of the palaeographic evolution: the first stage can be marked from the 3rd – 2nd millennium BC. During this period fine sediments, rich in Posidonia fibres, were deposited along the coast and in the bottom of the bay, which was oriented north, northwest. A meadow of Posidonia limited the influence of swells and currents (**Fig. 20: 10.1**). In the second millennium BC, in particular, a ridge of pebbles progressed northward due to the action of sea currents and coastal drift (**Fig. 20: 10.2**). The origin of this ridge is unknown. By the end of the 2nd millennium BC, the pebble ridge barrier reached the open sea at the site of *Bamboula* (**Fig. 20: 10.3**). This further protected the site from swells and storms (Callot et al., 2022b, pp. 25–54).

The second stage is from the beginning of the 1000 BC to the 2nd – 4th centuries AD. This is marked by the pebble spit continuing northward. The coastal sector of *Bamboula* corresponds to a natural, well-protected coastal shelter, where a port can be established (**Fig. 20: 10.4**). Communication with the sea must have been possible to the north by a passage. In the Classical Period, ramps and ship sheds were built and the site took the form of a military port (Callot et al., 2022, pp. 25–54).

The emphasis on the Classical period reconstruction within the publication is particularly evident, primarily due to the pivotal role played by the ship sheds and their significance in understanding the palaeogeography of Kition. In the portrayal of the port basin reconstruction (**Fig.** 20), the authors proposed that during the Classical period, the port basin featured a relatively shallow depth ranging from 3.50 m to 3.90 m, demanding considerable navigational skills for entering and exiting from the *neosoikoi* (Callot et al., 2023).

By the Roman period, the pebble spit had migrated so far north, that the access channels from the ports to the sea became unnavigable for ships. Eventually it filled the access points, and the environment became lagoonal. The faunas indicate the beginning of a progressive confinement of the environment. The connection with the sea was not entirely cut-off, but was drastically limited (see: Callot et al., 2022).

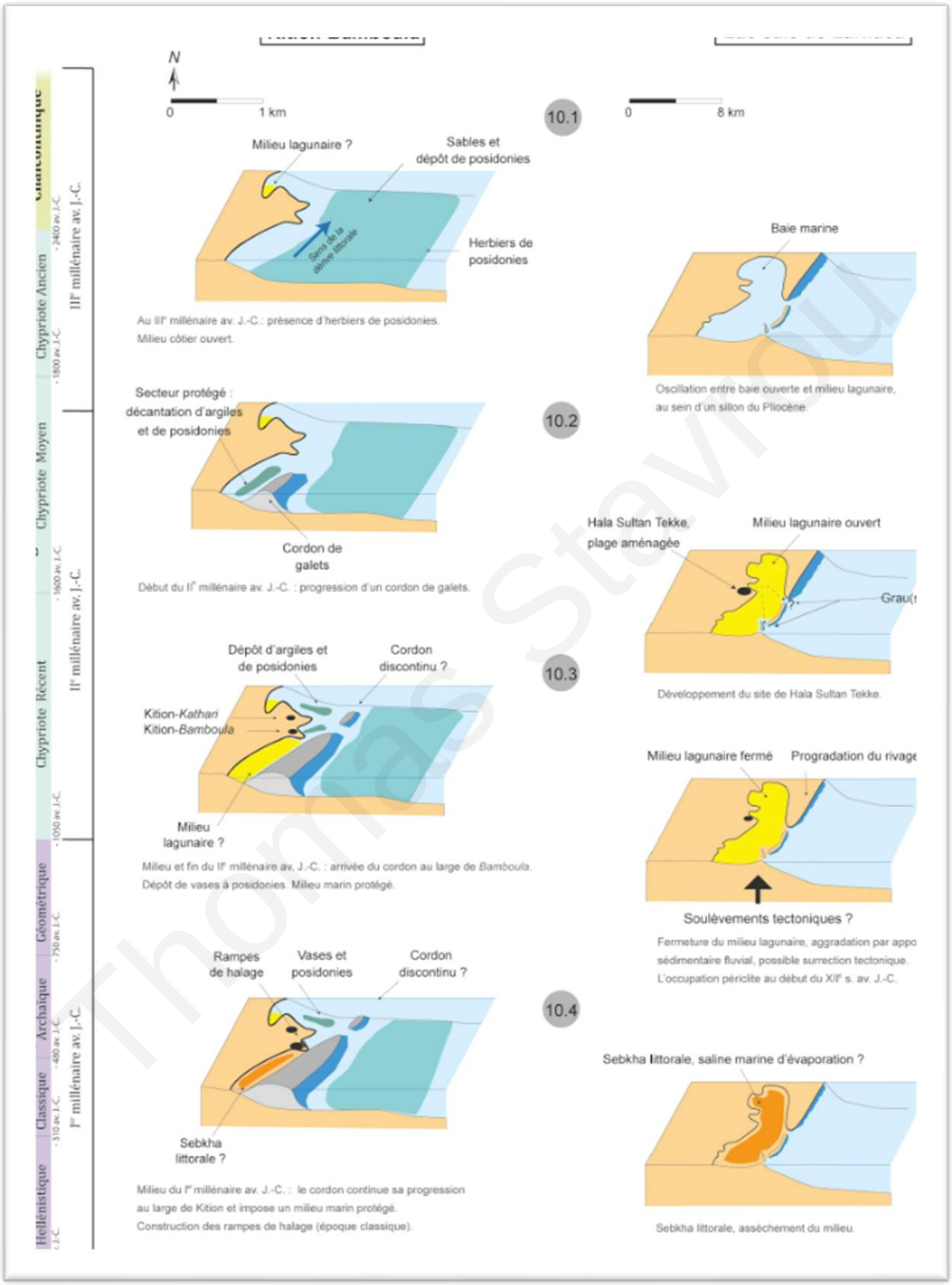

Figure 20: 4000 years of evolution of coastal landscape at Kition Bamboula and the Salt Lake of Larnaca (Callot et al., 2022)

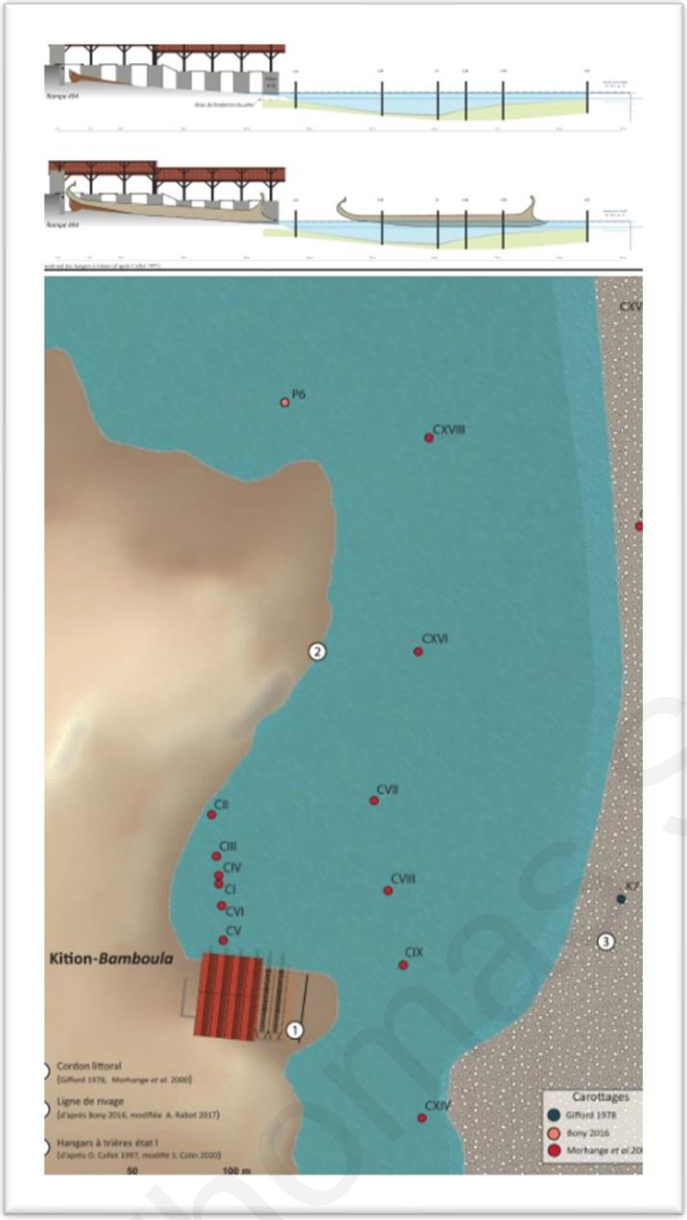

Figure 21: Plan view of the port basin in the Classical Period (Callot et al. 2022).

3.3 Relative Sea Level

An understanding of the local sea-level variation is integral for palaeogeography reconstructions, especially coastal sites. Local sea-level curves reflect global eustatic changes, regional isostatic adjustments of the crust to changing ice and ocean volumes and tectonically controlled crustal movements (Sivan et al., 2001). Reconstructions of Holocene sea-level changes in the Mediterranean are based on relative sea-levels (RSL) indicators that assess variations in sea level (Raban and Galili, 1985; Sivan et al., 2001; Benjamin et al., 2017; Polidorou et al., 2021).

Within the eastern Mediterranean alone, there can be variations from site to site. Recent studies from Greece by Evelpidou et al., (2019) indicate a RSL rise trend of an average of ~0.8 ± 0.2 mm/yr since ~5700 cal PB. While recent studies from Dor in Israel, a relatively tectonically stable region, indicates a period of low RSL of around -2.5 m below sea present sea level from the Middle Bronze Age to the Hellenistic Period (ca. 3500-2200 years BP). This was followed by a rapid rise to present levels, starting in the Hellenistic period and concluding during the Roman period (Yasur-Landau et al., 2021).

Examination of the shorelines of southeastern Cyprus shows that they have undergone significant changes during the Holocene, and more precisely during the last six millennia. Various indicators reveal relative variations in sea levels (Dalongeville et al., 2000, p. 13). There is ample evidence of RSL change: corrosion and organogenic construction (notches, kerbs, buldges), raised beaches and beachrock. Most of these reflections are based on observation points grouped on both sides of Larnaca, where different types of evidence of shoreline variations are associated (Dalongeville et al., 2000, p. 14).

As already mentioned, Morhange *et al*. (2000) sedimentological sequencing at the ancient harbour of Kition mentioned, reconstructed paleo-environments and coastal changes over the last 4 millennia, suggesting tectonic uplift of Kition, whereas Gifford (1980, 1985) suggested the opposite, a higher sea-level and subsidence in the same region. A pattern of uplift was also reported by Yon (1994) at Cape Kiti. According to Poole and Robertson, certain sections along the south and west coast of Cyprus show partially submerged beachrock deposits and archaeological sites, suggesting subsidence in certain areas of the island (Gifford, 1985, 1980; Poole and Robertson, 1991; Yon, 1994; Morhange et al., 2000; Galili et al., 2016, p. 212).

Dalongeville *et* al. (2000) identified three marine episodes corresponding to high relative sea levels along the southeastern coast between Mazotos and Larnaca (**Fig. 22**). Despite the very poor malacofauna, several radiocarbon dates were obtained from three levels of stepped beach deposits. These levels correspond to a relative sea-level increase from +2m (3329 and 2014 BC) to +1m (1169 BC and 235 AD) and +0.60m (1420 to 1530 AD) (Dalongeville et al., 2000; Callot et al., 2022).

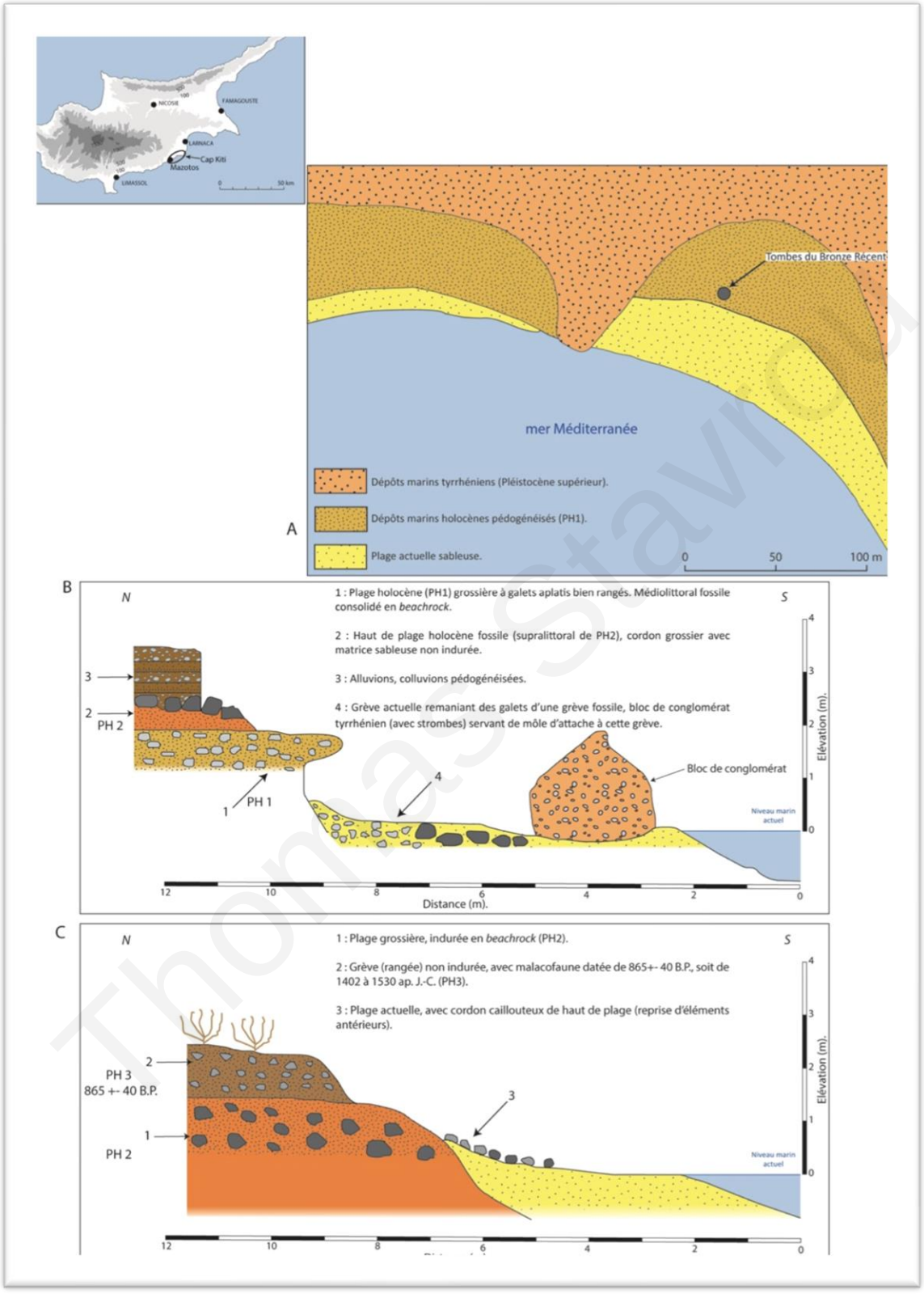

Figure 22: A: Outlines the Mazotos to Kiti coastline, Holocene beach deposits and Bronze Age tombs. B: Pervoila to Mazotos and C: Mazotos to Kiti coastline (Callot et al., 2022, pp. 25–54; Dalongeville et al., 2000)

These studies illustrate the contrasting findings on the direction, magnitude, and pace of vertical movements throughout the Late Holocene along the southeast coasts of Cyprus. In the tectonic context of Cyprus, at the border of the African plate and the Anatolian tectonic microplate, there is undoubtably the detection of tectonic movements (Altinok et al., 2011; Evelpidou et al., 2019). The quickness of evolution of Kition might be an indicator of tectonic impact on a lowland coastal environment (Koss et al., 1994). Under these circumstances, sea level signatures may be ambiguous (Morhange et al., 2000, p. 225). Given the considerable disparities in the local relative sea-level data across the coasts of Cyprus and the different methods employed across studies, makes it difficult to identify RSL when reconstructing the palaeogeography of Kition.

In addition, because there have been no RSL investigations conducted at Kition, addressing sea level changes from the Late Bronze Age through the Hellenistic and Roman period, this creates challenges when trying to apply a sea level to a particular historical period. As a result, the best course of action would be to apply the RSL indicators by Dalongeville et al. (2000), due to the close proximity along the coast, for the reconstruction of each historical period. This correlates to the second phase identified as a relative high sea-level of +1 m from 1169 BC to 235 AD.

4. 3D RECONSTRUCTION METHODOLOGY:

The following outlines the various methodological techniques, assumptions and outlines of the 3D reconstruction processes. An elevation marker is extracted from cores with precise radiocarbon dates. Cores lacking temporal markers are subjected to comparative analysis and correlation with their dated counterparts, thereby enabling the extrapolation of the similar stratigraphical unit. This will provide various elevations within each individual core for each historical period that will be used to create the paleo-DTM.

4.1 Coring data

Figure 23 illustrates a compilation of the comprehensive coring data collected within the vicinity of Kition over the past five decades (Bony et al., 2016; Gifford, 1980; Morhange et al., 2000). These sediment cores, when examined collectively, offer crucial insights into the stratigraphy and paleoenvironmental history of the region. Sediment cores provide valuable information regarding the paleoenvironment, past elevation dynamics, and other critical parameters that shed light on the historical development of this coastal site. By identifying distinct features within the sedimentological sequences and cross-referencing them with radiocarbon and pottery dating, it becomes possible to correlate key historical elements across multiple cores (Bony et al., 2016).

Figure 24 presents the stratigraphic sequence of cores (C 5, C 6, C 1, C 4, C 3, and C 2) retrieved from the ancient port of *Bamboula* (from Morhange *et al*., 2000). Through the various analytical techniques mentioned in the previous chapter, a strong correlation emerges among these cores, reflecting various evolutionary developments captured within the sediment. For instance, Core C 6, situated above the base Pleistocene Marly Substrate layer, consists of a clayey-sand mixture interspersed with Posidonia fibres. Radiocarbon dating indicates a timeframe from approximately 907-764 BC at the layer's base (-2.4 m below sea level) to 97-402 AD at the top (-2.0 m below sea level). This layer, consistently observed in cores C 5, C 1, C 4, and C 3, suggests that this area functioned as an open marine bay from at least the Iron Age to the Roman period, with a gradual elevation increase, likely due to natural sedimentation in the *Bamboula* port.

This interpretation is confirmed by subsequent sequence layers, reflecting a lagoonal environment with limited access to the open sea. The presence of gypsum deposits in core C6 at approximately -1.3 m below sea level, dated to 350 AD suggests full isolation of the *Bamboula* port from the sea (Morhange et al 2000; Callot et al. 2022).

Figure 25 highlights the broader *Bamboula* port basin and reveals a strong correlation within the sedimentological sequences of cores (C 15, C 14, C 9, C 8, C 7, C 16, and C18) (from Morhange *et al*., 2000). Radiocarbon dates from C 8 establish benchmark periods, which are used as reference points for other cores. The sediment sequence, spanning from -2.80 m to -2.20 m below current mean sea level, characterizes an open marine bay environment. Radiocarbon dating places this environment between 870-780 BC to 210 ± 350 AD. This pattern is consistently observed in cores C 14, C 9, C 7, C 16, and C 18. Furthermore, the cores demonstrate a sequence of sedimentological layers above the marine bay deposition layer. These

layers signify transitions from an open marine environment to a lagoonal environment, followed by a silted lagoon, ultimately leading to a marsh and Salt Lake environment.

Figure 26 focuses on the Kition coastal spit location, with C 11 providing the earliest radiocarbon date of 2855 ± 60 years BC at -7.50 m below sea level. This layer represents an open marine bay deposition environment, which prevailed until around 601 – 202 BC. This environment is also recorded in cores K 7 and P 4, with radiocarbon dates indicating a progressive formation of a coastal spit, fully established from K7 to P4 by approximately 536 ± 122 BC. Though some dating uncertainty exists, the establishment of this coastal spit is evident during the late Iron Age.

Lastly, **Figure 27** concentrates on the Kition *Kathari* area. Cores C 6, P 5, P 7, and P3 (from Morhange, 2000; Bony, 2016) provide the most comprehensive stratigraphic sequence compared to other core groups. Radiocarbon dates from C 6 at -2.40 and -2.10 m below sea level date from 907-764 BC to 97-402 AD, respectively. Core P 7 yields a radiocarbon date of 1151 ± 110 BC at -2.00 m below sea level. These dated sequence layers also align well with those of P 5 and P 3, collectively suggesting a marine bay environment from the Late Bronze Age through to the Roman Period. Evidence of shifting depositional layers characteristic of lagoonal and salt lake environments in C 6 may indicate earlier restriction from the sea compared to other cores in this group. However, this entire core group implies a successive evolution from a marine bay to a silted lagoon, eventually transforming into marshland before being filled with modern materials (Morhange, 2000; Bony, 2016).

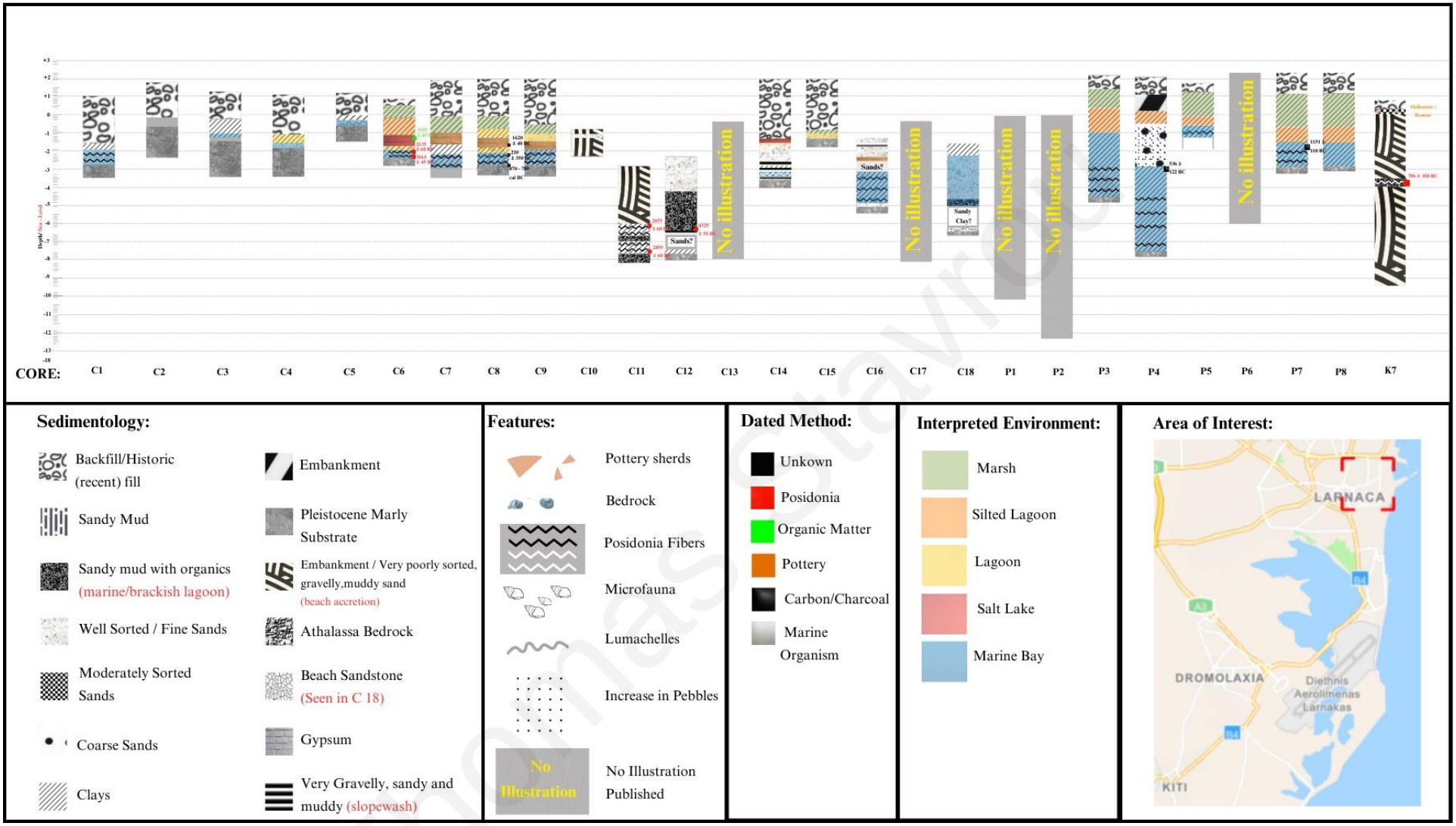

Figure 23: All cores extracted from Larnaca area of interest compiled into one chrono-stratigraphic illustration (after, Bony et al., 2016; Gifford, 1978; Morhange et al., 2000).

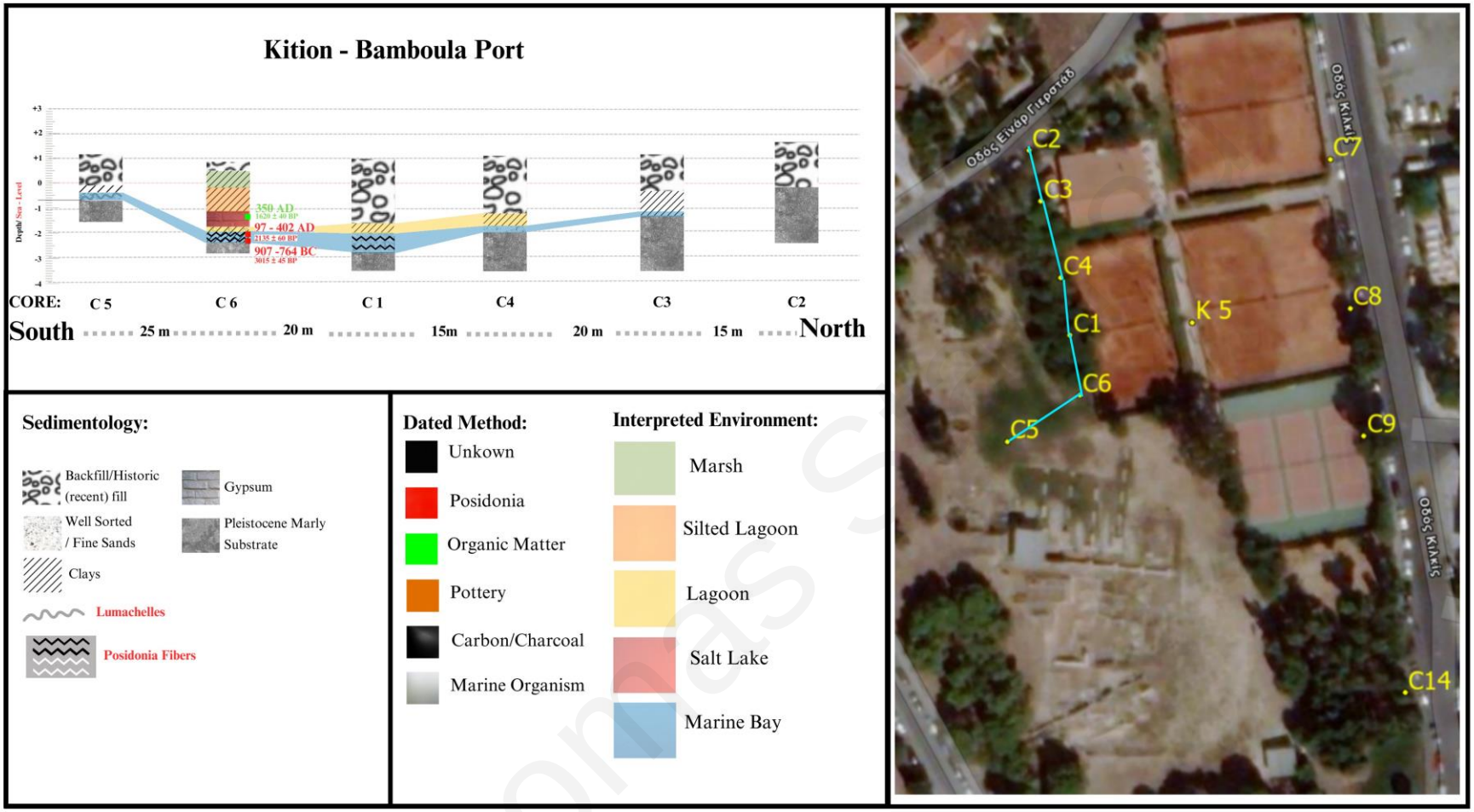

Figure 24: Chronostratigraphic transect of cores (C 1- 6) extracted from the Kition-Bamboula port basin (after Callot et al., 2022).

Figure 25: Chronostratigraphic transect of cores (C 7- 9, C 14-16, & C 18) from the Bamboula port basin (after Morhange et al., 2000; Callot et al., 2022

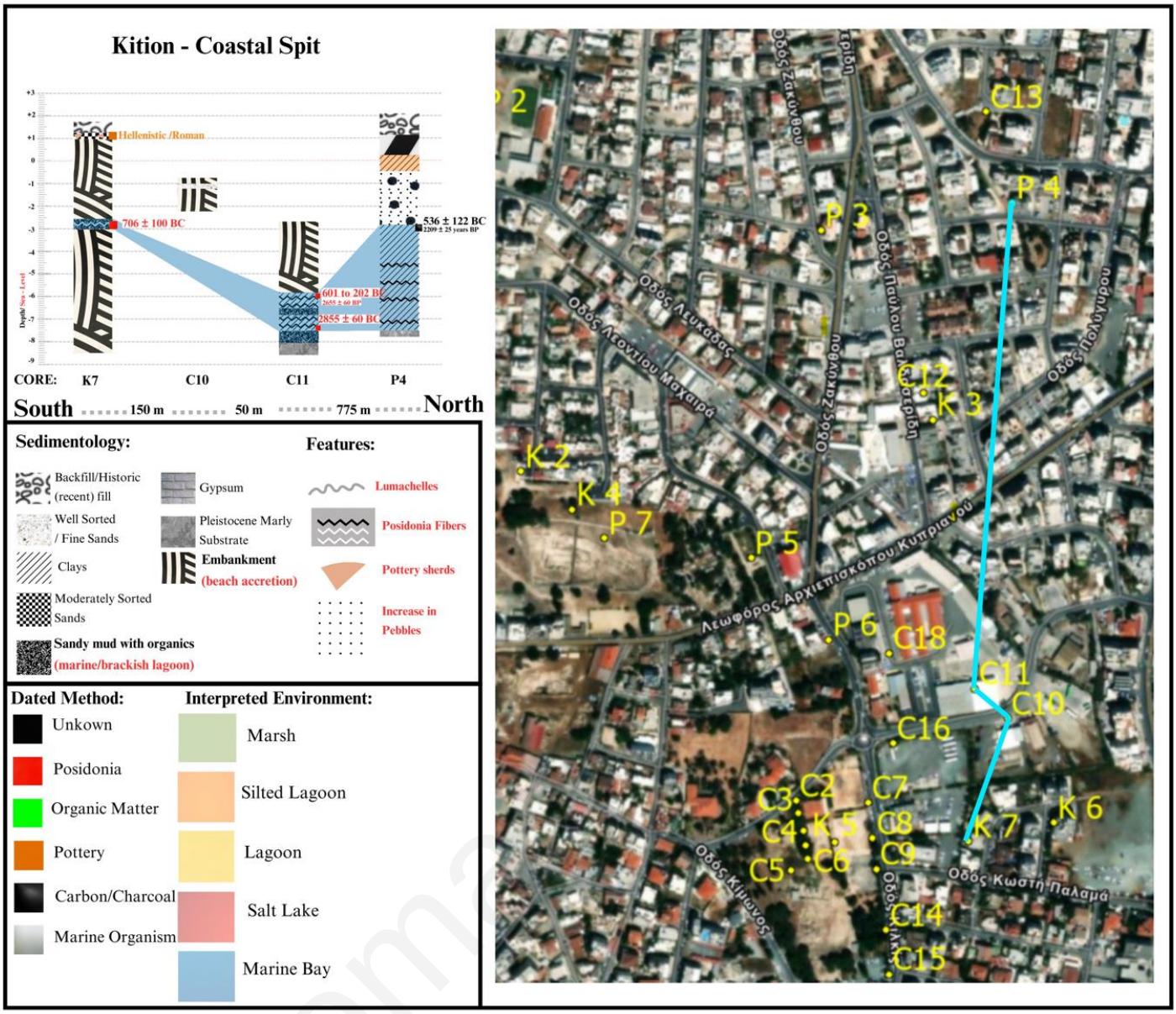

Figure 26: Chronostratigraphic transect of cores (K 7, C 10, C 11, P 4) from the Kition coastal spit location (after Gifford, 1980; Bony et al., 2016; Callot et al., 2022)

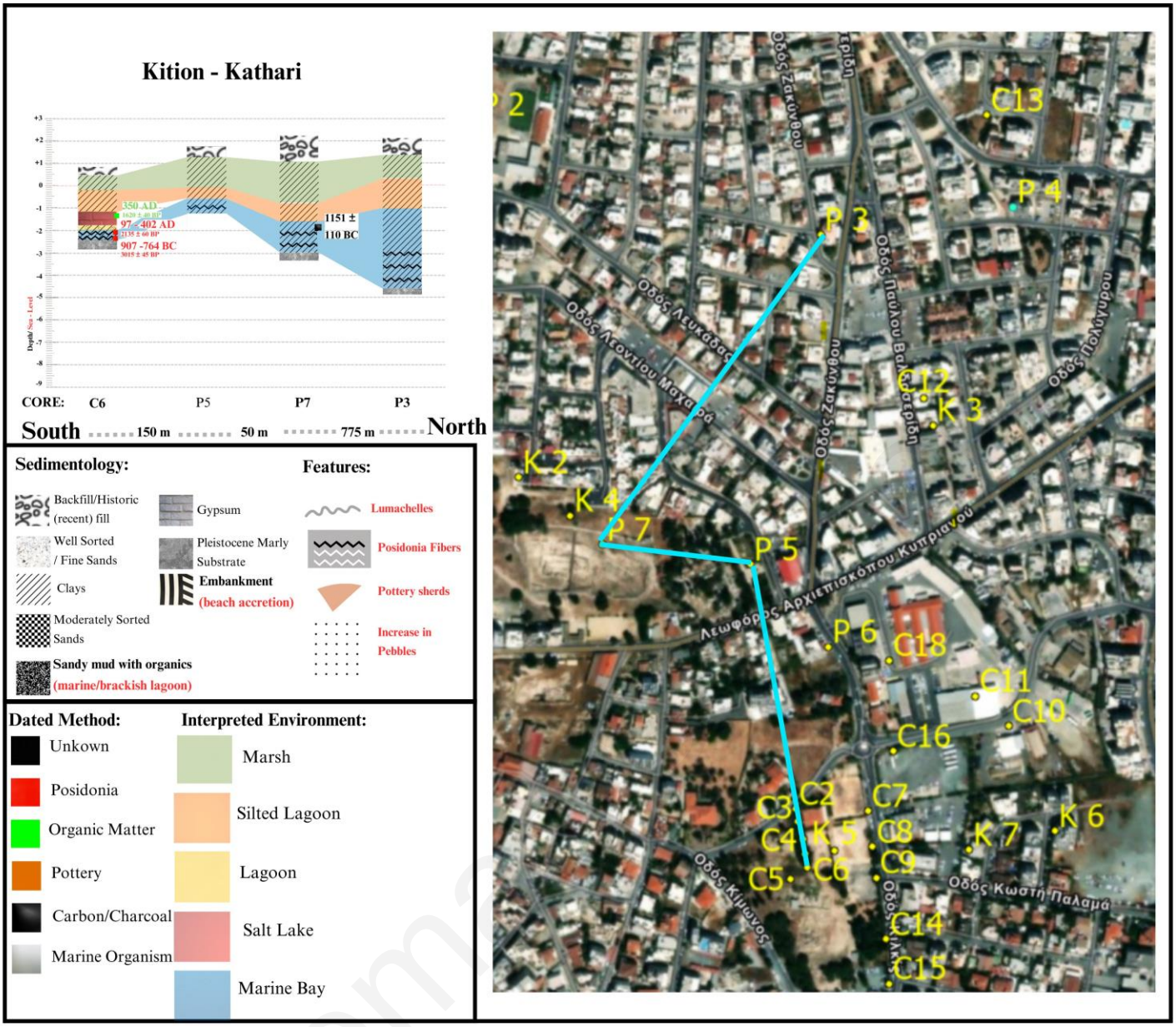

Figure 27: Chronostratigraphic transect of cores (C 6, P 5, P 7 & P 3) from the Kition-Kathari (after Bony et al., 2016)

4.1.1. GIS methodology

For all data processing, a uniform coordinate system, WGS 1984 World Mercator, was used. ArcGIS Pro 3.1 was employed for all interpolation methods. The interpolation extent was constrained to the Kition Area of Interest (KOI) (outlined in **Fig. 1**). Several interpolations were generated, but in the interest of conciseness, only the most pertinent DTMs will be discussed, along with the rationale for selecting the best one for the 3D reconstruction, which will be presented at the end of each chapter.

Using the geoprocessing tool Create Random Points, 50 points were generated within the AOI. 30 points were removed as they were plotted to the east of the proposed shoreline (Bony, 2016) and would have interfered with the interpolation data. This left 20 sample points that were paired with each period (Late Bronze Age, Iron Age, Classical period, and Hellenistic and Roman period) respectively. These Randomly Generated points (RP) received modern DTM elevation points which will be used for all the following interpolations.

4.2 Elevation & Sea-Level Adjustments

Relative sea level adjustments were made to the coring data in order to better portray palaeogeography DTM for each period. For this we considered the relative sea-level indicators from Dalongeville et al. (2000) due to their proximity to Kition and their dating overlapping this study's concerned periods. Elevation from each core was taken at levels where dated material was extracted from. Cores that did not have any radiocarbon dating, were measured at levels that correlate to those that are radiocarbon dated.

Tables 1 – 4, provide the elevation of each core used in each period reconstruction, with the adjusted elevation based on RSL changes. These adjusted elevation points served as the input values for the interpolation methods.

It is crucial to emphasize that the most distinct indicator of the ancient sea level is discernible at the tow ramps of *Bamboula*. Calculations suggest that the foundation of the first row of pillars (aligned with pillar 818) was submerged approximately -1 m below relative sea-level. Consequently, it can be inferred that the last rows stood approximately 2.2 m above relative sea level (Callot et al., 2022). Following this rationale, four supplementary elevation points (each corner pillar) from the ship sheds were incorporated into the Classical period and the Hellenistic and Roman elevation data. No adjustments were applied to these elevations since the relative sea level remains consistent with the findings of this study.

Table 2: Table of the Elevation points based on Core (C ,P & K) and random sample (RP) points with adjusted elevation points based on Relative sea-level of Late Bronze Age.

LBA Elevation Points

FID	Name:	Elevation	Adjusted Elevation
0	C11	-6.50	-5.50
1	P7	-1.60	-0.60
2	P3	-2.90	-1.90
3	C6	-2.40	-1.40
4	P4	-6.00	-5.00
5	K7	-3.00	-2.00
6	C1	-2.80	-1.80
7	C4	-2.10	-1.10
8	C3	-1.30	-0.30
9	C5	-0.70	0.30
10	C8	-2.80	-1.80
11	C9	-2.70	-1.70
12	C16	-5.15	-4.15
13	C7	-2.80	-1.80
14	RP1	10.12	11.12
15	RP2	10.08	11.08
16	RP3	10.14	11.14
17	RP4	9.26	10.26
18	RP5	8.09	9.09
19	RP6	10.98	11.98
20	RP7	12.87	13.87
21	RP8	7.20	8.20
22	RP9	9.92	10.92
23	RP10	9.08	10.08
24	RP11	12.78	13.78
25	RP12	10.21	11.21
26	RP13	9.80	10.80
27	RP14	6.70	7.70
28	RP15	8.36	9.36
29	RP16	6.98	7.98
30	RP17	10.16	11.16
31	RP18	9.20	10.20
32	RP19	10.50	11.50
33	RP20	7.66	8.66

Table 3: Iron Age elevation points based on Core (C ,P & K) and random sample (RP) points with adjusted elevation points based on Relative sea-level.

Iron Age Elevation Points

FID	Name:	Elevation	Adjusted Elevation
0	C6	-2.40	-1.40
1	C1	-2.80	-1.80
2	C4	-2.10	-1.10
3	C3	-1.25	-0.25
4	C14	-3.30	-2.30
5	C9	-2.70	-1.70
6	C8	-2.80	-1.80
7	C7	-2.80	-1.80
8	C16	-5.10	-4.10
9	C18	-4.90	-3.90
10	C11	-6.10	-5.10
11	P4	-3.10	-2.10
12	K7	-3.00	-2.00
13	P5	-1.30	-0.30
14	P3	-2.90	-1.90
15	C5	-0.70	0.30
16	RP1	10.12	11.12
17	RP2	10.08	11.08
18	RP3	10.14	11.14
19	RP4	9.26	10.26
20	RP5	8.09	9.09
21	RP6	10.98	11.98
22	RP7	12.87	13.87
23	RP8	7.20	8.20
24	RP9	9.92	10.92
25	RP10	9.08	10.08
26	RP11	12.78	13.78
27	RP12	10.21	11.21
28	RP13	9.80	10.80
29	RP14	6.70	7.70
30	RP15	8.36	9.36
31	RP16	6.98	7.98
32	RP17	10.16	11.16
33	RP18	9.20	10.20
34	RP19	10.50	11.50
35	RP20	7.66	8.66

Table 4: Classical Period elevation points based on Core (C ,P, K), Ship shed pillars (Pillars1-4) and random sample (RP) points with adjusted elevation points based on Relative sea-level.

Classical Period Elevation Points			
FID	**Name:**	**Elevation**	**Adjusted Elevation**
0	C5	-0.60	0.40
1	C6	-2.30	-1.30
2	C1	-2.40	-1.40
3	C4	-1.90	-0.90
4	C3	-1.20	-0.20
5	K7	-1.00	0.00
6	C11	-5.80	-4.80
7	P4	-2.85	-1.85
8	P5	-0.70	0.30
9	P7	-1.70	-0.70
10	P3	-1.20	-0.20
11	C8	-2.50	-1.50
12	C7	-2.50	-1.50
13	C9	-2.40	-1.40
14	C16	-4.10	-3.10
15	C18	-3.50	-2.50
16	C14	-3.10	-2.10
17	Pillar1	-1.00	-1.00
18	Pillar3	2.20	2.20
19	Pillar4	2.20	2.20
20	Pillar2	-1.00	-1.00
21	RP1	10.12	11.12
22	RP2	10.08	11.08
23	RP3	10.14	11.14
24	RP4	9.26	10.26
25	RP5	8.09	9.09
26	RP6	10.98	11.98
27	RP7	12.87	13.87
28	RP8	7.20	8.20
29	RP9	9.92	10.92
30	RP10	9.08	10.08
31	RP11	12.78	13.78
32	RP12	10.21	11.21
33	RP13	9.80	10.80
34	RP14	6.70	7.70
35	RP15	8.36	9.36

Table 5: Hellenistic and Roman period elevation points based on Core (C ,P, K), Ship shed pillars (Pillars1-4) and random sample (RP) points with adjusted elevation points based on Relative sea-level.

Hellenistic and Roman Period Elevation Points			
FID	**Name**	**Elevation**	**Adj_ele**
0	C5	-0.40	0.60
1	C6	-2.00	-1.00
2	C1	-2.05	-1.05
3	C4	-1.80	-0.80
4	C3	-1.10	-0.10
5	K7	1.20	2.20
6	C10	-0.80	0.20
7	C12	-2.70	-1.70
8	P4	0.90	2.10
9	P5	-0.55	0.45
10	P7	-1.10	-0.10
11	C8	-2.20	-1.20
12	C7	-2.10	-1.10
13	C16	-3.40	-2.40
14	C18	-2.40	-1.40
15	C14	-3.00	-2.00
16	C9	-1.90	-0.90
17	Pillar1	-1.00	-1.00
18	Pillar2	-1.00	-1.00
19	Pillar3	-2.20	-2.20
20	Pillar4	-2.20	-2.20
21	RP1	10.12	11.12
22	RP2	10.08	11.08
23	RP3	10.14	11.14
24	RP4	9.26	10.26
25	RP5	8.09	9.09
26	RP6	10.98	11.98
27	RP7	12.87	13.87
28	RP8	7.20	8.20
29	RP9	9.92	10.92
30	RP10	9.08	10.08
31	RP11	12.78	13.78
32	RP12	10.21	11.21
33	RP13	9.80	10.80
34	RP14	6.70	7.70
35	RP15	8.36	9.36
36	RP16	6.98	7.98
37	RP17	10.16	11.16
38	RP18	9.20	10.20
39	RP19	10.50	11.50
40	RP20	7.66	8.66

4.3 Interpolation and DTM Methods

A Digital Terrain Model (DTM) approximates a part or the whole of the continuous terrain surface by a set of discrete points with unique height values over 2D points. Heights are in approximation vertical distances between terrain points and some reference surface or geodetic datum (Hirt, 2014, p. 1) A more commonly used term of a Digital Elevation Model (DEM) can be defined as the digital representation of the land surface elevation with respect to any reference datum and is frequently used to refer to any digital model of a topographic surface. While DEM and DTM are often considered synonymous in some regions, their interpretation differs in this context.

Specifically, a DTM enhances a DEM by incorporating linear features representing the bare-earth terrain (Heidemann, 2018, p. 48). Several methods are available in literature and GIS software for spatial interpolation and the choice of the most suitable of them for building DTM depends on many factors, particularly on the distribution of the sampled points, therefore, on the morphology of the area to be mapped (Alcaras et al., 2019, p. 1654).

Interpolation is a procedure used to predict values at a location using sample points for which there is no recorded observation. Interpolation techniques are based on the principles of spatial autocorrelation, which assumes that the closer points are more similar compared to farther ones (Arun, 2013, p. 134). Interpolation methods can be classified in a number of ways, including local/global, exact/approximate, and deterministic/geostatistical methods. Global interpolators determine a single function that is mapped across the whole region, whereas local interpolators apply an algorithm repeatedly to a small portion of the total set of points. Exact interpolators honour data points on which the interpolation is based, whereas approximate interpolators are used when there is some uncertainty about the given surface values (Erdogan, 2009).

Due to the small sample size of elevation points within each period’s dataset, a variety of interpolations will be used to best determine the different techniques. Almost all the historical elevation points are in the centre right of the interest area, while the land elevation points are randomly scattered, this will inevitably influence the different methods implemented.

4.3.1. Inverse distance weighted

Inverse Distance Weighted (IDW) is an exact local deterministic interpolation method that constructs a raster surface from given points utilizing inverse weighted techniques. The output value for each cell in IDW is bounded by the range of values employed for interpolation. This is due to IDW's nature as a weighted distance average: the average value cannot exceed the highest or fall below the lowest input. Hence, IDW cannot create ridges or valleys if those extremes have not been previously sampled. It is imperative to ensure that the input sampling is sufficiently dense to capture local variations accurately. In cases of sparse or uneven sampling, IDW may not adequately represent the desired surface (Philip and Watson, 1982; ESRI, 2023).

IDW is one of the most widely used methods for surface modelling. It is based on the intuitive idea that the closest observations must carry more weight in determining the interpolated value in one point (Aguilar et al., 2005, p. 806).

4.3.2 Kriging

Kriging is a geostatistical method of interpolation and is known by the acronym BLUE which stands for “Best Linear Unbiased Estimator” (Rishikeshan et al., 2014). It is a computationally intensive statistical interpolation method with a wide range of applications, including health sciences, geochemistry, and pollution modelling. Kriging relies on the assumption that the spatial correlation between sample points' distances or directions can explain the surface's variation. Predicted values are derived using a weighted average technique based on the relationship among samples, often exceeding the value ranges of the sample points. There are several types of Kriging, such as: simple, ordinary, universal, indicator, disjunctive and probability Kriging, of which: simple, ordinary and universal are linear predictors. Ordinary Kriging, a specific type of Kriging, assumes no constant mean over the data area (i.e., no trend).

Kriging uses the semivariogram, which measures the average degree of dissimilarity between unsampled values and nearby values, to define the weights that determine the contribution of each data point to the prediction of new values at unsampled locations. Kriging requires a user with geostatistical knowledge to consider the autocorrelation structures of elevation for defining optimal weights (Krivoruchko and Gotway, 2004; Erdogan, 2009, p. 368; Arun, 2013, p. 138; ESRI, 2023).

4.3.3 Local Polynomial

Local polynomial interpolation fits multiple polynomials into a surface, each within specified overlapping neighbourhoods. The search neighbourhood can be configured by adjusting the size, shape, number of neighbours, and sector configuration. Local polynomial interpolation fits the specified order (zero, first, second, third and so on) polynomial using points only within the defined neighbourhood. The neighbourhoods overlap, and value used of each prediction is the value of the fitted polynomial at the centre of the neighbourhood. Local polynomial interpolation is most suitable for datasets with short-range variations (Szypuła, 2017, p. 50; ESRI, 2023).

Local polynomial interpolation relies on several assumptions; the samples were taken on a grid (samples are equally spaced apart) and that the data values within the searching neighbourhoods are normally distributed. In practice, most datasets will not conform to these assumptions, and in these cases the predicted values will be affected but not as much as the prediction standard errors (Szypuła, 2017, p. 50).

4.3.4 Natural neighbour

Natural neighbour interpolation identifies the closest subset of input samples to a query point and applies weights based on proportionate areas for interpolation. It is also known as Sibson, or “area-stealing’ interpolation Its basic properties are that it’s local, using only a subset of samples that surrounded a query point, and that interpolated heights are guaranteed to be within the range of the samples used (Rishikeshan et al., 2014, p. 667). This method, while similar to IDW, tends to work well with clustered scatter points. The overall interpolation equation in natural neighbour is analogous to that used in IDW (Childs, 2004, p. 35).

Additionally Natural neighbours is a local interpolation, and it does not infer trends and does not create peaks within the generated DEM. The natural neighbours of any point are those associated with neighbouring Voronoi (Thiessen) polygons (or pixels in a raster format map). The calculation of natural neighbour is based on a set of input points and their corresponding Voronoi diagram (You and Zhang, 2012; ESRI, 2023).

4.4 Paleo-DTMs

4.4.1 Late Bronze Age DTM

To create Late Bronze Age DTMs, various interpolated tools were employed. This diversity is essential for several reasons. Firstly, each interpolation interacts differently with the input data, producing distinct interpretations of paleo-elevation points. Secondly, it allows for comparisons among interpolated data, aiding in the identification of common features across all interpolated maps. Four distinct interpolated surfaces were generated for the Late Bronze Age.

Subsequently, past reconstructions, encompassing both urban features and natural topography, were georectified and employed as markers to discern any similarities and differences. Valuable references for this analysis include the suggested shoreline from Bony et al. (2016) around 3000 years BP and the comprehensive layout of Kition's defensive rampart outlined by Smith (2008). Despite only partial sections of the defensive structure being unearthed and recorded by Nikolaou (1976, pp. 52–63), it is reasonable to infer that this layout likely defines the absolute maximum extent of the Late Bronze Age defensive rampart.

The first reconstruction was generated using IDW, as shown in **Figure 28**. The initial IDW parameters created problematic data, particularly manifesting as a characteristic bullseye pattern west of *Bamboula*. Several IDW DTMs were produced by adjusting the power and search radius parameters, with the majority having higher power a fixed search radius proving ineffective. Despite this, the IDW with a power of 0.7 and variable search radius proved most effective. The shoreline roughly correlated in shape with the proposed shoreline by Bony et al. (2016). However, certain features such as the northerly migrating pebble beach were not evident in this reconstruction (**Fig. 18 & 19 in chapter 3)**.

Regarding archaeological features, the coastline shape matched well with the walled city's location. Temple 1 and the Workshops of *Kathari* are located above sea-level. About half of the archaeological site of *Bamboula* is above sea-level. Both sites offer a protective anchorage, with *Kathari* being the better of the two.

Table 6: Parameters for Late Bronze Age IDW DTM map.

Input Features:	Late Bronze Age Elevation
Z values field	Adjusted Elevation
Output cell size	3
Power	0.7
Search Radius	Variable

The Kriging interpolation demonstrated a distinctive sensitivity to lower-level cores (C 11 & P4: see **Fig. 26 in chapter 3**), resulting in the creation of a distinct rivulet, visually depicting a narrow channel or depression between elevated areas and those below sea-level (**Fig. 29)**. To enhance accuracy, semivariogram properties were adjusted, including the use of an Ordinary Kriging method, a lag size of 6.9 and a spherical semivariogram model (see Table 2).

The ordinary Kriging assumed the constant mean is unknown, which is useful in this area of interest, namely a coastline with positive and negative elevation points. The lag size allows for the adjustment of distance between centre points of the neighbouring bins in the semivariogram analysis. The Spherical semivariogram model allow for a decrease (or in other cases an increase) in spatial correlation until some distance, beyond which autocorrelation is zeros (ESRI, 2023).

These refinements aimed to adapt the method to the specific characteristics of the data. However, despite these efforts, Kriging faced challenges due to the spatial distribution and constraint of elevation points. Sparse or uneven sampling limited its ability to accurately represent the Late Bronze Age period's terrain. Given additional and well-distributed data points may have improved the results.

Table 7: Late Bronze Age Kriging Interpolation DTM parameters.

Input Features:	Late Bronze Age Elevation
Z values field	Adjusted Elevation
Semivariogram properties	Spherical 6.908034
Output cell size	7.26825443898514
Search Radius	Variable 15

The Local Polynomial interpolation tool provided a greater degree of data manipulation, which could be problematic if not applied with caution. The maps tended to create very sharp features when no smooth search radius was applied. Some of the similar features are the sharpness between the elevation values. Attempting to smooth this data resulted in an unrealistic, eastward shoreline. The southeastern corner of the map (**Fig. 30)**, below the *Bamboula* sector, exhibited elevated surfaces above sea level due to limited default search radius settings. Different order polynomials were projected, however, only the first order polynomial produced an qualified map. This is because higher polynomials work only if there are a sufficient number of points, in which case there are not.

The First order polynomial followed the default parameter settings as seen in Table 7. All Late Bronze Age features are located above sea level, at various elevations between 3-7 m above the sea-level. The interpolation technique produced a relatively straight coastline, with a somewhat protected bay south of *Bamboula*. Although the coast is a generally well-defined feature, there are sharp elevated features off the coast to the south. This is a common attribute for all the local polynomial interpolations produced in this section and is a result of a number of factors, with the main issue being the distribution of the data points (Late Bronze Age elevation points) not being normally distributed on a grid (equally spaced apart).

Table 8: Parameters for Local Polynomial Interpolation using the first order polynomial kernel function (map in Figure 3).

Input Features:	Late Bronze Age Elevation
Z values field	Adjusted Elevation
Output cell size	7.26825
Order of polynomial	1
Search Neighborhood	NBRTYPE=Standard S_MAJOR=611.612328892591 S_MINOR=611.612328892591 ANGLE=0 NBR_MAX=15 NBR_MIN=10 SECTOR_TYPE=ONE_SECTOR
Kernal Function	Exponential
Output surface type	PREDICTION

The Natural Neighbour tool, in contrast, offers limited options for user manipulation, as it primarily relies on default parameters. The resulting Late Bronze Age DTM (**Fig. 31)** exhibits a gradual, smooth decline in elevation from west to east. This gradual slope reflects the inherent behaviour of the interpolation method, which extends the processing extent according to the provided Late Bronze Age elevation points.

In this DTM, the Late Bronze Age Temple 1 and Workshops of *Kathari* are notably situated above the shoreline at the 0 m contour level. Similarly, the Late Bronze Age wells of *Bamboula* also maintain elevations above this reference level. Although some sections of the rampart are positioned below the 0 m contour line, the general shape of the rampart closely follows the shoreline. Consequently, this DTM stands out as the most plausible representation, suggesting two viable anchorages in the coves/bays of *Kathari* and *Bamboula*. This alignment with archaeological findings enhances its credibility in terms of historical accuracy.

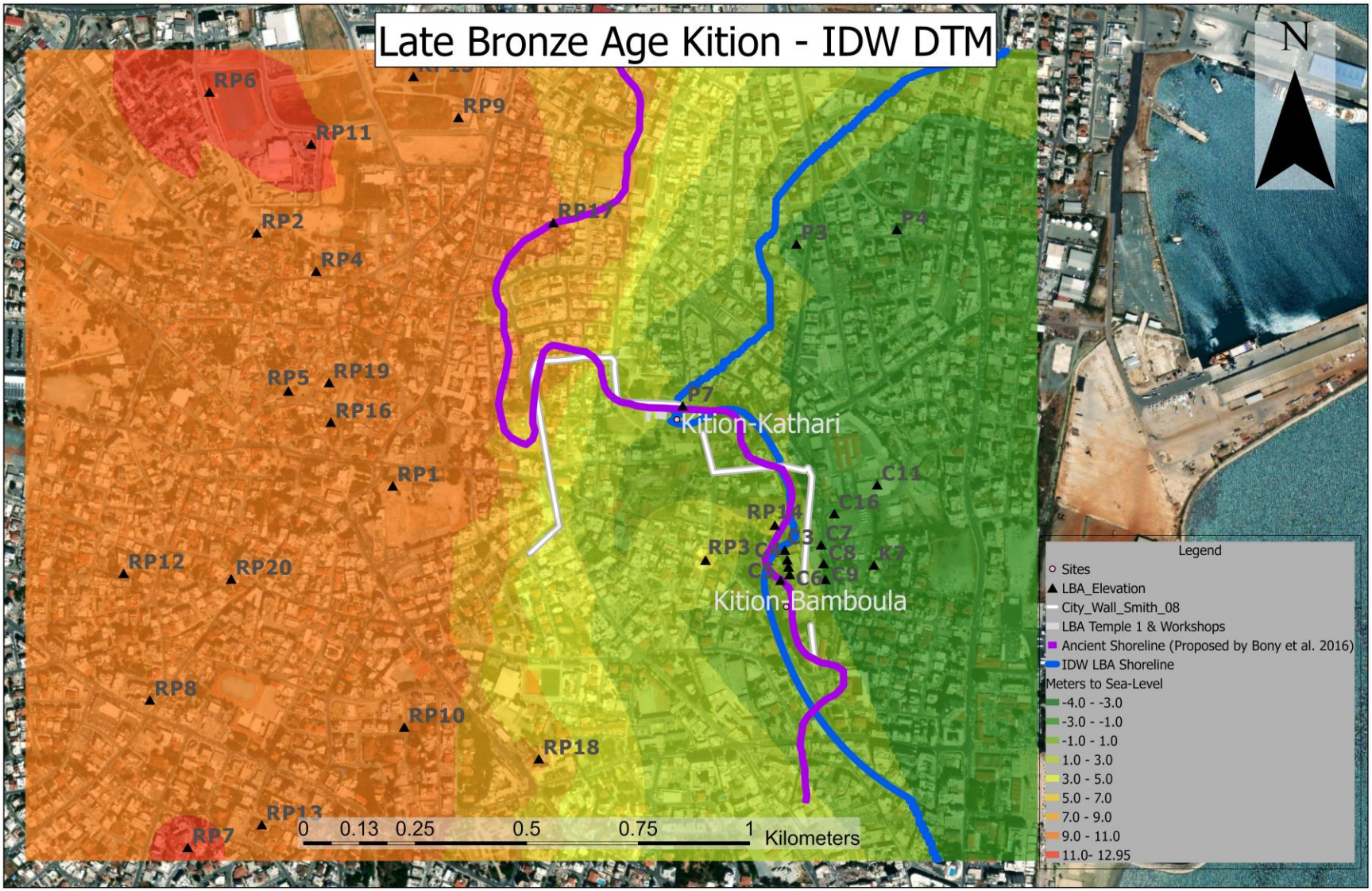

Figure 28: Late Bronze Age DTM created using IDW interpolation technique.

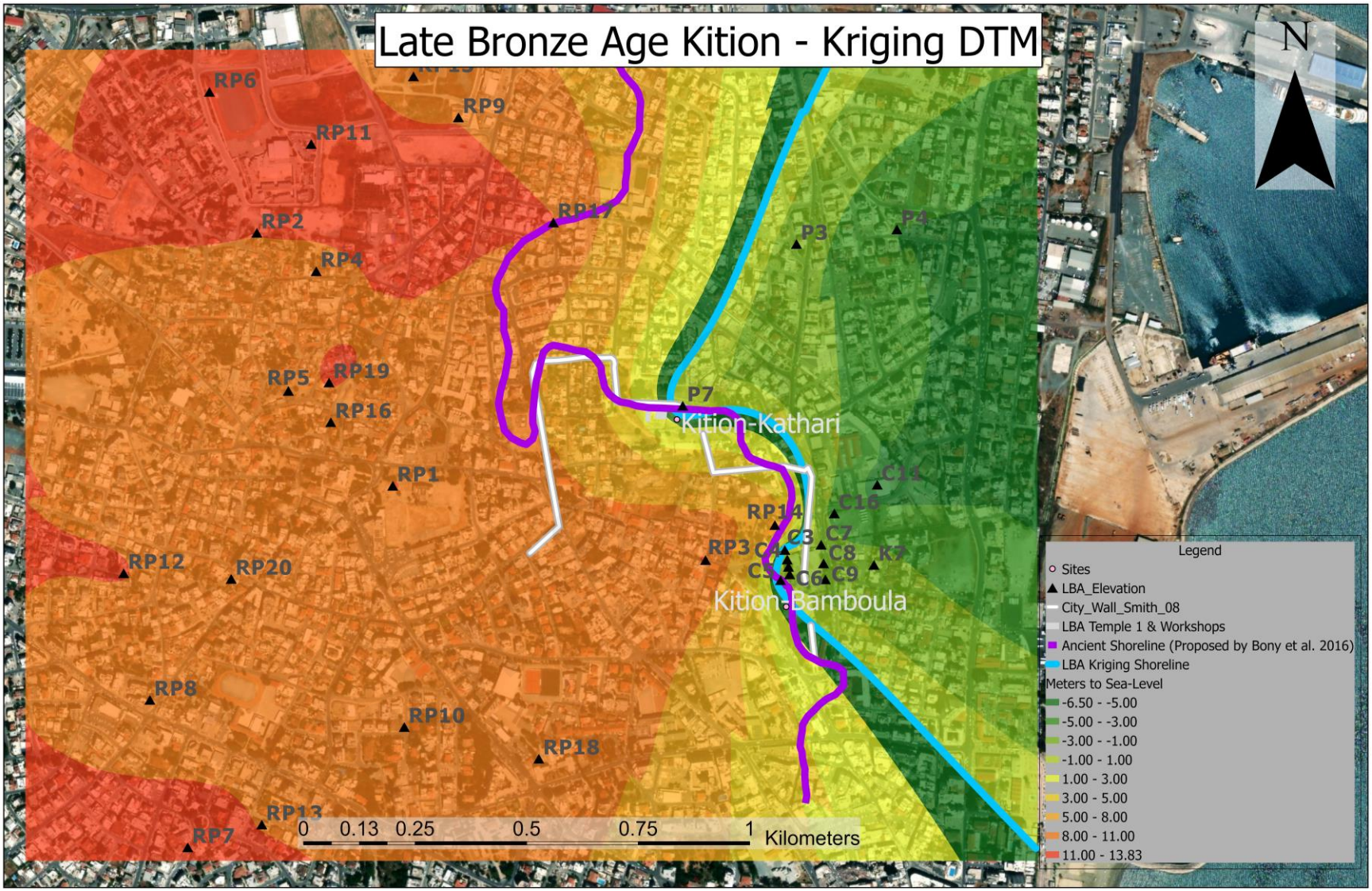

Figure 29: Late Bronze Age DTM created using Kriging interpolation technique.

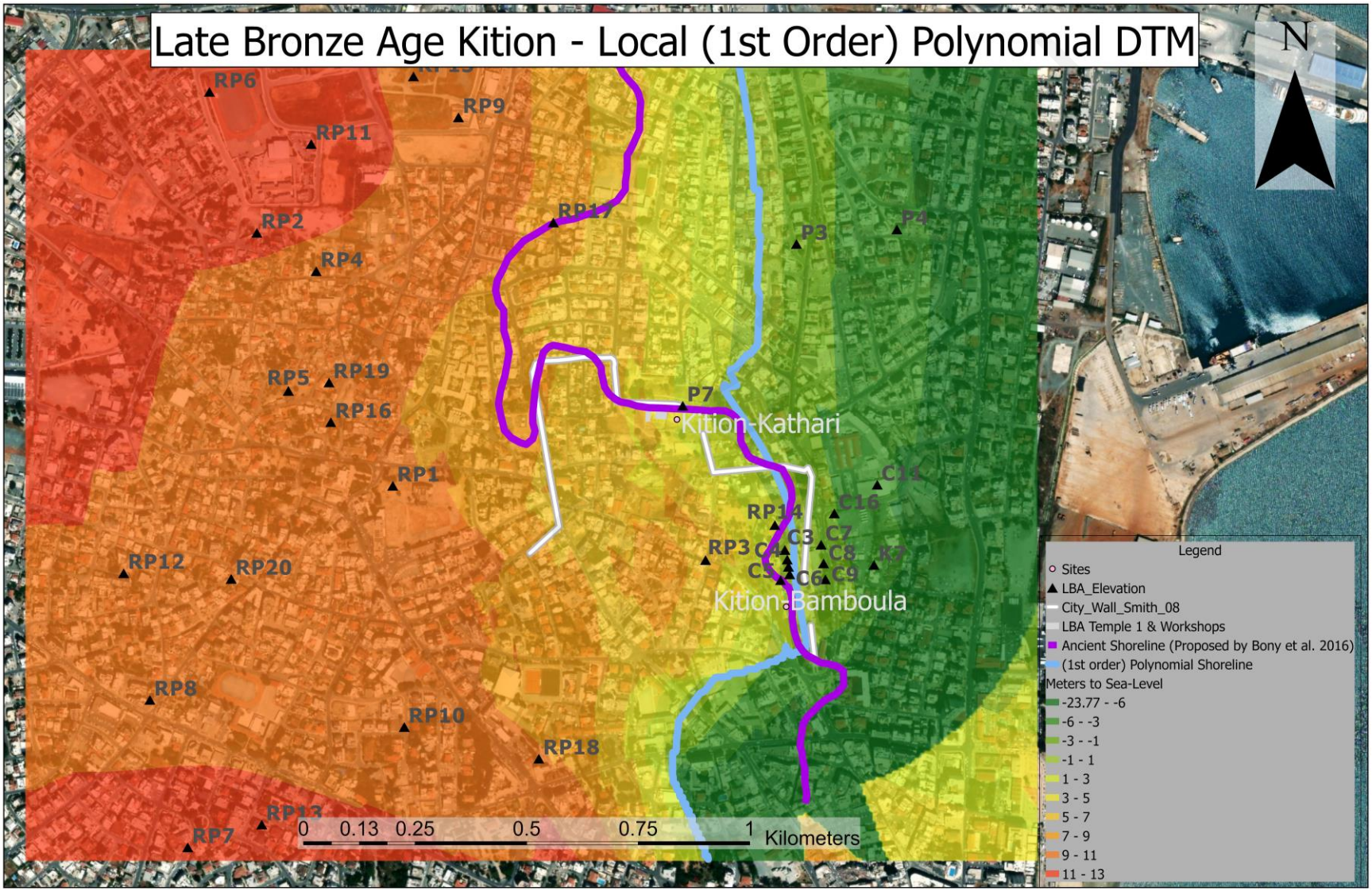

Figure 30: Late Bronze Age DTM created using local polynomial interpolation technique.

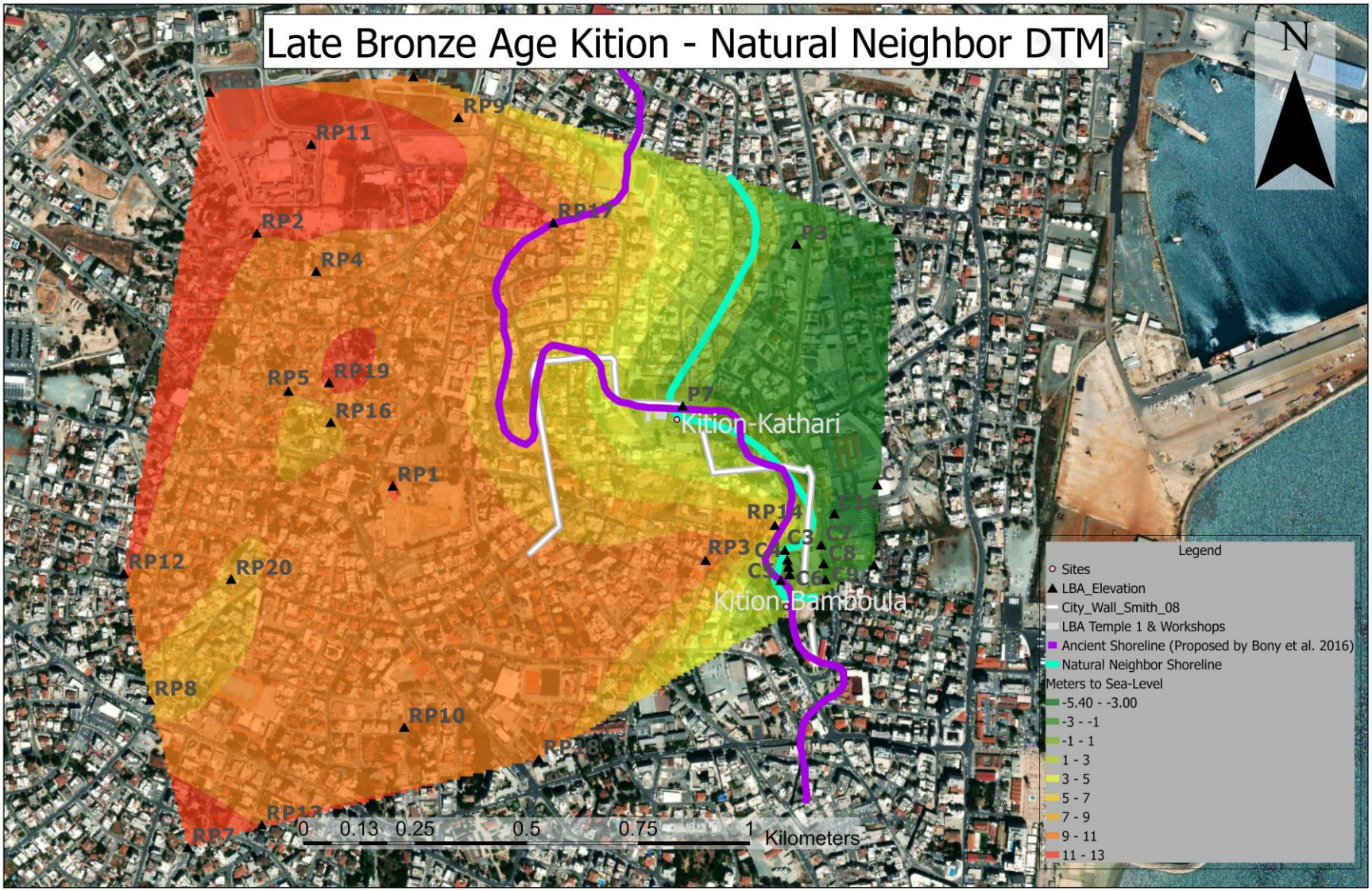

Figure 31: Late Bronze Age DTM created using Natural Neighbour interpolation technique.

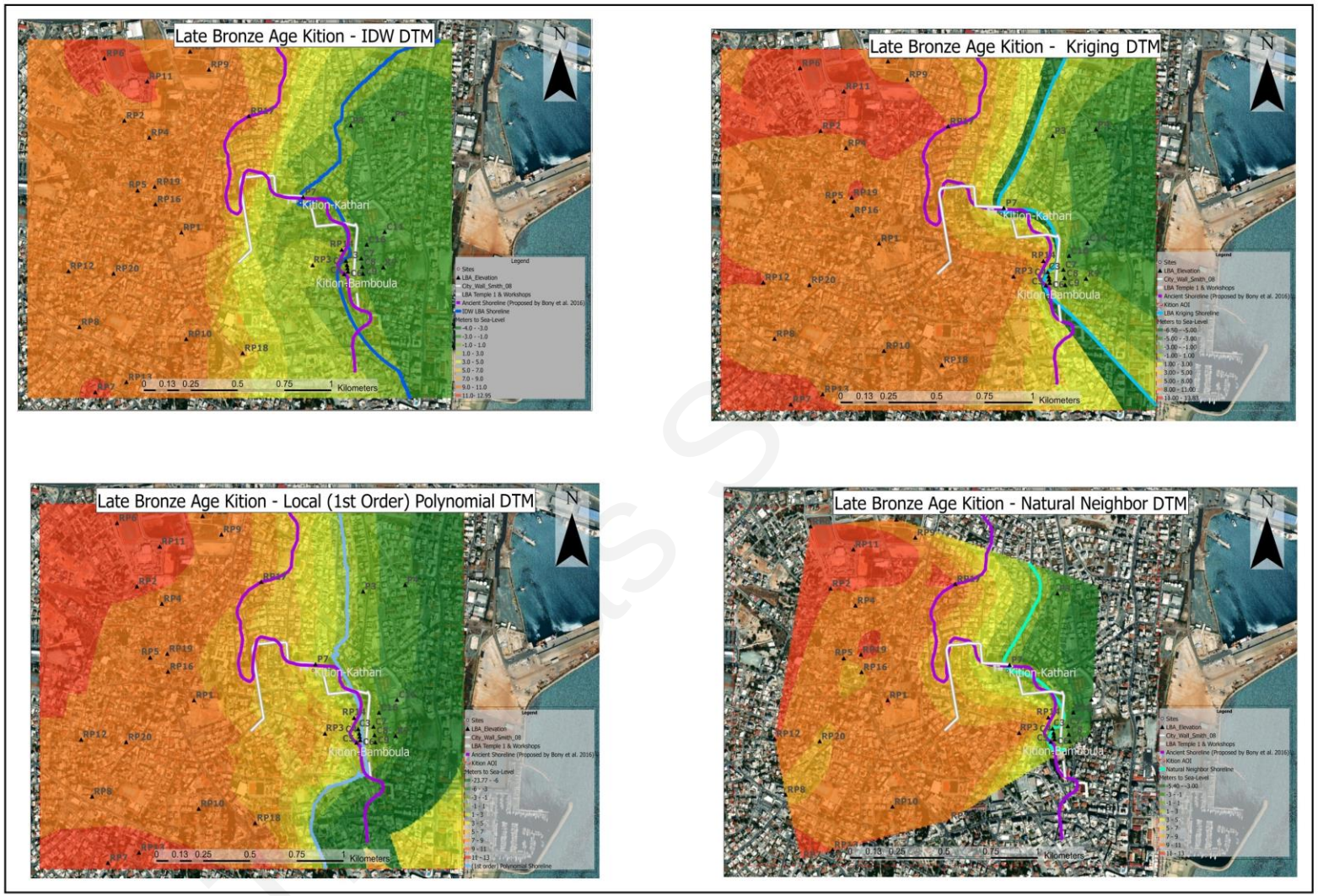

Figure 32: All interpolated DTMs for the Late Bronze Age Kition.

The interpolated DTMs in this section offer diverse insights into the palaeogeographic landscape of ancient Kition, showcasing how processing techniques and parameters affect the results. With only 35 data points and their somewhat clustered distribution, these techniques provide valuable insights when compared to one another (**Fig. 32**).

IDW and Natural Neighbour methods performed well with the clustered Late Bronze Age coring elevations, consistently depicting reliable coastal anchorages at *Kathari* and *Bamboula*. IDW extended the coastline northward in alignment with previous reconstructions. In contrast, Kriging produced a fanning-out coastline influenced by clustered Late Bronze Age coring elevations. Local Polynomial interpolation yielded a straight coastline with sharp elevation features due to uneven elevation point distribution.

The IDW interpolation method proved the most promising for realistic Late Bronze Age Kition paleogeography reconstructions. While not an exact replication of previous research, it closely aligns with prior work. The IDW DTM's shoreline shape resembles previous studies, though its exact location may vary. Notably, it identifies two small coves in *Kathari* and *Bamboula*, housing Late Bronze Age remains near the paleo-coastline. This also correlates well with the sedimentology of the coring data extracted from both sites (*Bamboula:* C 5, C 6, C 1, C 4, C 3, C 2, and *Kathari*: P7 & P 5: see **Fig. 24 & 27**) which consists of a clayey sand material with Posidonia fibers, which is indicative of an open marine bay. Consequently, the IDW DTM was chosen for the 3D reconstruction.

4.4.2 Iron Age DTM

The Iron Age elevation levels do not vary significantly from the Late Bronze Age elevations. This is due to the fact that radiocarbon dates are very close (ca. 1100 – 900 BC). The creation of the Iron Age DTMs followed the same protocol as the previous. There is not much change in the elevation between the cores, however there is the addition of core P5. P5 was originally excluded from the LBA due to its rather high elevation, however, its resemblance to the sedimentological features dated to the Iron Age of C6 is too similar to have been excluded from the Iron Age reconstruction. The paleo-shoreline proposed by Bony et al. (2016) for ca. 3000-years calibrated BP will be used again as a reference for the Iron Age DTM.

The first reconstructed DTM was generated using IDW, as shown in **Figure 33**. A number of different parameters were tested, including higher powers (1-2) which rendered much of the archaeological features of *Bamboula* below the sea level. The best parameters that maintained a reliable Iron Age DTM in regard to the Bamboula port basin and the archaeological remains are in **Table 8.**

The overall DTM created a large area of high elevation of 10 – 11.18 m above sea-level in the west of the study area, which gradually lowers to the shoreline. The IDW interpolation was effective in two regards. Firstly, all Iron Age archaeological features are located above sea-level except for the Iron Age Sanctuary of *Bamboula*. The sanctuary is located along the shoreline, with its northeastern corner reaching -0.20 m below sea level. and secondly, the presence of two small inlets located at *Kathari* and *Bamboula* attest to the capabilities of Kition having two anchorage locations.

Although the Iron Age and Late Bronze Age DTM's have similar elevation inputs and use similar parameters, there is a substantial difference between the DTMs produced. Firstly, the Iron Age coastline is more straight moving north to south, with sharpers features such as the *Kathari* anchorage. Additionally, the coastline south of *Bamboula* is less pronounced and follows a straight line.

Table 9: Parameters for Iron Age IDW DTM map.

Input Features:	Iron Age Elevation
Z values field	Adjusted Elevation
Output cell size	3
Power	0.27
Search Radius	Variable 12

The Kriging interpolation yielded a moderately effective DTM for the Iron Age (**Fig. 34**). While the parameters closely mirrored those employed for the Late Bronze Age interpolation, distinctions were introduced in the semivariogram characteristics and search radius (refer to Table 9). The lag size was maintained at 6.9. Notably, all locations, excluding Bamboula, register elevations above the shoreline.

As usual, the DTM generated a higher elevation in the west with particular elevated areas in the northwest and southwest corners of the AOI. The overall configuration of the shoreline markedly contrasts with the Late Bronze Age scenario, presenting a "C" shaped shoreline as opposed to a "W" fanned coastline. This change in shape would have definitely diminished protection to the bays at *Kathari* and *Bamboula*. Despite employing analogous parameters and similar settings, discernible differences exist between the two interpolated DTMs.

Numerous attempts were undertaken to manipulate the data for a more convincing representation of the shoreline; however, achieving a reliable map proved ineffective, culminating in the version presented below. Again, the interpolation may have produced a better DTM had there been additional and well-distributed data points may have improved the results.

Table 10: Iron Age Kriging Interpolation DTM parameters

Input Features:	Iron Age Elevation
Z values field	Adjusted Elevation
Semivariogram properties	Spherical 6.00
Output cell size	7.26825443898514
Search Radius	Variable 12

The local Polynomial interpolation of the Iron Age DTM (**Fig. 35**) provided mixed results. The interpolations' ability to experiment with its many parameters, allows for greater flexibility with the input data. This allowed for a number of changes to the parameters in order to generate a reliable DTM.

Again, the sanctuary in *Bamboula* is located along the shoreline, with its northeastern corner located below the 0 m contour. Although, all other features are located some distance from the shoreline, and work well with the DTM. The Iron Age local polynomial DTM is very similar to the Late Bronze Age. Many of the higher elevated areas are the same shape and location and the coastline follows a very similar path. However, there is a smoother more realistic island or spit feature of the coast of the Iron Age local polynomial.

One interesting feature of the DTM is the land in the southeastern corner off the coastline. This feature matches well with the growing spit identified by Morhange et al. (2000) and further reinforced by Boney et al (2016). The height of this feature is between 0-5m above sea-level. The overall coastline follows a relatively straight north – south line, with a small cove at *Kathari* and a bigger one south of *Bamboula*.

Table 11: Parameters for Local Polynomial Interpolation using the first order polynomial kernel function (map in Figure 3).

Input Features:	Iron Age Elevation
Z values field	Adjusted Elevation
Output cell size	6.00
Order of polynomial	1
Search Neighborhood	NBRTYPE=Standard S_MAJOR=550 S_ MINOR=650 ANGLE=0 NBR_MAX=20 NBR_MIN=10 SECTOR_TYPE=ONE_SECTOR
Kernal Function	Exponential
Output surface type	PREDICTION

The Natural Neighbour DTM (**Fig. 36**) did not produce a reliable DTM. The overall model created a relatively flat plateau ranging between 5 – 8 m that predominantly covers most of the DTM. The shoreline, similar to previous reconstruction, follows a wavy pattern from north to south, with both *Kathari* and *Bamboula* exhibiting possible safe anchorage points for ships.

This DTM again, places all archaeological sites, except *Bamboula*, above sea-level. Although, some parts of the site are above the shoreline, the Iron Age sanctuary is over the shoreline. The *Kathari* temples are located further from the coastline, as the diminished influence of core P 7 is presented. This contrasts with the previous Natural Neighbour DTM, where in the Late Bronze Age a more pronounced bay is present at *Kathari.* The port of *Bamboula* is similar but again, less pronounced as the Late Bronze Age Natural Neighbour DTM.

Table 12: Parameters for Iron Age Natural Neighbour DTM map.

Input Features:	IronAge_Elevation
Z values field	Adjusted Elevation
Output cell size	3
Power	0.27
Search Radius	Variable 12

Figure 37 highlights the different interpolation methods used in this section for the Iron Age DTM. Once again, the sample data in this section encountered challenges due to its low quantity and dense distribution, leading to varied effectiveness across the different interpolation methods.

Each DTM, to varying degrees, struggled to delineate a shoreline that retained all archaeological context above the shoreline. This challenge arose from the concentrated below sea-level elevations derived from coring data. The *Bamboula* Sanctuary was partially below sea-level in all examples. Presuming the continued use of the Late Bronze Age (LBA) rampart during the Iron Age, it would likely have intersected with the Iron Age shoreline in numerous areas.

The IDW and Kriging DTMs both favored *Kathari* as the primary anchorage point for the Iron Age. Conversely, the Natural Neighbor method leaned towards *Kathari* but also suggested Bamboula as a potential anchorage point. The Local Polynomial method generated a relatively straight coastline that did not strongly support either location, introducing a third potential option south of Bamboula, behind the spit.

Despite the challenges faced by each method, the Kriging interpolation emerged as the most effective for the Iron Age 3D reconstruction among the four. As with the previous interpolation, the Kriging tool also identified an open marine bay as suggested by the sedimentological interpretation (*Bamboula:* C 5, C 6, C 1, C 4, C 3, C 2, and *Kathari*: P7 & P 5: see **Fig. 24 & 27**). Additionally, the coastline aligns closely with the findings of Boney et al. (2016). While not without its drawbacks, particularly in placing the Bamboula sanctuary below sea level, the correspondence with past reconstructions is noteworthy.

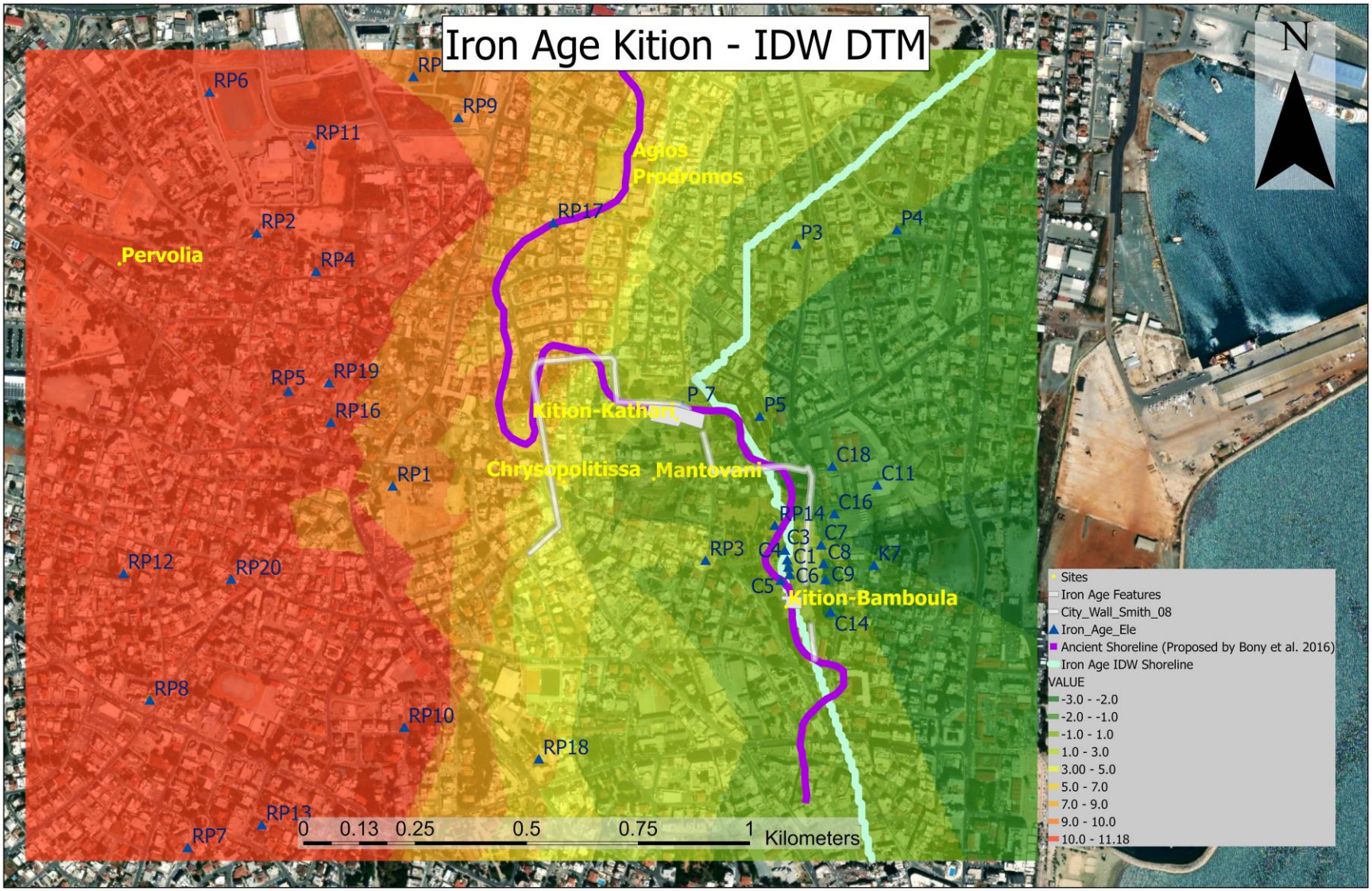

Figure 33: Iron Age DTM created using IDW interpolation technique.

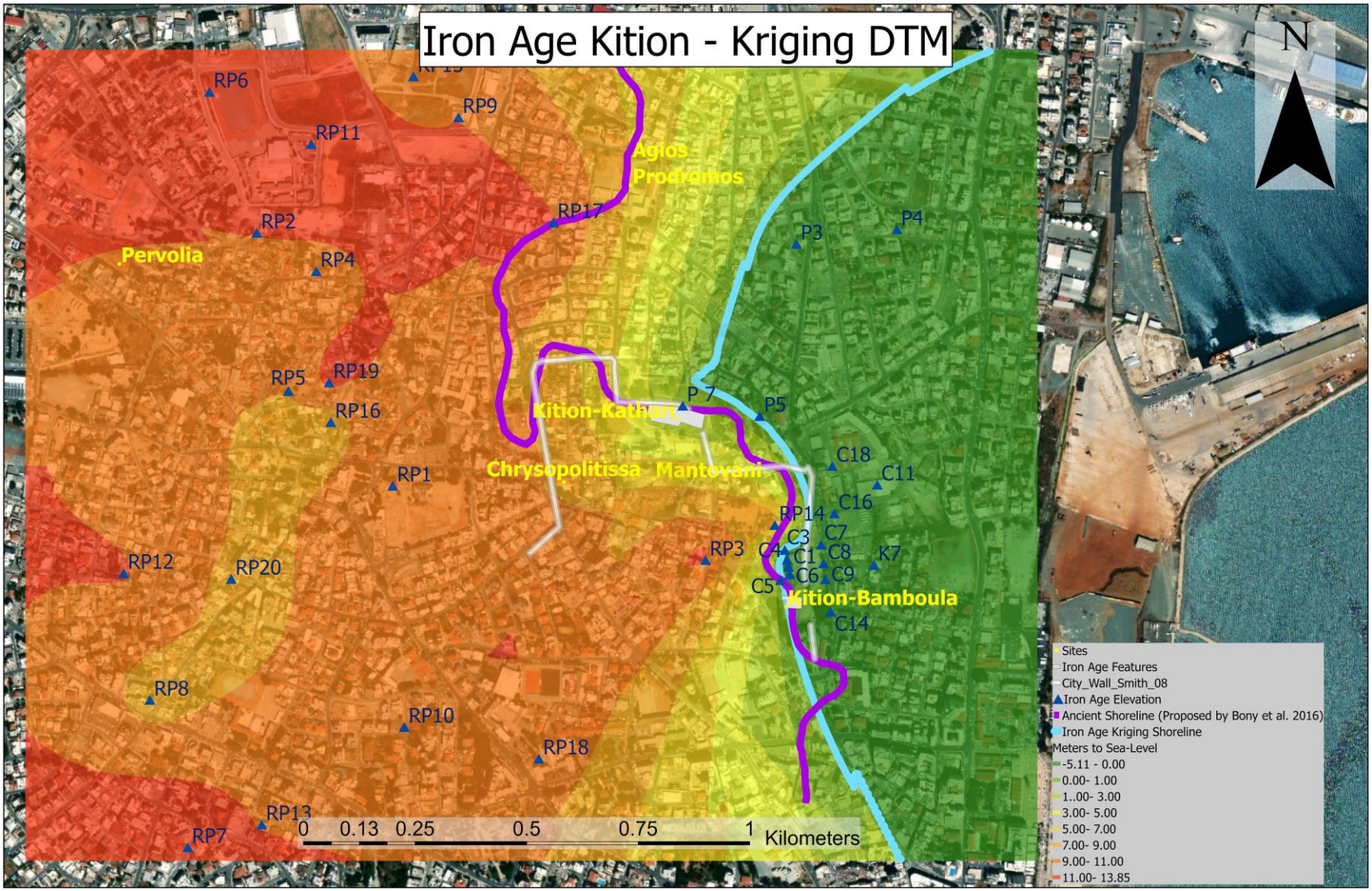

Figure 34: Iron Age DTM using the Kriging interpolation technique.

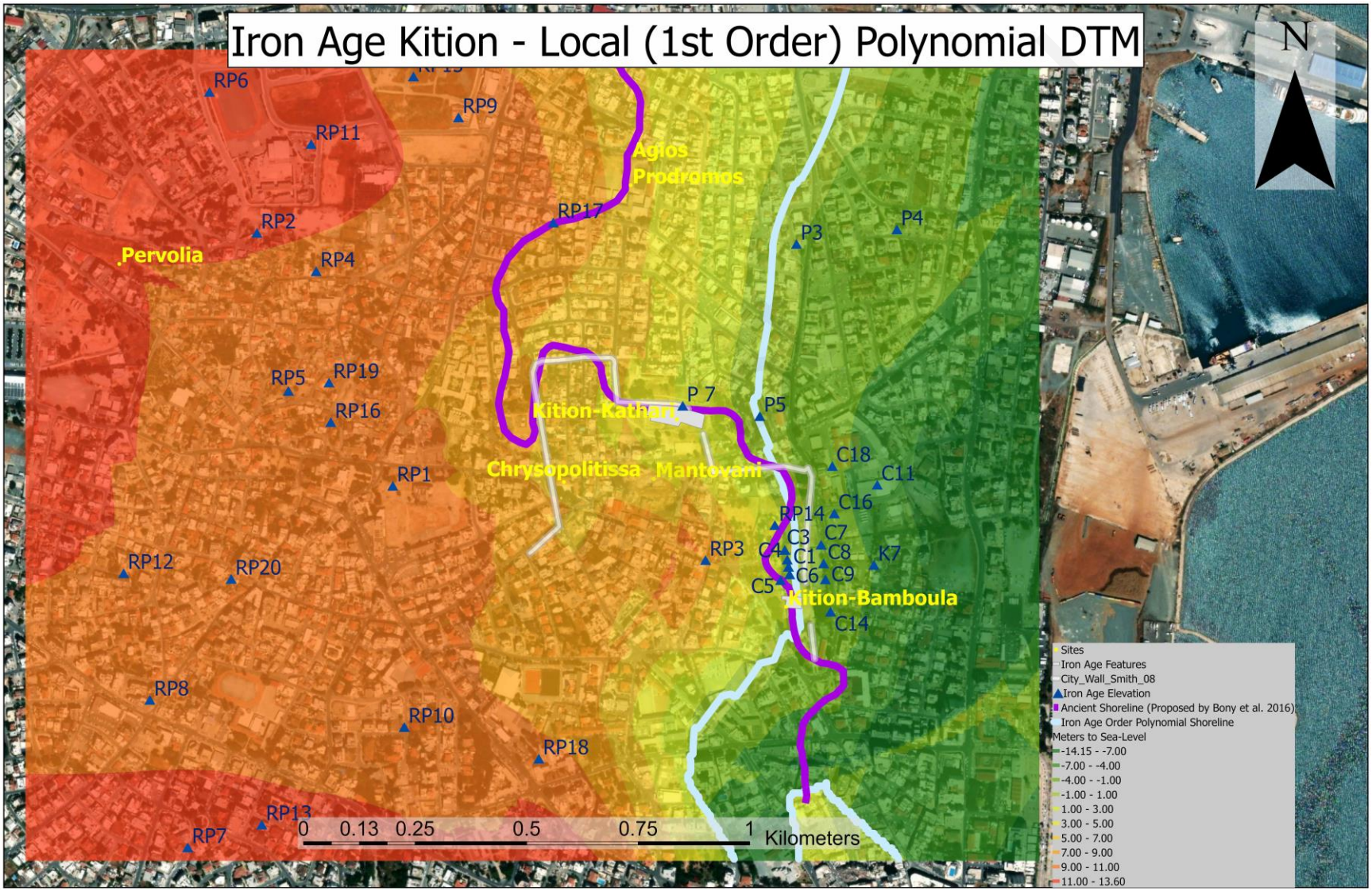

Figure 35: Iron Age DTM using the Local first Order Polynomial interpolation technique.

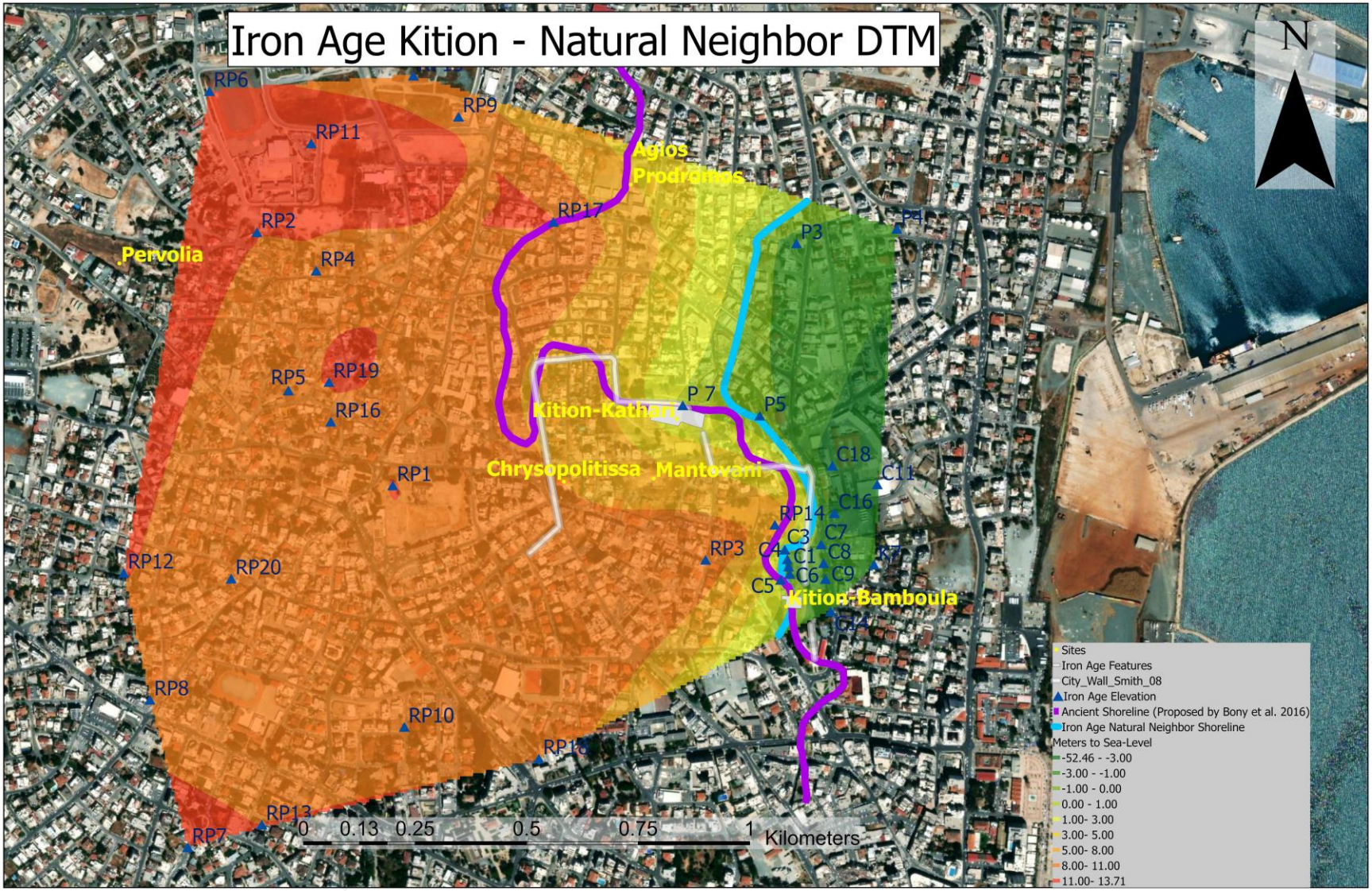

Figure 36: Iron Age DTM using the Natural Neighbor interpolation technique.

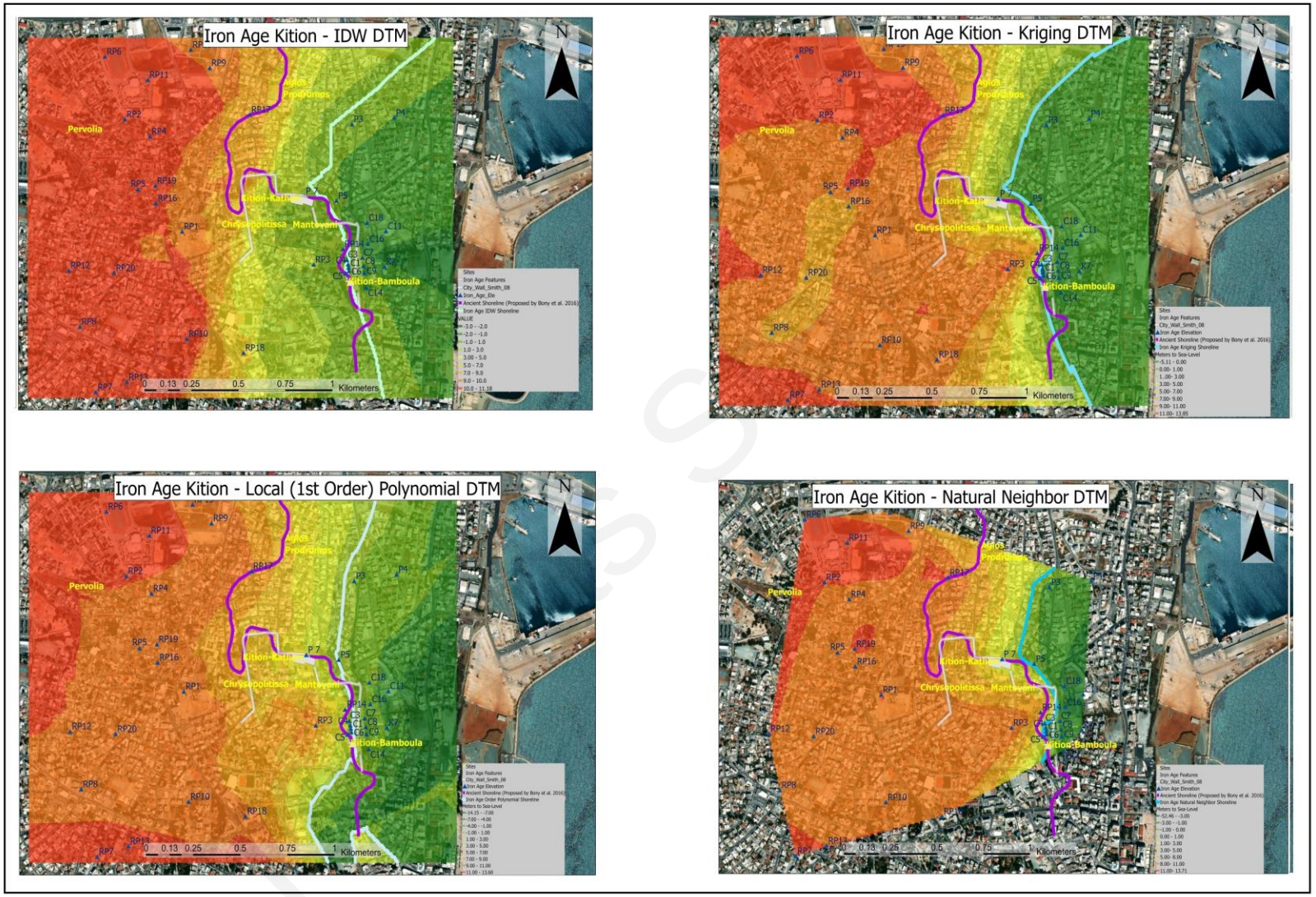

Figure 37: All interpolated DTMs for the Iron Age.

4.4.3 Classical DTM

The elevation points used for the Classical Period differ quite substantially from those of the Iron Age. The addition of the 4 points from the ship shed also enhance the accuracy of the interpolation near *Bamboula*. This is especially useful considering this is the most extensively Classical site excavated of Ancient Kition. The creation of the Classical period DTM follows the same protocol as above.

The first interpolated DTM generated for the Classical Period was with the IDW tool as seen in **Figure 38**. As usual a number of different parameters were tested, with the best suited shown in **Table 12**. The overall DTM follows a decrease in elevation from west to east, with small, scattered hills along the way to the shoreline. The shoreline itself differs from Morhange et al. (2000), with no coastal spit.

Unfortunately, there are some inconsistencies with the elevation of some of the archaeological sites. Namely, the elevation of the temple precinct of *Kathari* being located partially below the shoreline. The port of *Bamboula* was successfully generated in the DTM. The shipsheds have an ideal entrance to the open marine bay in a -1 m – -3 m below sea level elevation for ships to navigate. The over effectiveness of the additional elevation points of the shipshed is clearly visible in this DTM.

Table 13: Parameters for Classical period IDW DTM.

Input Features:	Classical Period Elevation
Z values field	Adjusted Elevation
Output cell size	7.29
Power	2
Search Radius	Variable 12

The second Classical Period DTM was generated using the Kriging interpolation tool, as shown in **Figure 39**. The parameters set are shown in **Table 13**. The overall DTM follows an increased in elevation in its northwest and southwest extremities, followed by a gradual decrease towards the coast. There are some elevated areas between *Chrysopolitissa* and *Bamboula* with an elevation between 11-13.85 m. The shoreline is somewhat similar to that of Morhange et al. (2000), in regard to the west. It differs in the identification of the coastal spit.

In terms of the archaeological context, the *Bamboula* site pairs well with this DTM. Each boat hold has direct access to the sea and the port is located within a small cove that would offer additional protection from the elements. At *Kathari* the shoreline partially touches the temple precinct, however, the fortified defensive wall would have likely protected it in this scenario.

Table 14: Classical period Kriging Interpolation DTM parameters

Input Features:	Classical Period Elevation
Z values field	Adjusted Elevation

Semivariogram properties	Spherical 6.91
Output cell size	7.26825443898514
Search Radius	Variable 12

The third interpolation technique used for the creation of the Classical period DTM of Kition was the local polynomial technique (**Figure 40**). The parameters of which are shown in Table 14. The overall DTM depicts a gradual decline in elevation from west to east, with a large hill located just north of *Bamboula*. The shoreline is jagged, with noticeable bays located east of *Kathari* and south of *Bamboula*. The shoreline has no resemblance to any previous reconstructions of the same period.

In terms of archaeological contexts, the shoreline for this DTM does follow a similar layout to the city wall but not to the suggested ports of Kition. The port of *Kathari*, is located quite far east. Regarding the ship sheds of *Bamboula*, the shoreline cuts through the eastern section, leaving 3-4 boat holds with no direct access to the sea.

Table 15: Parameters for Local Polynomial Interpolation using the first order polynomial kernel function (map in Figure 3).

Input Features:	Classical Period Elevation
Z values field	Adjusted Elevation
Output cell size	6.00
Order of polynomial	1
Search Neighborhood	NBRTYPE=Standard S_MAJOR=450 S_MINOR=650 ANGLE=0 NBR_MAX=20 NBR_MIN=10 SECTOR_TYPE=ONE_SECTOR
Kernal Function	Exponential
Output surface type	PREDICTION

The last DTM created for the Classical period used the natural neighbour interpolation tool, as shown in **Figure 41**. The parameters set are shown in **Table 15**. The overall elevation follows a gradual decrease from northwest to east. The shoreline somewhat follows previous interpretations, with the possibility of two ports: one at *Kathari* and the other at *Bamboula*. The *neosoikoi*, works well with this DTM, in which all boat holds have direct access to the sea and is located within a small cove that further protects the port.

Table 16: Parameters for Classical period Natural Neighbour DTM map.

Input Features:	Classical Period Elevation
Z values field	Adjusted Elevation
Output cell size	3

When paired together (**Fig. 42**), the different interpolations and their outcomes are noticeable. It is also evident that the benefit of the four additional elevation points added from the *neosoikoi* greatly enhanced the reconstruction of the *Bamboula* port. Unfortunately, no reconstruction was able to identify the spit. This is due to the fact that the elevation points of the cores (K 7, C 10, C11 & P 4) are still below 0, even after relative sea-level adjustments were made.

The most successful is the IDW for several reasons. Mainly the shoreline to the west, from *Bamboula* to *Kathari,* agrees with that of Morhange et al (2000) reconstruction for the Classical period. Although the interpolation was able to capture the elevated surface of the growing spit (cores K 7, C 10, C 11, P 4 in **Fig. 26)** was not possible to be identified discretely in this interpolation. Furthermore, the DTM works well with the archaeological remains of Kition. However, assuming the defensive wall was somewhat still in use, parts remain past the shoreline.

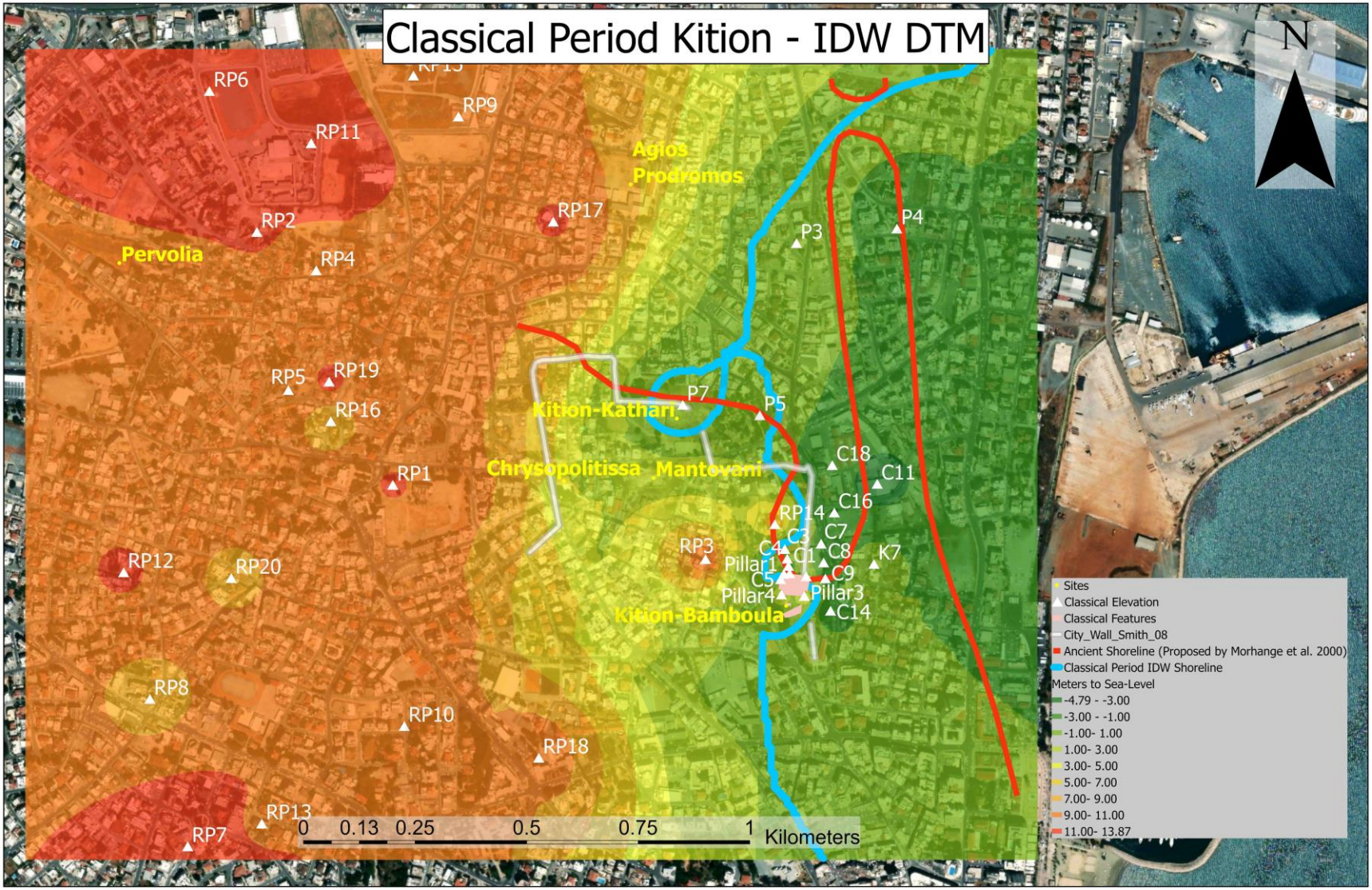

Figure 38: Classical period DTM created using IDW interpolation technique.

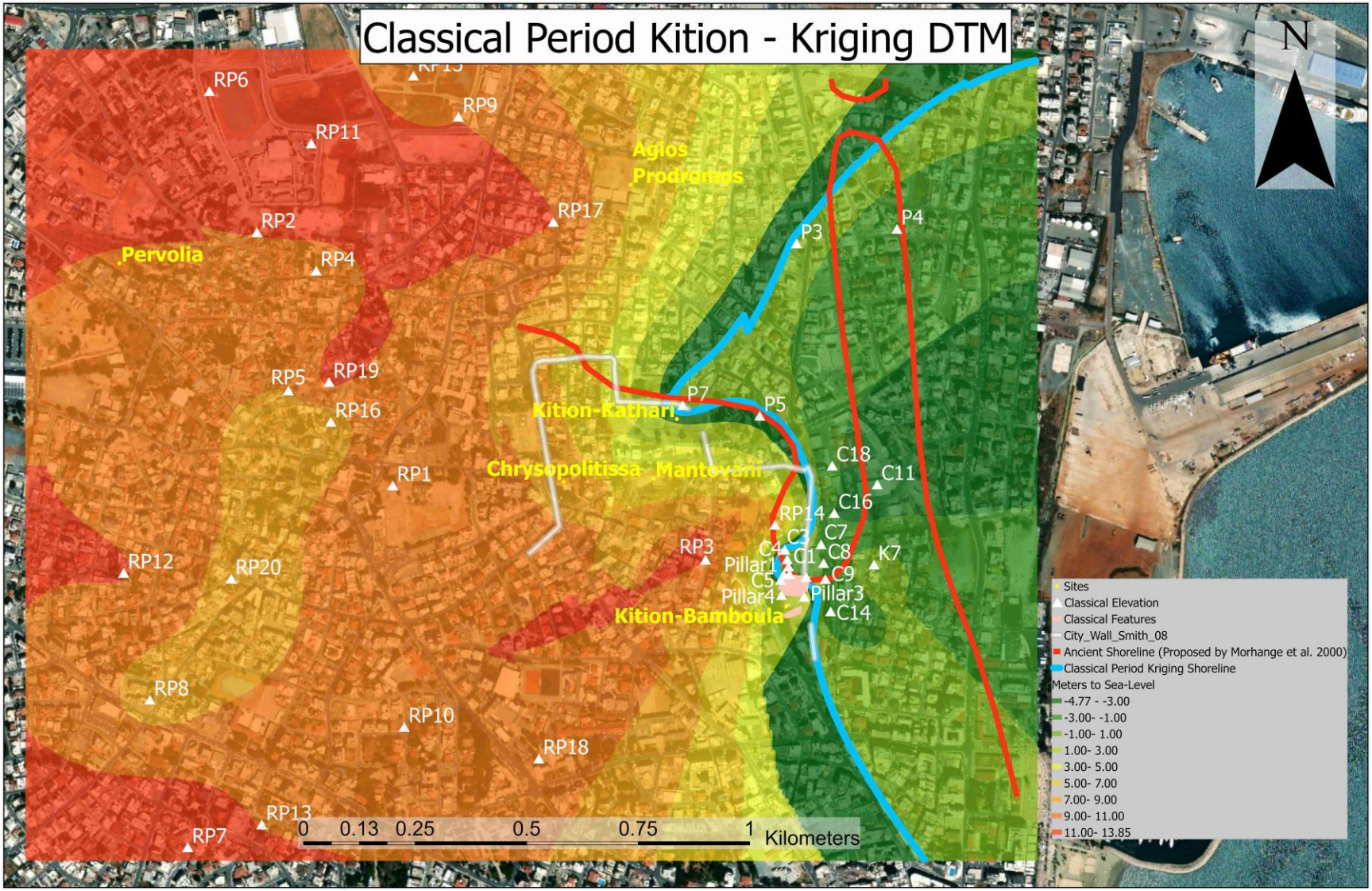

Figure 39: Classical Period DTM using the Kriging interpolation technique.

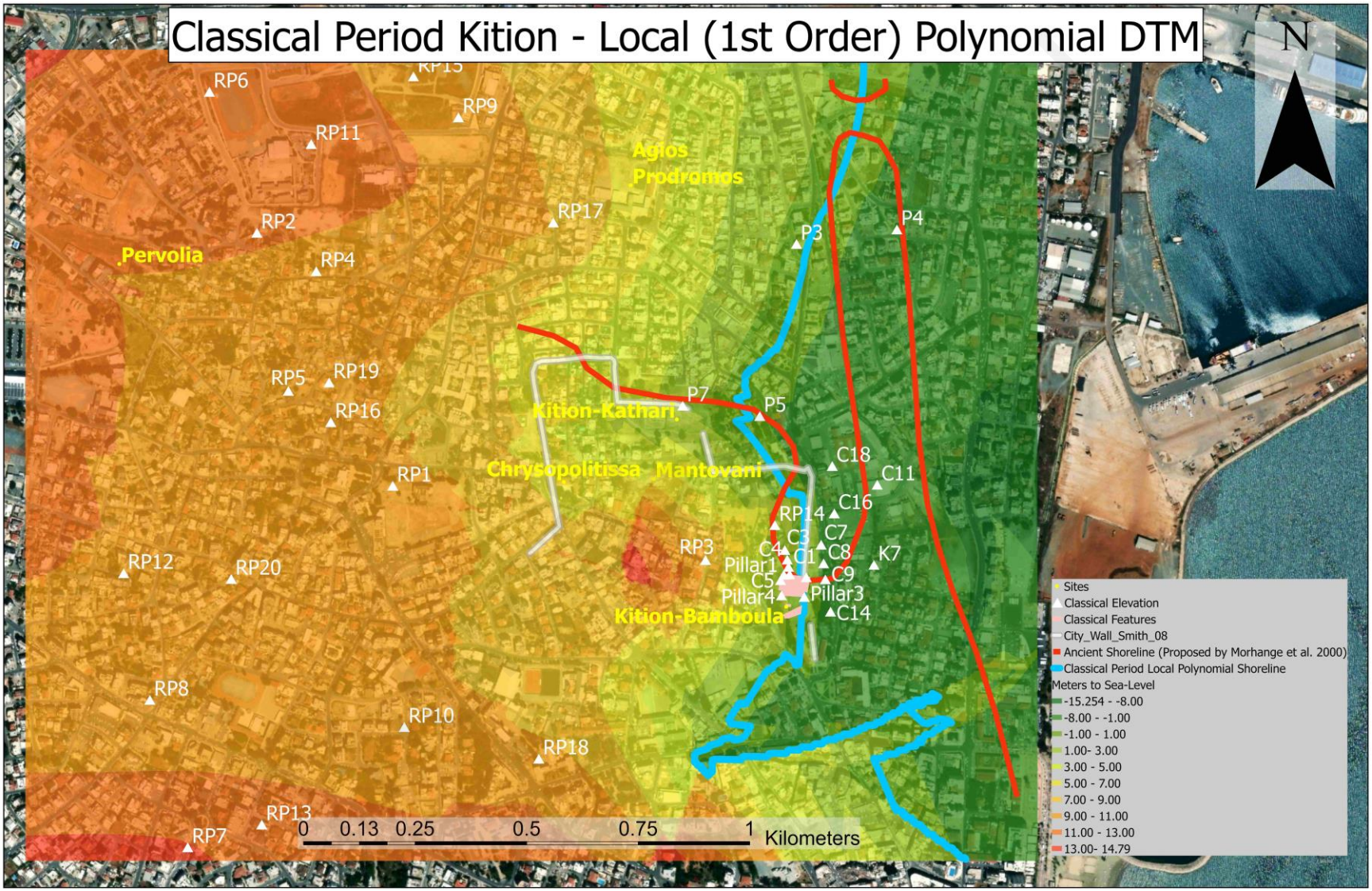

Figure 40: Classical Period DTM using the Local first Order Polynomial interpolation technique.

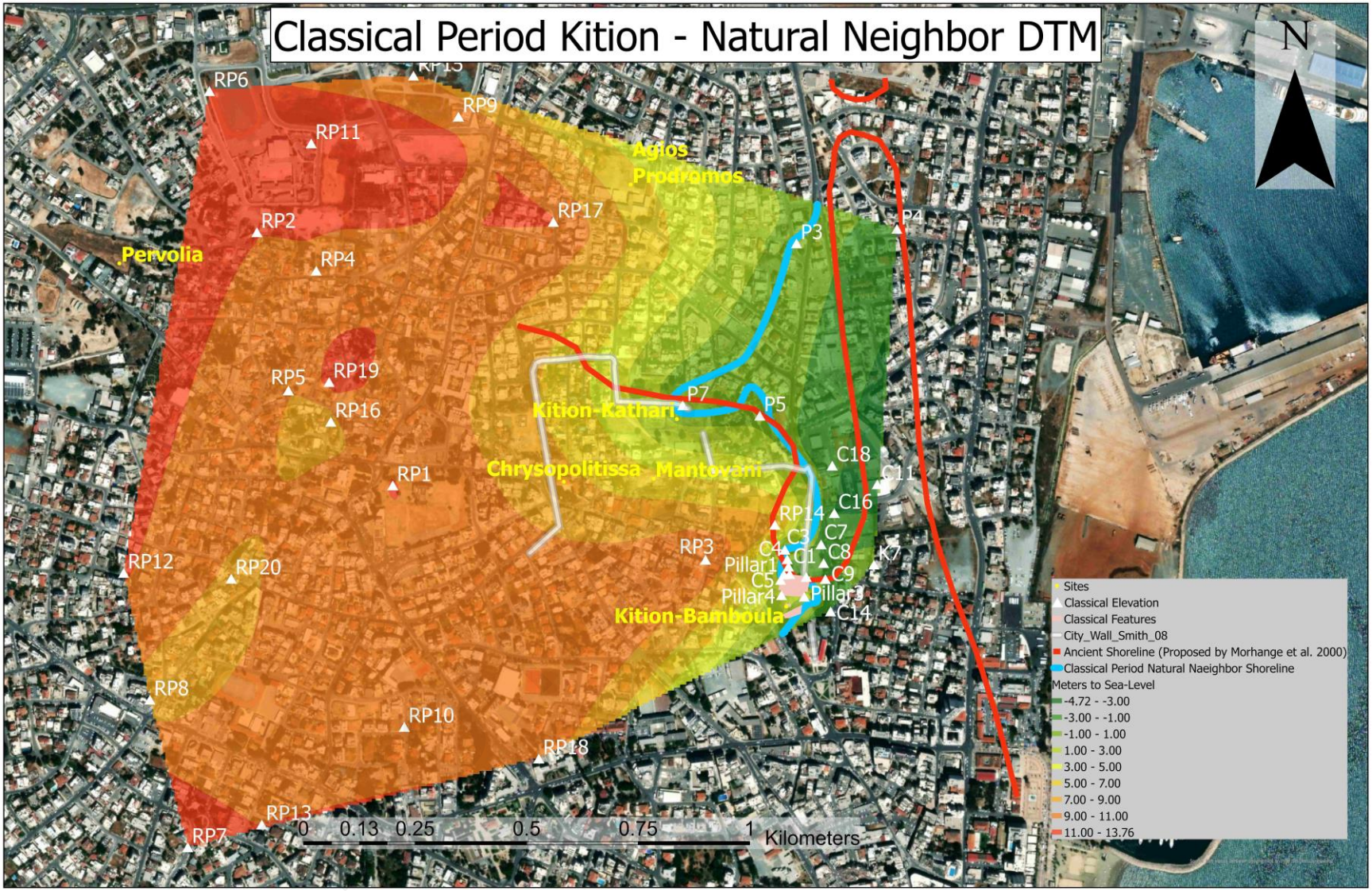

Figure 41: Classical Period DTM using the Natural Neighbor interpolation technique.

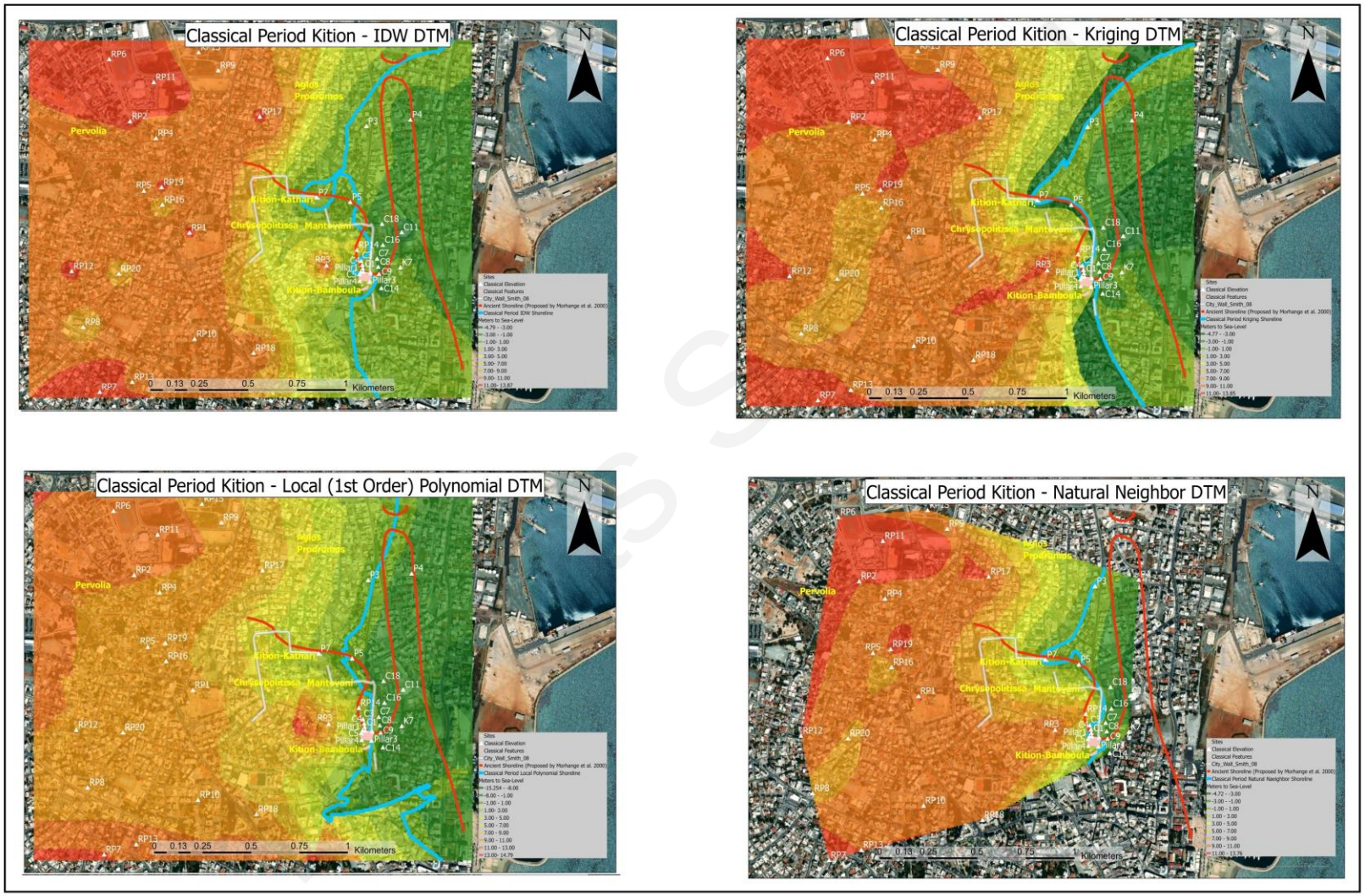

Figure 42: All Interpolated DTMs for the Classical Period.

4.4.4 Hellenistic and Roman DTM

The elevation points utilized for the Hellenistic and Roman periods exhibit only slight variations from the preceding period. The four additional points from the ship shed remain consistent, under the assumption that no significant sea-level changes occurred. While Gifford's (1978) reconstruction of the ancient harbor of Hellenistic Kition (**Fig.** 14) serves as a useful comparison, more recent works offer an enhanced understanding through the incorporation of additional cores and analytical procedures. Consequently, the shorelines of the interpolated DTMs were juxtaposed with the Classical/Hellenistic reconstruction by Morhange et al. (2000). Elevation points from two cores (K7 & P4) notably increase in elevation from the previous period, attributed to the presence of Hellenistic and Roman pottery fragments and similarities between the two cores (Refer to **Table 4** & **Figure 26**). The protocol for generating the Hellenistic and Roman period DTM aligns with that of the preceding periods.

The first DTM was created using the IDW interpolation technique (**Fig. 32**). The parameters set are in Table 16. The overall DTM follows a decrease in elevation from west to east, with small, hills in the northwest and southwest, as well as scattered hillocks along the way to the shoreline. The shoreline itself differs from Morhange et al. (2000), with no coastal prominent spit. However, a few small islands were present around cores K 7 and C 10, as well as a small spit in the northern section of the bay. A small salt lake is also captured at *Kathari*, which is reminiscent of the small bodies of water identified in Giffords (1978) reconstruction of the eastern coast of Hellenistic Kition.

There is no longer any protected cove located at *Kathari*, However the *Bamboula* port is well protected in a small cove behind the island. Other than the suggested city wall, the DTM works well with the archaeological context, particularly with the ship shed along the shoreline. The water column, however, is relatively narrow, with a maximum depth of -2.36m.

Table 17: Parameters for Hellenistic and Roman Period IDW DTM

Input Features:	Hellenistic and Roman Period Elevation
Z values field	Adjusted Elevation
Output cell size	7.29
Power	1.5
Search Radius	Variable 12

The second DTM was created using the Kriging interpolation technique, as shown in **Figure 44**. The parameters set are shown in Table 17. The overall DTM follows the similar pattern with higher elevations in the west and decreases going east. However, the due to the elevation increase of the Hellenistic and Roman elevations, the land continues eastward, creating lagoonal environment with an entrance to the sea east of core P 5.

The shoreline starts and ends along the easternmost extremity of the DTM, establishing a semi-closed environment. Both *Kathari* and *Bamboula* present viable anchorage points. While the shoreline deviates from Morhange's (2000) depiction, it suggests a comparably enclosed

environment in theory. Once again, the maximum depth of the water column is recorded at -2.37 m.

Table 18: Hellenistic and Roman Period Kriging Interpolation DTM parameters

Input Features:	Hellenistic and Roman Period Elevation
Z values field	Adjusted Elevation
Semivariogram properties	Spherical 7.27
Output cell size	7.27
Search Radius	Variable 12

The third DTM was created using the local polynomial interpolation technique, as shown in **Figure 45**. The parameters set are shown in **Table 18**. The DTM differs from others, in that the highest elevation points are located around *Bamboula.* Several different parameters changes were tested, but to no avail. The DTM and the shoreline work well with the archaeological context.

The shoreline is separated into three sections, with the largest connecting Kition with the sea via a northeastern passageway. Again, both *Kathari* and *Bamboula* are both viable ports, with the later more protected within the semi-closed environment. The archaeological context works well with this DTM. The maximum water depth in the partially closed bay is -6.76 m.

Table 19: Parameters for Local Polynomial Interpolation for Hellenistic and Roman period DTM (map in Figure 3).

Input Features:	Hellenistic and Roman Period Elevation
Z values field	Adjusted Elevation
Output cell size	7.27
Order of polynomial	1
Search Neighborhood	N BRTYPE=Standard S_MAJOR=400 S_MINOR=425 ANGLE=0 NBR_MAX=12 NBR_MIN=10 SECTOR_TYPE=ONE_SECTOR
Kernal Function	Exponential
Output surface type	PREDICTION

The final Hellenistic and Roman period DTM was created using the natural neighbour interpolation technique, as shown in **Figure 46**. The parameters set are shown in **Table 19**. The DTM has high elevation points in the northwest, which gradually decreases east.

The shoreline probably best matches that of proposed by Morhange et al (2000). However, given the nature of the processing extent of natural neighbour, large sections that would be valuable are absent from the map. Overall, the DTM works well with the archaeological context. The

maximum water depth is -2.34 m, which again, is relatively shallow and would need considerable skill to navigate.

Table 20: Parameters for Hellenistic and Roman period Natural Neighbour DTM map.

Input Features:	Hellenistic and Roman Period Elevation
Z values field	Adjusted Elevation
Output cell size	3

When paired together (**Fig. 47**) the different interpolations and their outcomes are noticeable. When compared to the previous period, the elevated levels of the cores extracted from the spit location (K 7, C10, C 11 & P 4), all effected the DTM quite drastically. Both the Kriging and local polynomial techniques generated semi-closed environments, with limited access to the sea to the east. Similar observations apply to the Natural Neighbor interpolated DTM, although the extent limitation prevents a conclusive statement. The IDW interpolation did not create a semi-closed environment but did create a number of islands and spit feature that resembles to other reconstructions somewhat.

Despite the utility and insightful contributions of all the DTMs, the IDW DTM stands out as the most effective. Unlike the other interpolations, it avoids creating a semi-closed lagoonal environment. The alignment of the shoreline from *Bamboula* to *Kathari* closely corresponds to previous reconstructions and works well with the sedimentological sequence of the cores outlined in **Figure 26**. Given that much of the focus for this period centers around *Bamboula*, the accuracy of this coastal stretch holds greater value. As such, the IDW DTM will be selected for the 3D reconstruction.

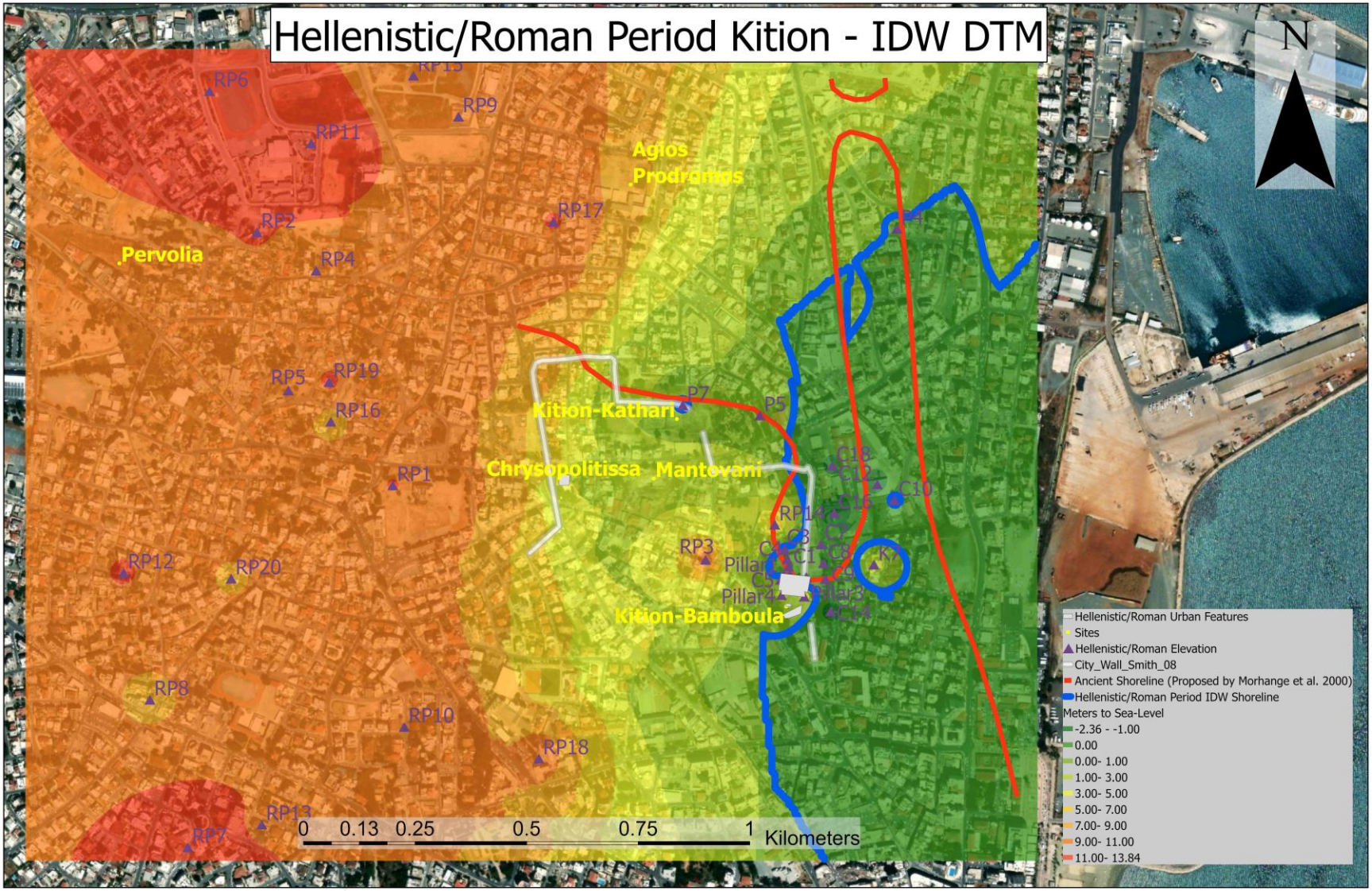

Figure 43: Hellenistic and Roman Period DTM created using IDW interpolation technique.

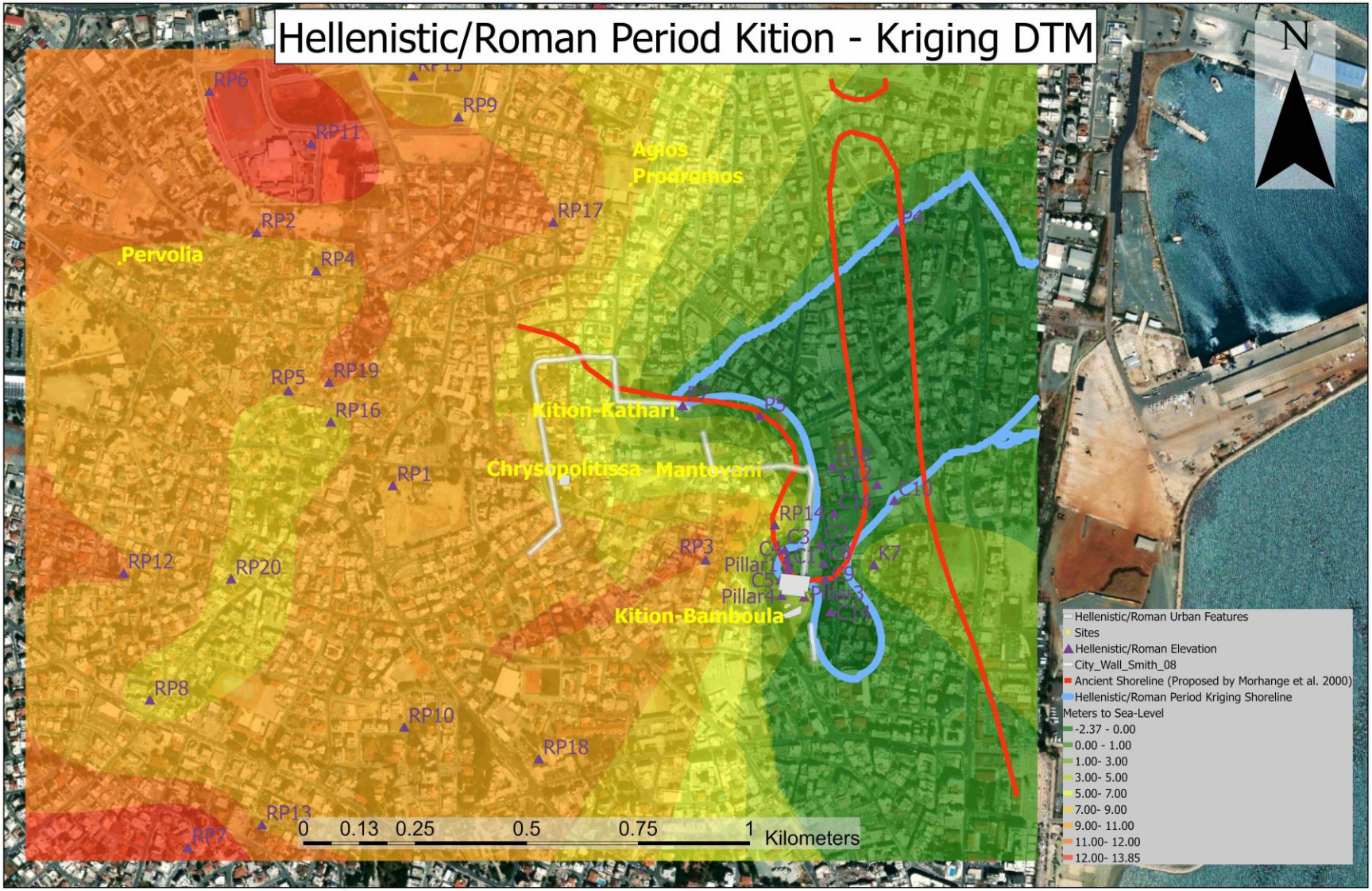

Figure 44: Hellenistic and Roman Period DTM using the Kriging interpolation technique.

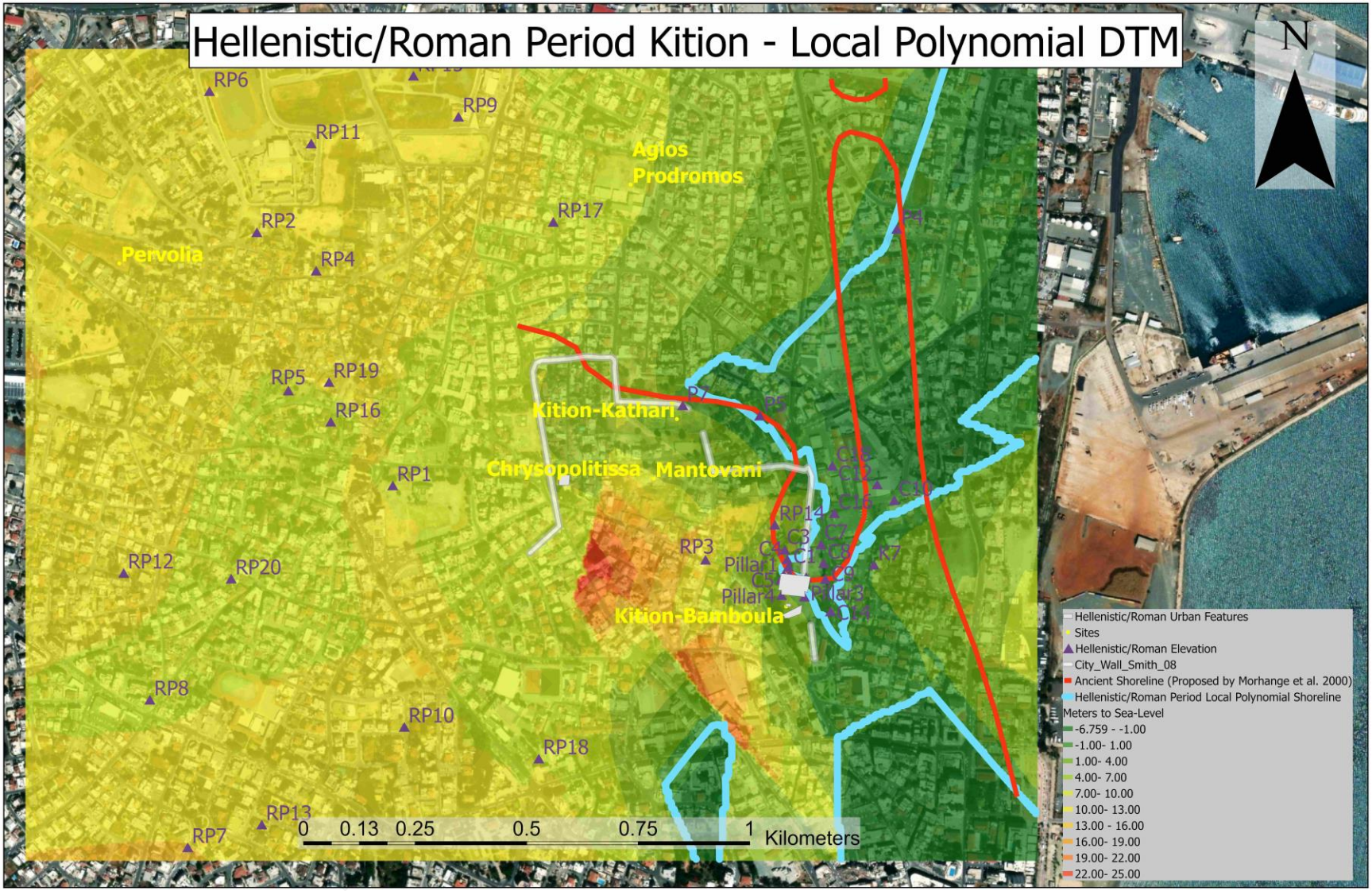

Figure 45: Hellenistic and Roman Period DTM using the local polynomial interpolation technique.

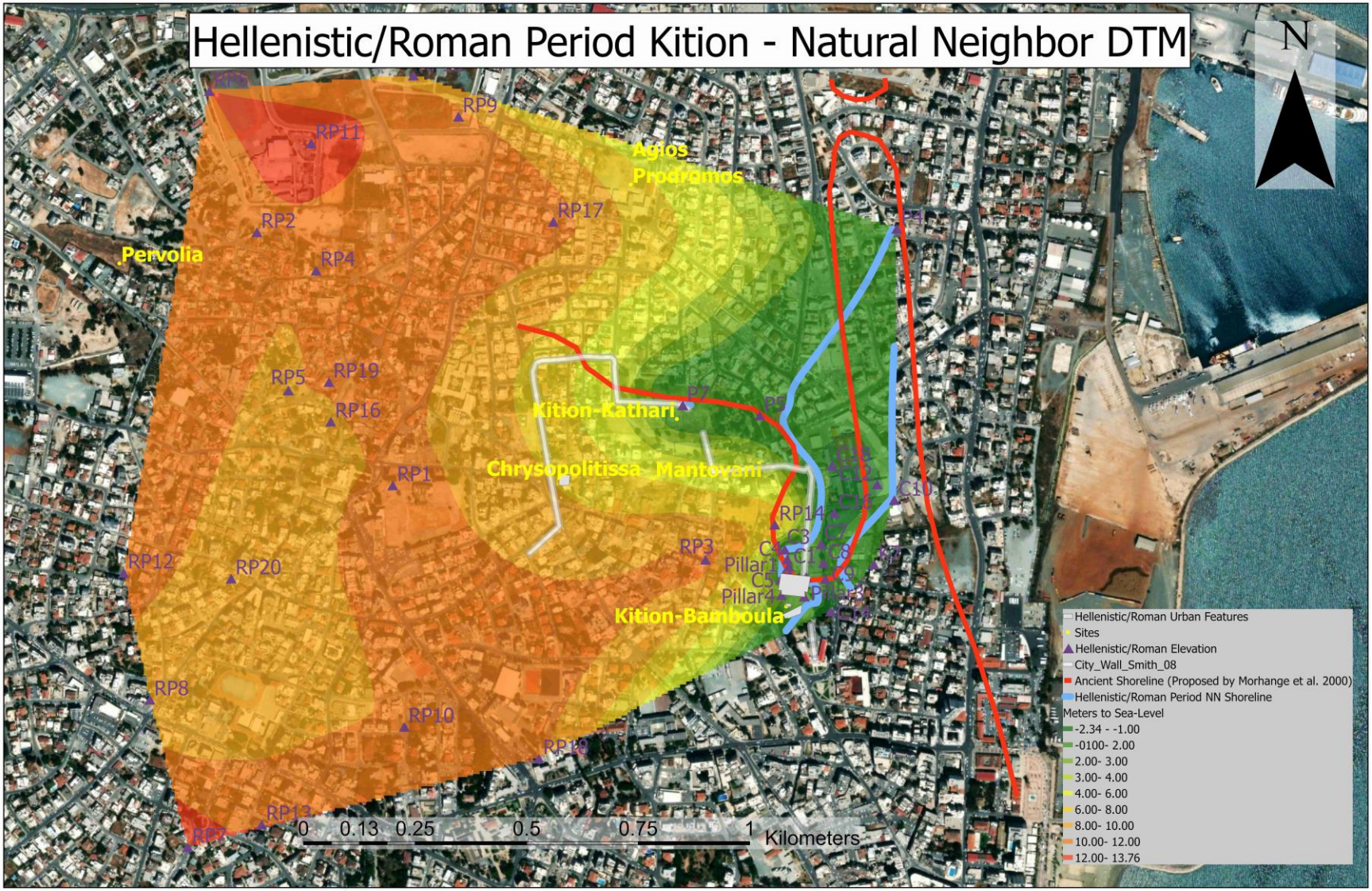

Figure 46: Hellenistic and Roman Period DTM using the Natural Neighbor interpolation technique.

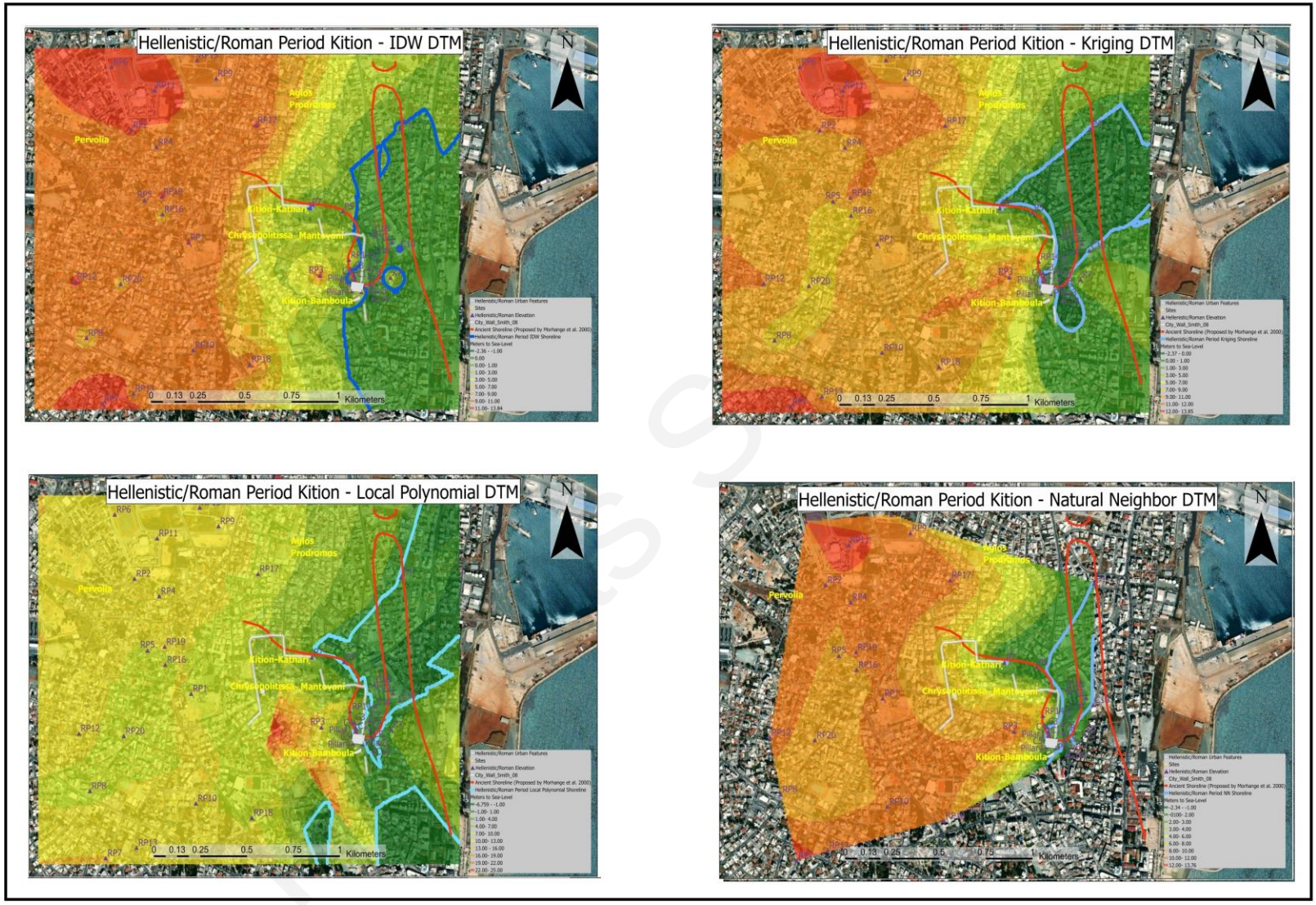

Figure 47: All interpolated DTMs for Kition during the Hellenistic and Roman Period. .

4.5 Georectification and 3D structures

To provide every urban feature documented and recorded for each historical period would take too long and is outside the scope of this thesis. In this case, only the best documented and important urban architectural features will be rendered onto the DTM's chosen for each period. Naturally, this would mean that the two areas that are of significance are the *Kathari* and the *Bamboula* sectors as they are the best documented and of importance due to their respective history as ports or access points to the sea.

The main objective of recreating these structures isn't necessarily to provide an accurate architectural depiction of each individual feature, but rather to place it in space and time within the historical period they were constructed. Each feature was georectified into ArcGIS based on excavation plans and in some cases accessed through online database (ArcGIS online).

The 3D recreations were conducted in ArcGIS Pro (ArcScene). **Table 20** highlights the key urban features chosen for each historical period. In order to add depth and dimension to the reconstructions, small houses and settlements were added in places already discussed above for each period.

Table 21: List of main archaeological features that will be 3D reconstructed with their respective date and location.

Feature	**Period:**	**Location:**
Temples 1 – 5	Late Bronze Age	*Kathari*
Workshops	Late Bronze Age	*Kathari*
Small Settlements and Wells	Late Bronze Age	*Bamboula*
Rampart	Late Bronze Age – Roman	Kition
Sanctuary	Iron Age	*Bamboula*
Temples	Iron Age	*Kathari*
Small Settlement?	Iron Age	*Kathari*
Neosoikoi (Ship sheds and Ramp)	Classical	*Bamboula*
South Building	Classical	*Bamboula*
Sanctuary	Classical	*Kathari*
Neosoikoi (Ship sheds and Ramp)	Classical/Hellenistic	*Bamboula*
Sanctaury	Classical/Hellenistic	*Bamboula*
South Building	Classical/Hellenistic	*Bamboula*
Baths	Hellenistic	*Chrysopolitissa*

5. 3D RECONSTRUCTION RESULTS

This following section highlights the results of the 3D reconstructed DTMs derived from the findings presented in the previous chapter for each historical period.

5.1 Late Bronze Age (ca. 1100-1050 BC)

An overview of Late Bronze Age Kition 3D reconstructed architectural features was performed using Inverse Weighted Distance Interpolation (**Fig. 48**). A series of temples (ca. 1125-1050 BC) were established along the city walls of *Kathari*. The defensive walls surround the northern and eastern limits and enter the sea in some areas (**Fig. 49**). Most of the archaeological remains from the Late Bronze Age are located near the *Kathari* and *Bamboula* sectors of the city. For this reason, main urban clusters of houses are concentrated in those two areas with scattered houses or farmsteads filling the rest of the area.

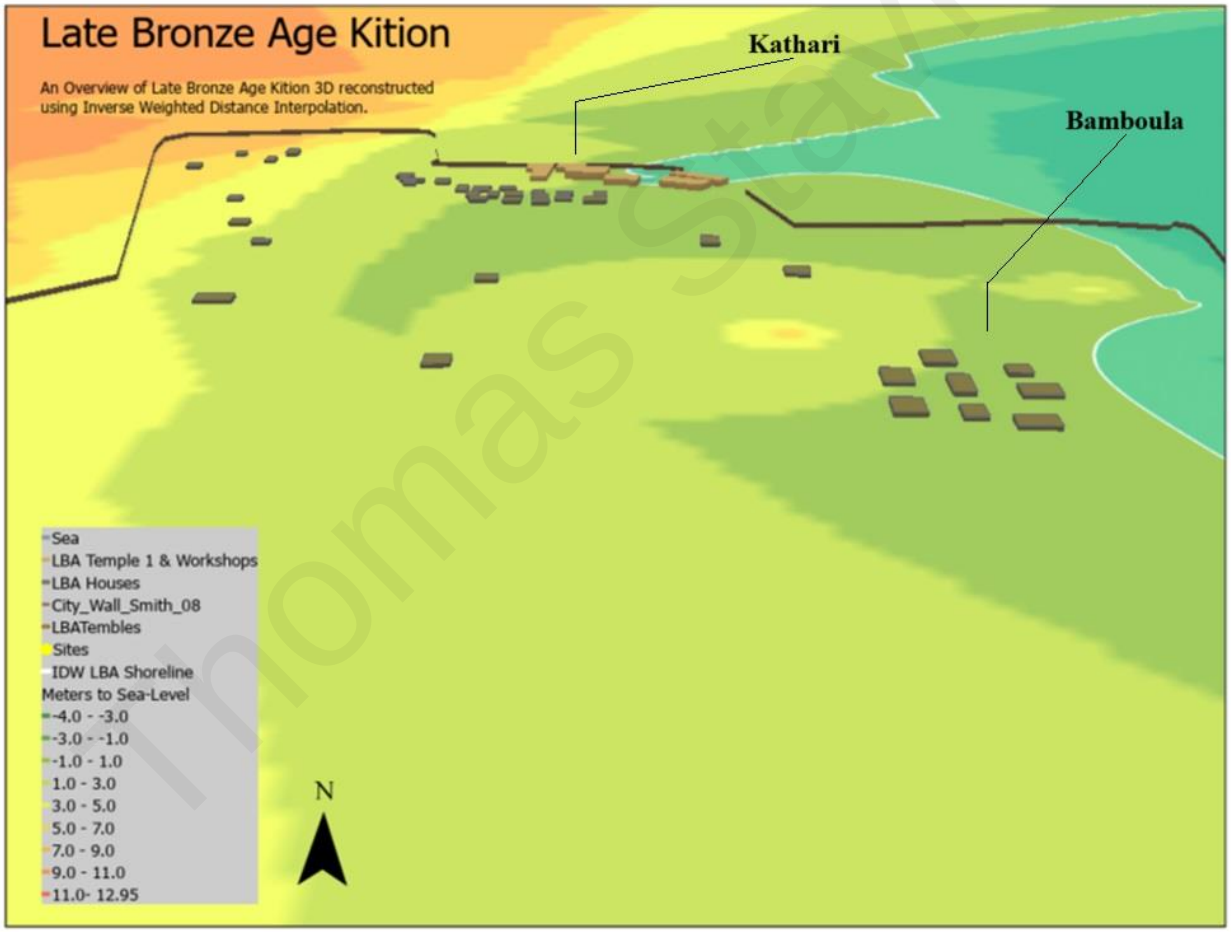

Figure 48: Overview of 3D reconstructed Late Bronze Age Kition.

Figure 49: 3D reconstructed Kition – Kathari during the Late Bronze Age.

5.2 Iron Age (ca. 850-707 BC)

An overview of Iron Age Kition 3D was reconstructed using Kriging interpolation (**Fig. 50**). Two temples dated to ca. 850-707 BC were reconstructed at the *Kathari* Sector along the city walls of *Kathari*. The overall reconstruction suits well for the *Kathari* Sector. However, the *Bamboula* sector is not well captured as the Archaic sanctuary is located in -1,00 m elevation zone. The defensive walls follow the pattern in some sections of the DTM (west and north) while being partially in the sea. Following the same principle as before, most of the archaeological remains from the Iron Age are located near the *Kathari* and *Bamboula* sectors of the city. For this reason, main urban clusters of houses are clustered in those two areas with scattered houses or farmsteads filling the rest of the area (**Fig. 51**).

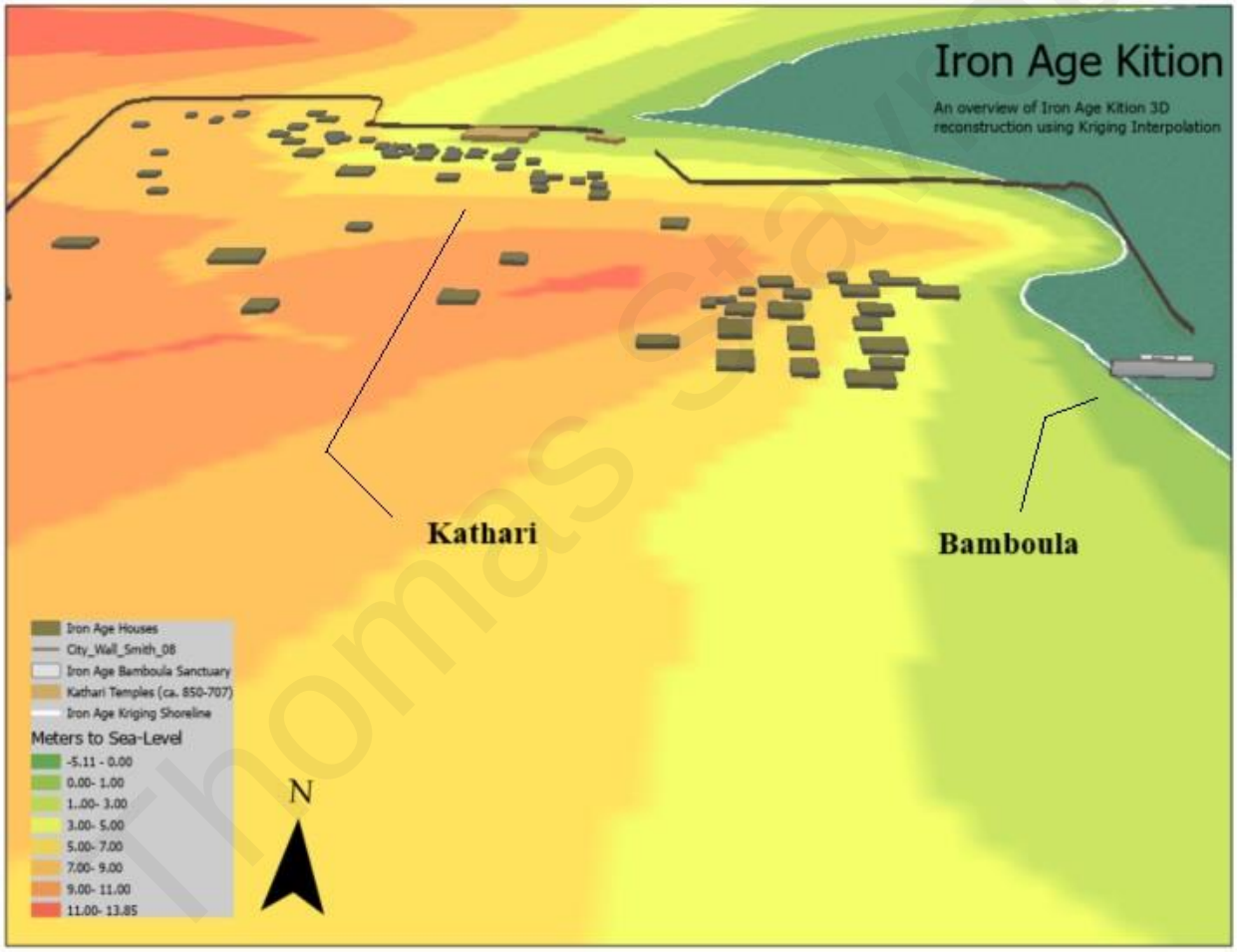

Figure 50: Overview of 3D reconstructed Iron Age Kition.

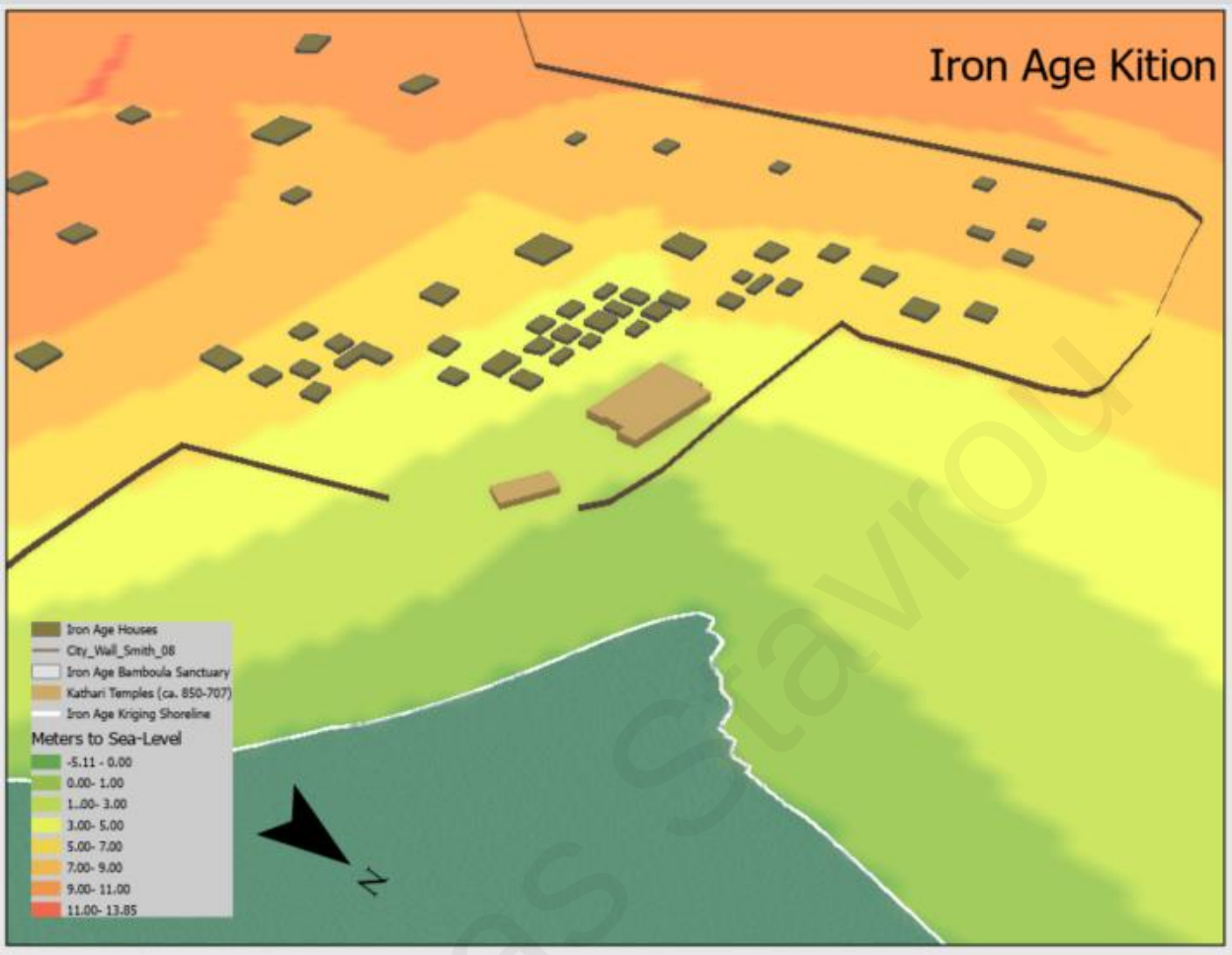

Figure 51: 3D reconstructed Kition – Kathari during the Iron Age.

5.3 Classical period (ca. 500 – 400 BC)

An overview of Classical Period Kition is presented in 3D through IDW interpolation (**Fig. 52**). The reconstruction is particularly fitting for the *Bamboula* sector, benefiting from additional points derived from the foundation of the *neosoikoi* pillar bases. Defensive walls exhibit a discernible pattern in certain DTM sections (west and north) while partially extending into the sea. Given the archaeological evidence of prosperity during the Classical Period, the reconstruction reflects an increase in houses compared to the preceding era. Subsequently, the majority of archaeological remnants from the Classical period are concentrated around *Bamboula* (**Fig. 53**).

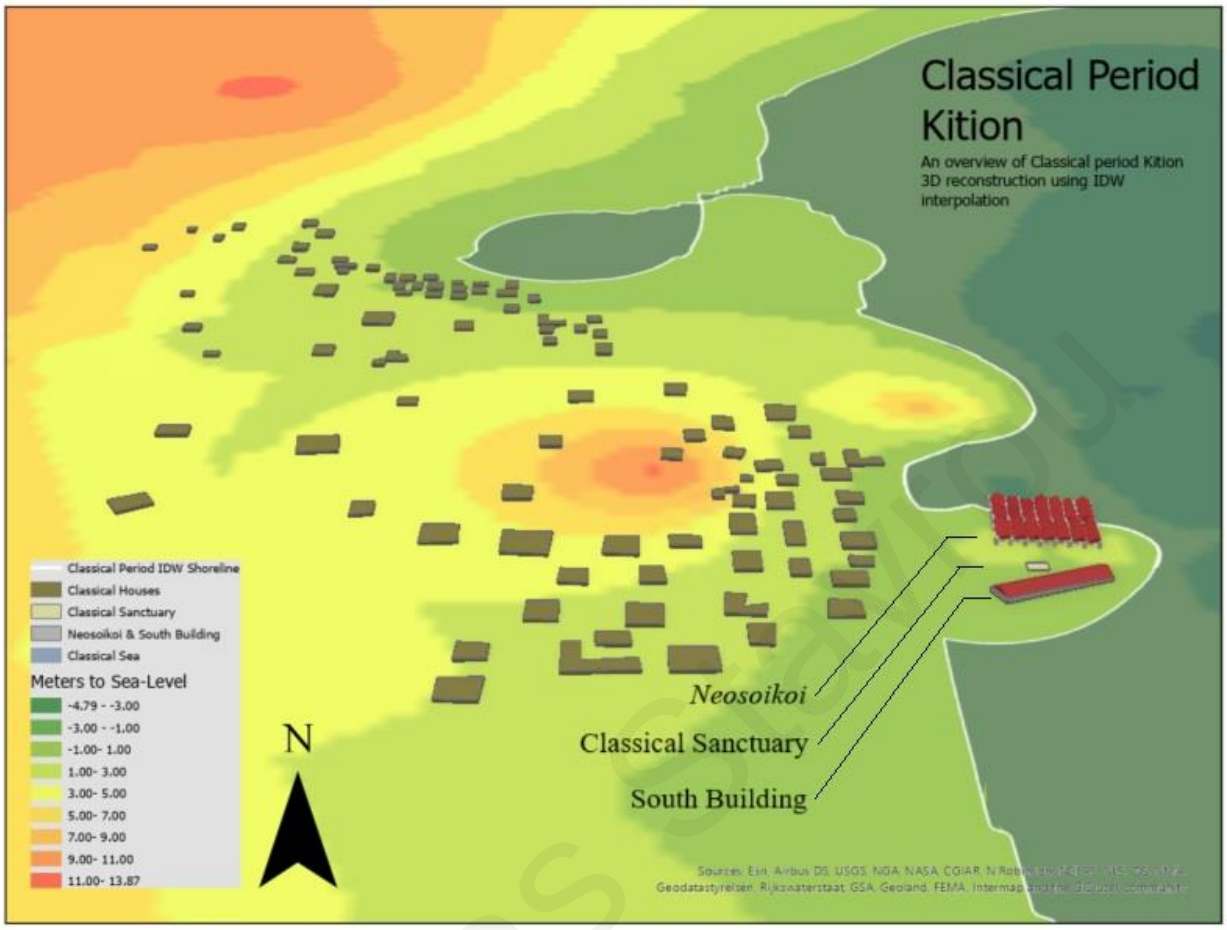

Figure 52:Overview of 3D reconstructed Classical period Kition.

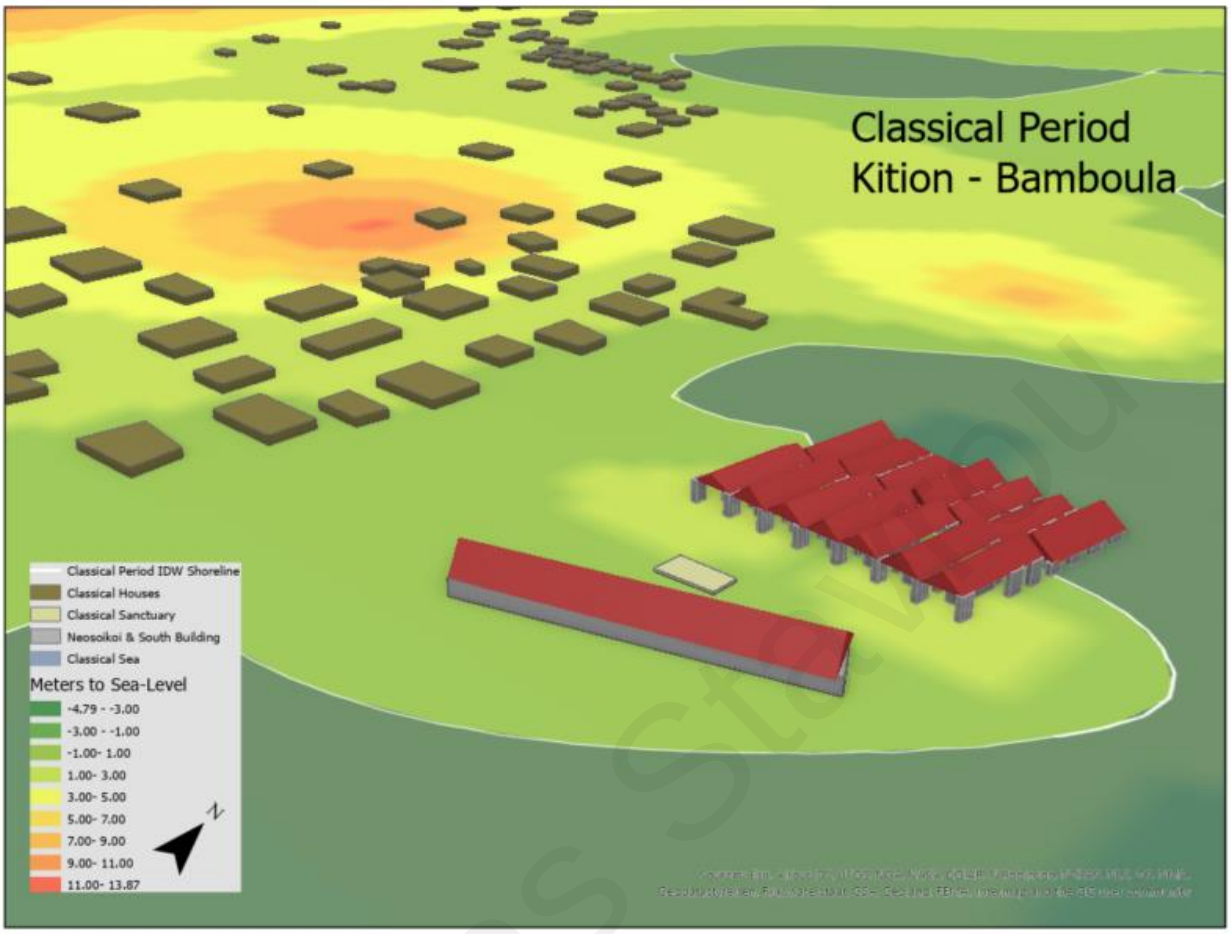

Figure 53: 3D reconstructed Kition – Bamboula during the Classical Period.

5.4 Hellenistic and Roman period (ca. 3rd to 1st century BC)

An overview of Kition during the Hellenistic and Roman period is presented in 3D through IDW interpolation (**Fig. 52**). Again, the reconstruction is particularly fitting for the *Bamboula* sector, benefiting from additional points. Due to the archaeological remains, suggesting a decline in urban prosperity, the portrayal of this is done by removing much of the settlement features. Again, *Bamboula* serves as the main 3d reconstructed feature, with the addition of the Roman baths from *Chrysopolitissa* (**Fig. 53**).

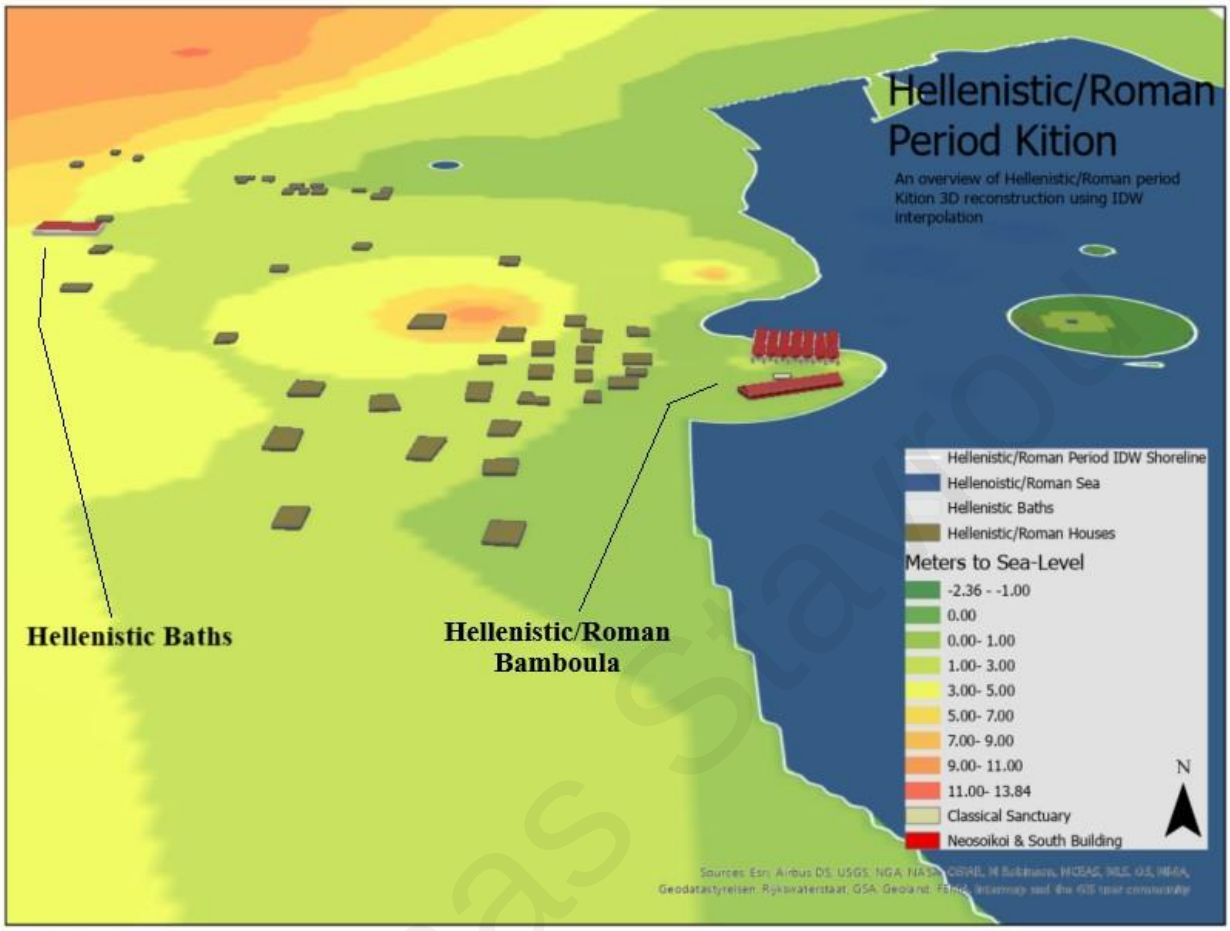

Figure 54:Overview of 3D reconstructed Kition during the Hellenistic and Roman period.

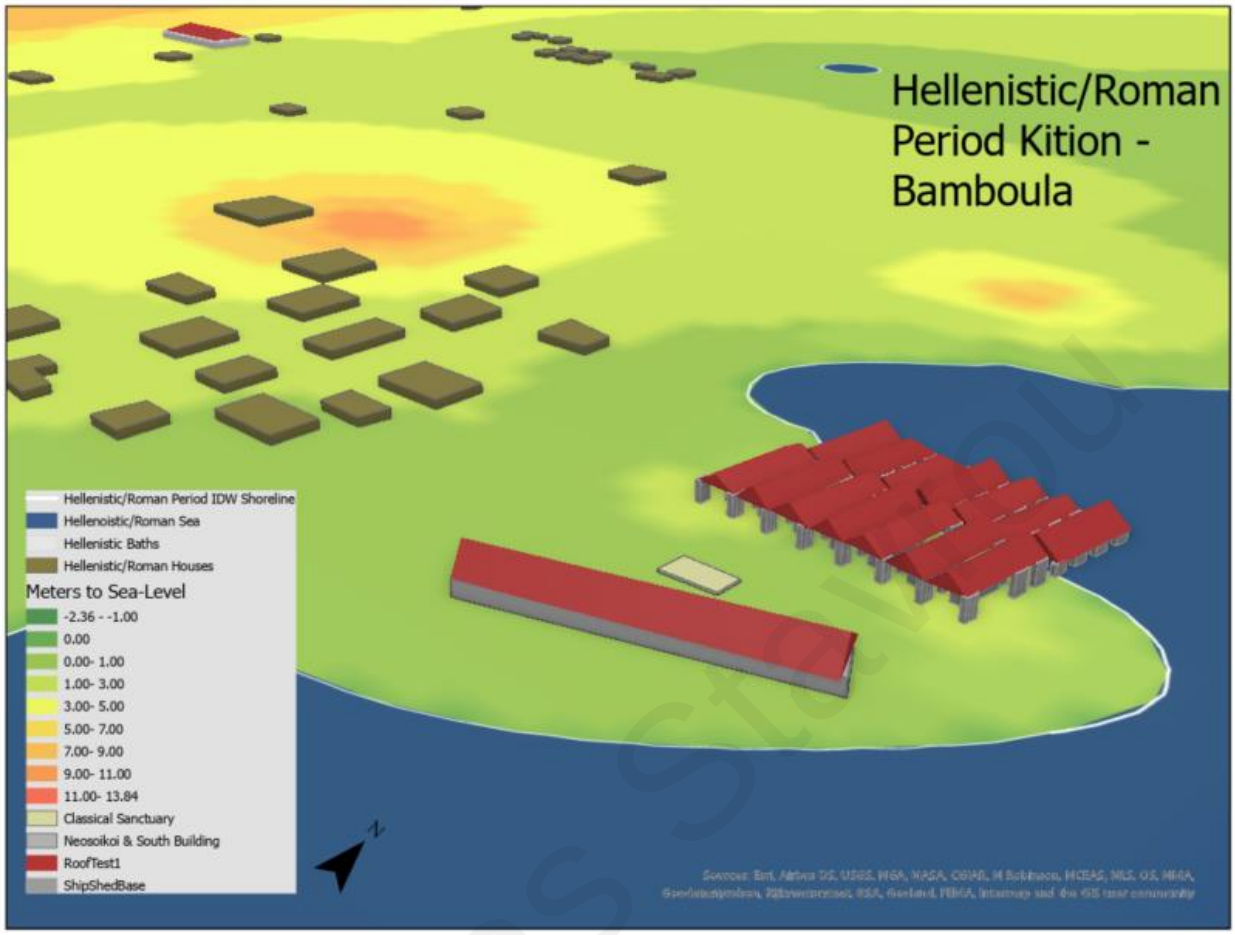

Figure 55: 3D reconstructed Kition – Bamboula during the Hellenistic and Roman Period, with the Hellenistic bath from Chrysopolitissa in background.

6. DISCUSSION

The overall methodology employed in this study proved effective in achieving 3D reconstructions using various interpolated methods. The coring data with their dated elevation levels was valuable in creating a shoreline and water depth of certain coastal features when paired with the modern elevation points used. However, a notable challenge surfaced with the absence of offshore-coastal features compared to previous reconstructions, attributed to the low elevation of the dates recorded in the sedimentological sequence of the cores. This raises considerations about the potential influence of factors like material compression over time and minor tectonic activity, impacting the accuracy of these elevation points.

A recurring issue in the reconstruction involves the positioning of archaeological features along or within the shoreline. These discrepancies were influenced by various factors affecting the interpolation accuracy. Addressing this necessitates nuanced consideration of the methods used and their limitations, potentially prompting adjustments in the interpretation of these features.

In the broader context of the archaeological discussion on the topography of Kition, this study provides valuable insights by exploring alternative approaches to reconstructing the palaeogeography of the region. The implementation of various interpolation methods allows for calculated manipulations of data related to ancient elevation levels, contributing to a more comprehensive understanding of Kition's historical landscape. The application of interpolation emerges as a dependable method for reconstructing Kition's palaeogeography that has yet to be applied. The technique provides a credible contribution to the ongoing discussion among previous reconstructions and presenting an alternative approach for reconstructing paleoenvironments.

While successful, the interpolations underline the need for additional well-spaced coring data to enhance overall accuracy. Challenges such as uncertainties in dating techniques limiting temporal markers, the density of coring data affecting reliable terrain survey for interpolation methods, and the potential for improvement through additional elevation points from archaeological excavation layers have been identified. Despite its success, the study identifies areas for enhancement, emphasizing the importance of more strategically placed cores along the coastline to refine precision and reliability, especially when considering later periods.

Nevertheless, this study demonstrates that utilizing interpolation from coring data, in conjunction with archaeological features, offers a novel and reliable approach to deriving a digital terrain model for ancient Kition. The method provides multiple theoretical 3D models, showcasing the potential for alternative techniques archaeological and geographical reconstructions.

7. CONCLUSION

The first objective of this thesis was to provide a 3D reconstruction of the urban and coastal landscape of ancient Kition during the Late Bronze Age, Iron Age, Classical period, Hellenistic and Roman periods. The palaeogeographic reconstructions of Kition presented in this research, by providing a comprehensive insight into the city's evolution, offering a fresh perspective on urban topography and the changing environmental conditions—from an open bay connected to the Mediterranean Sea to a more enclosed setting over time. The amalgamation of urban topography with palaeogeography DTMs forms a vital framework for comprehending the city's historical development throughout time.

A major challenge encountered was the scarcity of elevation points on land near archaeological sites, impacting the Late Bronze Age and Iron Age interpolations. This resulted in low-lying cores influencing land features, placing them partially below sea level. Addressing this limitation through additional coring and incorporating publicly available information on excavated layers would significantly enhance the accuracy of these DTMs. Furthermore, increased coring data, especially from the east of *Kathari* and *Bamboula*, would also improve the precision of interpolations, contributing to a more detailed representation of offshore coastal features like the spit and improving the reliability of the reconstructed port basins.

Noteworthy findings from the interpolation tools include challenges in generating shorelines within the proposed Late Bronze Age defensive wall limits, questioning the accuracy of the wall's layout as suggested by previous studies. The second objective was to compare interpolated DTM shorelines with other palaeogeographic reconstructions. The thesis illustrates that the interpolated DTMs were successfully compared to other reconstructions that was able to challenge new perspectives on the possible shape of the coastline over time.

Additionally, the delayed appearance of the coastal spit, proposed to have originated in the Classical Period, became evident in this study only in the Hellenistic and Roman Period DTM, potentially indicating the need for further coring data. The only period to reliably capture offshore features is in the Hellenistic and Roman periods. In the best-chosen IDW DTM, the elevation of the small island features is between 1-3 m above sea level, likely suggesting that this low-lying sandy island did not act as a hindrance to ships navigating to and from the port of Bamboula.

The third objective was to test the effectiveness of Interpolation as a method of portraying palaeogeography. Employing various interpolation methods, this study successfully demonstrated the versatility in recreating Kition's palaeogeography with limited sample points obtained from coring data. The IDW and Kriging interpolation tools emerged as particularly effective for the given dataset, showcasing adaptability with the dense and incomplete dataset, as well as their capabilities of parameter manipulation. Specifically, IDW proved most valuable for creating DTMs in the Late Bronze Age, Classical, Hellenistic and Roman periods, while Kriging demonstrated improved presentation for the Iron Age.

The framework and methodology of this research can be applied to other sites, particularly those of coastal sites, demonstrating the broader relevance and potential applicability of the innovative

3D reconstruction approach in archaeological studies. Introducing interpolated DTMs as a means to recreate the palaeogeography of Kition in a 3D model offers an unprecedented approach to understanding the evolution of the site through time. This study lays the groundwork for future research of better understanding Kition within a 3D approach, which can be built on. Prospective research endeavors employing GIS techniques, encompassing spatial, network, density, or terrain analyses, will offer substantial insights from the reconstructed findings of this study.

8. BIBLIOGRAPHY

Aguilar, F.J., Agüera, F., Aguilar, M.A., Carvajal, F. (2005). Effects of Terrain Morphology, Sampling Density, and Interpolation Methods on Grid DTM Accuracy. *Photogramm Eng Remote Sensing*, *71*, 805–816. https://doi.org/10.14358/PERS.71.7.805

Alcaras, E., Parente, C., Vallario, A. (2019). Comparison of different interpolation methods for DTM production, University of Naples 'Parthenope', Naples, Italy. *IJATCSE*, *6*, 1654–1659. https://doi.org/10.30534/ijatcse/2019/91842019

Altinok, Y., Alpar, B., Özer, N., Aykurt, H. (2011). Revision of the tsunami catalogue affecting Turkish coasts and surrounding regions. *Nat. Hazards Earth Syst. Sci.*, *11*, 273–291. https://doi.org/10.5194/nhess-11-273-2011

Arun, P.V. (2013). A comparative analysis of different DTM interpolation methods. *The Egyptian Journal of Remote Sensing and Space Science*, *16*, 133–139. https://doi.org/10.1016/j.ejrs.2013.09.001

Astrom, P., Nys, K. (2001). Trial excavations north of Area 6 in 1999, in: P. Åström (ed.), 57–61.

Barnes, C. (2022). Monumental stonework at Kition Kathari : a spatial analysis of a Late Cypriot built environment. (T). Electronic Theses and Dissertations (ETDs) 2008+.University of British Columbia https://doi.org/10.14288/1.0413131

Benjamin, J., Rovere, A., Fontana, A., Furlani, S., Vacchi, M., Inglis, R.H., Galili, E., Antonioli, F., Sivan, D., Miko, S., Mourtzas, N., Felja, I., Meredith-Williams, M., Goodman-Tchernov, B., Kolaiti, E., Anzidei, M., Gehrels, R. (2017). Late Quaternary sea-level changes and early human societies in the central and eastern Mediterranean Basin: An interdisciplinary review. *Quaternary International*, *449*, 29–57. https://doi.org/10.1016/j.quaint.2017.06.025

Bony, G., Carayon, N., Flaux, C., Marriner, N., Fourrier, S., Morhange, C. (2016). Évolution paléo-environnementale de la baie de Kition: mise en évidence d'un possible environnement portuaire (Larnaca, Chypre). *44e Supplément à la Revue Archéologique de Narbonnaise*, 369-380.

Callot, O., Fourrier, S., Yon, M. (Eds.) (2022). *Kition-Bamboula VIII: Le port de guerre de Kition.* MOM Éditions. https://doi.org/10.4000/books.momeditions.13617

Caubet, A., Fourrier, S., Yon, M. (2015). *Kition-Bamboula VI. Le sanctuaire sous la colline (Travaux de la Maison de l'Orient et de la Méditerranée 67), Lyon.*

Cannavò, A. (2022). Kition de Chypre : du royaume phénicien à la cité hellénistique. *Ktèma : Civilisations de l'Orient, de la Grèce et de Rome antiques, 47*, 155-174.

Childs, C. (2004). Interpolating Surfaces in ArcGIS Spatial Analyst. *ESRI Education Services*, 32–35.

Dalongeville, R., Bernier, P., Prieur, A., Le Campion, T. (2000). Les variations récentes de la ligne de rivage du sud-est de Chypre / The Early Changes of Southeastern Cyprus Shorelines. *morfo, 6*, 13–19. https://doi.org/10.3406/morfo.2000.1039

Devillers, B., Brown, M., Morhange, C. (2015). Paleo-environmental evolution of the Larnaca Salt Lakes (Cyprus) and the relationship to second millennium BC settlement. *Journal of Archaeological Science: Reports, 1*, 73–80. https://doi.org/10.1016/j.jasrep.2014.11.004

Erdogan, S. (2009). A comparison of interpolation methods for producing digital elevation models at the field scale. *Earth Surf. Process. Landforms, 34*, 366–376. https://doi.org/10.1002/esp.1731

ESRI (2023). An overview of the Interpolation toolset. *An overview of the Interpolation toolset-ArcGIS Pro | Documentation.*

Evelpidou, N., Pavlopoulos, K., Vouvalidis, K., Syrides, G., Triantaphyllou, M., Karkani, A., Paraschou, T. (2019). Holocene palaeogeographical reconstruction and relative sea-level changes in the southeastern part of the island of Samos (Greece). *Comptes Rendus Geoscience, 351*, 451–460. https://doi.org/10.1016/j.crte.2019.09.001

Fischer, P.M. (2019). Hala Sultan Tekke, Cyprus: A Late Bronze Age Trade Metropolis. *Near Eastern Archaeology, 82*, 236–247. https://doi.org/10.1086/705491

Fischer, P.M., Bürge, T. (2017). Peoples Up-to-Date. New Research on Transformations in the Eastern Mediterranean in the 13th–11th Centuries BCE. *Contributions to the Chronology of the Eastern Mediterranean, 35*. Vienna, Austrian Academy of Sciences.

Fischer, P.M. (2023). Interregional trade at Hala Sultan Tekke, Cyprus: Analysis and chronology of imports. *Journal of Archaeological Science: Reports, 47*, 103722. https://doi.org/10.1016/j.jasrep.2022.103722

Fourrier, S. (2015a). The Iron Age city of Kition: the state of research 85 years after the Swedish Cyprus Expedition's excavations. *Ancient Cyprus Today*, 129–139.

Fourrier, S. (2015b). The Iron Age topography of Kition, *in the website: Kyprios Character. History, Archaeology & Numismatics of Ancient Cyprus:* 1–12.

Fourrier, S. (2014). Étude d'une ville chypro-phénicienne : Kition à l'âge du Fer (de la seconde moitié du xi^{e} s. à la fin du iv^{e} s. av. J.-C.), *Mémoire d'habilitation à diriger des recherches, Université d'Aix-Marseille*.

Fourrier, S., Georgiadou, A., Chamel, B., Denninger, N., Gardeisen, A., Papayanni, K., Theodoropoulou, T. (2021). The death of infants in Early Iron Age Cyprus. A jar burial from Kition-Bamboula. *OpAthRom, 14*, 281–304. https://doi.org/10.30549/opathrom-14-13

Fourrier, S., & Rabot, A. (2020). Un puits à roue élévatrice de Kition-Bamboula. *Bulletin de Correspondance Hellénique, 144*, 705-776https://doi.org/10.4000/bch.1195

Frost, H. (1982). On a sacred Cypriot anchor. *Archéologie au Levant. Recueil à la mémoire de R. Saidah.*, 161–166.

Galili, E., Şevketoğlu, M., Salamon, A., Zviely, D., Mienis, H.K., Rosen, B., Moshkovitz, S. (2016). Late Quaternary beach deposits and archaeological relicts on the coasts of Cyprus, and the possible implications of sea-level changes and tectonics on the early populations. *SP, 411*, 179–218. https://doi.org/10.1144/SP411.10

Georgiadou, A., Georgiou, A. (2019). Spinning, Weaving and Purple Dyeing at Kition: New evidence for the textile industry at the settlement of Bamboula during the Late Bronze-Earl. *cchyp, 103–128.* https://doi.org/10.4000/cchyp.457

Georgiou, A. (2012). Pyla-Kokkinokremos, Maa-Palaeokastro and the settlement histories of Cyprus in the twelfth century BC [PhD thesis], *University of Oxford.*

Georgiou, A., Georgiadou, A., Fourrier, S. (2023). Traditions and innovations during the 12th-to11th century BC transition in Cyprus: new data from Kition-Bamboula. *Cahiers du Centre d'Etudes Chypriotes*, 117–151.

Gifford, J.A. (1985). Post-Bronze Age coastal change in the vicinity of Kition. In: Karageorghis, V. & Demas, M. (eds) Excavations at Kition V. The Pre- Phoenician Levels, Volume 1. Department of Antiquities, Lefkosia, Cyprus.

Gifford, J.A. (1980). Paleogeography and archaeological sites of the Larnaca lowlands, Southern Cyprus. Nivmer, 6-7.

Gifford, J.A. (1978). Paleography of archaeological sites of the Larnaca Lowlands, Southeastern Cyprus. [PhD thesis], University of Minnesota.

Gjerstad, E. (1960). Pottery Types, Cypro-Geometric to Cypro-Classical, in «OpAth» 3, 105–122.

Heidemann, H.K. (2018). Lidar base specification (ver. 1.3, February 2018): *U.S. Geological Survey Techniques and Methods*, book 11, chap. B4 (Techniques and Methods), Techniques and Methods.

Hirt, C. (2014). Digital Terrain Models, in: Grafarend, E. (Ed.), *Encyclopedia of Geodesy*. Springer International Publishing, Cham, 1–6. https://doi.org/10.1007/978-3-319-02370-0_31-1

Iacovou, M. (2007). Site Size Estimates and the Diversity Factor in Late Cypriot Settlement Histories. *Bulletin of the American Schools of Oriental Research, 348*, 1–23. https://doi.org/10.1086/BASOR25067035

Iacovou, M. (2018). From the Late Cypriot Polities to the Iron Age 'Kingdoms': understanding the Political Landscape of Cyprus from within. In *Les royaumes de Chypre à l'épreuve de l'histoire: Transitions et ruptures de la fin de l'âge du Bronze au début de l'époque hellénistique*, A. Cannavo & L. Thely (Eds.), Athènes: École Française d'Athènes.

Karageorghis, V. (1982). Cyprus, from the Stone Age to the Romans, *Ancient peoples and places.* Thames and Hudson, London.

Karageorghis, V., Demas, M. (1985). Excavations at Kition. *Vol. 5, The Pre-Phoenician Levels.* Nicosia: Department of Antiquities.

Karageorghis, V. and Demas, M. (1988). Excavations at Maa-Palaeokastro 1979–1986. *plat: Plates* Nicosia.

Karageorghis, V., Kassianidou, V. (1999). Metalworking and Recycling in Late Bronze Age Cyprus – the Evidence from Kition. *Oxford J Archaeology, 18*, 171–188. https://doi.org/10.1111/1468-0092.00078

Knapp, A.B. (2018). Seafaring and seafarers in the Bronze Age Eastern Mediterranean. Sidestone Press, Leiden.

Given, M., Knapp, A.B., Coleman, D. (2003). The Sydney Cyprus Survey Project: Social Approaches to Regional Archaeological Survey. *Monumenta archaeologica*. Cotsen Institute of Archaeology, University of California, Los Angeles.

Koss, J.E., Ethridge, G., Schumm, S.A. (1994). An Experimental Study of the Effects of Base-Level Change on Fluvial, Coastal Plain and Shelf Systems. *SEPM JSR Vol. 64B.* https://doi.org/10.1306/D4267F64-2B26-11D7-8648000102C1865D

Krivoruchko, K., Gotway, C.A. (2004). Creating exposure maps using Kriging. *Public Health GIS News and Information, 56*, 11–16.

Kumar, A. (2011). Granulometry, in: Singh, V.P., Singh, P., Haritashya, U.K. (Eds.), *Encyclopedia of Snow, Ice and Glaciers.* Springer Netherlands, Dordrecht, 477–477. https://doi.org/10.1007/978-90-481-2642-2_222

Morhange, C., Goiran, J.-P., Bourcier, M., Carbonel, P., Le Campion, J., Rouchy, J.-M., Yon, M. (2000). Recent Holocene paleo-environmental evolution and coastline changes of Kition, Larnaca, Cyprus, Mediterranean Sea. *Marine Geology, 170*, 205–230. https://doi.org/10.1016/S0025-3227(00)00075-X](https://doi.org/10.101

Nikolaou, K. (1976). The Historical Topography of Kition. *Studies in Mediterranean archaeology*. P. Åström, Göteborg.

Paladio-Hernandez, A., Salles, P., Arriaga, J., López-González, J. (2022). Characterization of the Morphological Behavior of a Sand Spit Using UAVs. *Journal of Marine Science and Engineering, 10*(5), 600. https://doi.org/10.3390/jmse10050600

Parpas, A.P. (2022). The Maritime Economy of Ancient Cyprus in Terms of the New Institutional Economics, *Archaeopress.*

Peppe, D. J., & Deino, A. L. (2013). Dating Rocks and Fossils Using Geologic Methods. *Nature Education Knowledge, 4*(10), 1.

Philip, G.M., Watson, D.F. (1982). A Precise Method for Determining Contoured Surfaces. *Australian Petroleum Exploration Association Journal, 22*, 205–212.

Polidorou, M., Evelpidou, N., Tsourou, T., Drinia, H., Salomon, F., Blue, L. (2021). Observations on Palaeogeographical Evolution of Akrotiri Salt Lake, Lemesos, Cyprus. *Geosciences, 11*, 321. https://doi.org/10.3390/geosciences11080321

Poole, A.J., Robertson, A.H.F. (1991). Quaternary uplift and sea-level change at an active plate boundary, Cyprus. *JGS, 148*, 909–921. https://doi.org/10.1144/gsjgs.148.5.0909

Pococke, R. (1745). A description of the East and some other countries, vol. 2 (in 2 parts). W. Bowyer, London.

Raban, A., Galili, E. (1985). Recent maritime archaeological research in Israel—A preliminary report. *International Journal of Nautical Archaeology, 14(4)*, 321-356.

Rabot, A. (2020). Kition, Larnaca: French Archaeological Mission of Kition (dir. Sabine Fourrier) https://storymaps.arcgis.com/stories/4428fc88b0a8485483e9068d85871162.

Rishikeshan, C.A., Katiyar, S.K., Mahesh, V.N.V. (2014). Detailed Evaluation of DTM Interpolation Methods in GIS Using DGPS Data. *In: 2014 International Conference on Computational Intelligence and Communication Networks.* Presented at the 2014 International Conference on Computational Intelligence and Communication Networks (CICN), IEEE, Bhopal, India, pp. 666–671. https://doi.org/10.1109/CICN.2014.148

Sivan, D., Wdowinski, S., Lambeck, K., Galili, E., Raban, A. (2001). Holocene sea-level changes along the Mediterranean coast of Israel, based on archaeological observations and numerical model. *Palaeogeography, Palaeoclimatology, Palaeoecology, 167*, 101–117. https://doi.org/10.1016/S0031-0182(00)00234-0

Smith, J.S. (2008). Art and Society in Cyprus from the Bronze Age into the Iron Age. *Cambridge.*

Strabo. (1917-1932). The Geography of Strabo. London : New York :W. Heinemann ; G.P. Putnam's Sons.

Szypuła, B. (2017). Geomorphometric comparison of DEMs built by different interpolation methods. *Landform Analysis, 32*, 45–58. https://doi.org/10.12657/landfana.032.004

Yasur-Landau, A., Shtienberg, G., Gambash, G., Spada, G., Melini, D., Arkin-Shalev, E., Tamberino, A., Reese, J., Levy, T.E., Sivan, D. (2021). New relative sea-level (RSL) indications from the Eastern Mediterranean: Middle Bronze Age to the Roman period (~3800–1800 y BP) archaeological constructions at Dor, the Carmel coast, Israel. *PLoS ONE, 16*, e0251870. https://doi.org/10.1371/journal.pone.0251870

Yon, M. (1994). Kition-Bamboula. In: Christou, D. (ed.) Chronique des fouilles des découvertes archéologiques à Chypre en 1993. *Bulletin de Correspondance Hellenique, 118.*

Yon, M., Caubet, A. (1987). Kition-Bamboula, III. *Kition-Bamboula III. Survey LN 13 (Recent Bronze and Geometric I).*

Yon, M., Childs, W.A.P. (1997). Kition in the Tenth to Fourth Centuries B. C. *Bulletin of the American Schools of Oriental Research, 308*, 9–17. https://doi.org/10.2307/1357405

You, S., Zhang, J. (2012). Constructing natural neighbor interpolation based grid DTM using CUDA. In: *Proceedings of the 3rd International Conference on Computing for Geospatial Research and Applications.* Presented at the COM.Geo ’12: 3rd International Conference on Computing for Geospatial Research and Application, ACM, Washington D.C. USA, pp. 1–6. https://doi.org/10.1145/2345316.2345349